



Universidad de Cantabria

**Escuela Técnica Superior de Ingenieros Industriales y de
Telecomunicación**

Departamento de Ingenierías Química y Biomolecular

**DEVELOPMENT OF NEW HIGH-PERFORMANCE
CONDUCTIVE MEMBRANES BASED ON POLYMERIZED
IONIC LIQUIDS FOR THEIR USE IN FUEL CELLS**

**“Desarrollo de nuevas membranas conductoras de altas
prestaciones basadas en líquidos iónicos polimerizados para su
aplicación en pilas de combustible”**

Memoria de tesis doctoral presentada para optar al título de
Doctor por la Universidad de Cantabria. Programa Oficial de Doctorado
en Ingeniería Química y de Procesos.

Mariana Díaz Vejo

Directores de tesis:

Profa. Dra. Inmaculada Ortiz Uribe

Dr. Alfredo Ortiz Sainz de Aja

Santander, 2017

Programa Oficial de Doctorado en Ingeniería Química y de Procesos (BOE núm. 36, de 10 de febrero de 2010. RUCT: 5311209) con Mención hacia la Excelencia (BOE núm. 253, de 20 de Octubre de 2011. Referencia: MEE2011-0031)

Este trabajo ha sido financiado por el Ministerio de Ciencia e Innovación y por el Ministerio de Economía y Competencia de España a través de los proyectos: CTQ2008-00690, *Investigación y desarrollo de separaciones reactivas. Contribución al desarrollo tecnológico sostenible*; y CTQ2012-31639, *Nuevos procesos de separación con control cinético basados en la utilización de materiales funcionalizados*.

Asimismo, Mariana Díaz Vejo ha disfrutado de una beca de Formación del Profesorado Universitario (F.P.U.) del Ministerio de Educación, Cultura y Deporte (Ref.: FPU2012-03721, BOE-A-2013-2942) para la realización de esta tesis doctoral.

Agradecimientos

Mi más sincero agradecimiento a la Prof. Inmaculada Ortiz Uribe por confiar en mí y darme la oportunidad de desarrollar mi tesis doctoral en el grupo de investigación Procesos Avanzados de Separación. Ha sido un privilegio trabajar con una persona que demuestre tanta pasión por su trabajo. Su rigor científico y su profesionalidad han hecho posible este trabajo.

Me gustaría agradecer de manera especial al Dr. Alfredo Ortiz Sainz de Aja por haberme guiado en este camino durante todos estos años. Mil gracias por orientarme con tanta paciencia y por mantenerme motivada cuando las cosas se torcían. Por muy ocupado que estuviese siempre sacaba un hueco para reunirnos y debatir nuevas ideas. Simplemente, no me imagino un supervisor mejor.

Quiero expresar también mi gratitud al resto del profesorado del Departamento de Ingenierías Química y Biomolecular, así como a todo el personal administrativo y técnico, quienes siempre han estado dispuestos a ayudar cuando ha sido necesario.

Gracias a todo el personal del Instituto para Materiales Fronterizos de la Universidad de Deakin, especialmente a Dr. Jenny Pringle por su orientación durante mi estancia doctoral. Especialmente quisiera agradecer a Danah Al-Masri su amistad la cual comenzó el primer día que llegué a Melbourne. Por su bondad, simpatía y disposición de ayudar a los demás sin quitar la sonrisa. Nunca olvidaré los meses que pasé en Australia.

Por otra parte, me gustaría agradecer al Prof. David Mecerreyes y al Dr. Alfonso Sáez por haberme orientado y aconsejado durante mi tesis doctoral y acogerme en sus grupos de investigación. También me gustaría agradecer a Francisco Javier Garzón, Amador Claver, Irati Lazarraga, Raquel Barbadillo y Luis Alberto Herrero su colaboración en esta tesis doctoral.

A mis compañeros del seminario 458, Álvaro, Sandra, Nazely, Beatriz, Marcos, Raúl y Arantxa. Gracias por vuestra compañía y apoyo durante todo este tiempo. A todos mis amigos del departamento por su tiempo y amistad durante todos estos años: Ana, Azu, Carlos, Carolina, Gabriel, Germán, Isa, Lucía, Sara, Andrés y Esther. Especialmente, gracias a Pablo por su amistad desde hace más de 20 años. Siempre sospeché que gran parte de la culpa de que yo me decidiera a estudiar una carrera universitaria fue suya, cuando me sentaron con él en el instituto y se me pegó un poco de su compromiso con los estudios. Además, me gustaría hacer una mención especial a aquellos con los que me he aficionado un poquito al café durante este doctorado. Realmente me siento muy afortunada con vosotros, no todo el mundo tiene la suerte de poder trabajar con amigos. Muchísimas gracias por todo!

A Nano y a Nieves, quienes han sido como unos segundos padres cuando los míos se tomaban unas merecidas vacaciones. Sin ninguna duda, sois los mejores vecinos del mundo y unas magníficas personas.

Por último pero no menos importe, esta tesis hubiera sido impensable sin el apoyo de mi familia. Quiero agradecer a Pepín y a Milagros el cariño y apoyo que me dieron desde la lejanía, y que afortunadamente ahora me pueden dar en persona. A mi abuela que estaría muy orgullosa de mí. A mis hermanos Eva, Susi y Asier, por ser un referente para mí y por motivarme a crecer cada día. A mi cuñado Marcos, que junto con mi hermana me han ayudado y apoyado en todos los sentidos posibles, por los incontables buenos momentos y por escucharme y aconsejarme cada vez que lo he necesitado. A mis sobrinas Jana y Victoria, por sacarme una sonrisa y conseguir que me olvide de cualquier problema. A mis padres, por enseñarme las cosas que realmente importan y no aparecen en los libros, por creer en mí incluso cuando yo no creía en mí misma. Sin vuestro apoyo y cariño no hubiese llegado hasta aquí.

Summary

Proton exchange membrane fuel cells (PEMFCs) offer a promising technology for sustainable energy production due to their high efficiency and low environmental impact. This alternative holds several advantages over conventional technologies, such as their high electrical efficiency, low pollutant emissions, ease of installation and rapid start-up. The core of a PEMFC is called the membrane electrode assembly (MEA) that is composed of the proton exchange membrane (PEM) placed between two electrodes. Nafion perfluorosulfonic acid ionomer is the most widely used proton exchange membrane in PEMFC devices because of its excellent chemical stability, high ionic conductivity and good mechanical strength. However, this is a highly expensive membrane strongly dependent on humidity which requires the use of external controlled humidity systems. The lack of water in these membranes compromises the proton transport mechanisms leading to high ionic resistance electrolytes with deficient fuel cell performance. For this reason, the development of electrolytes with high ionic conductivity capable of working under non-humidified conditions constitutes an interesting scientific challenge. Many efforts have been made in order to develop proton exchange membranes capable of working under anhydrous conditions. Particularly, ionic liquids (ILs) are attracting interest as electrolytes for electrochemical applications due to their exceptional properties such as negligible volatility, non-flammability, high thermal and electrochemical stability and outstanding ionic conductivity even under anhydrous conditions.

In light of these facts, this thesis focuses on the development and application of innovative polymeric membranes for proton exchange membrane fuel cells without external humidification using ionic liquids as favorable proton exchange medium.

Firstly, in chapter 1 an overview of the current worldwide energy situation is presented, emphasizing the use of the fuel cell technology as an advantageous

alternative for energy production. The state of the art of proton exchange membranes was reviewed to establish the basis for the present thesis.

The methods and equipment used in this work are described in chapter 2. The fundamentals of the techniques used for the membrane characterization as well as the description of the experimental set-up, including the membrane-electrodes assembly and the protocol for fuel cell testing are included in this section.

In order to improve the low performance under non-humidified conditions reported for commercial perfluorosulfonic membranes, an impregnation procedure with two different protic ionic liquids 1-methyl-3-(4-sulfobutyl)-imidazolium bis(trifluoromethylsulfonyl)-imide ([HSO₃-BMIm][Tf₂N]) and 1-butyl-3-(4-sulfobutyl)-imidazolium trifluoromethanesulfonate ([HSO₃-BBIIm][TfO]) was carried out in chapter 3. Fuel cell performance and ionic resistance of these modified membranes were studied and compared with the behavior of unmodified perfluorinated membranes at different temperature and humidity conditions.

Having demonstrated the viability of protic ionic liquids as proton carriers under non-humidified conditions, the next step analyzed the design of high performance electrolytes under non-humidified conditions avoiding the use of expensive perfluorinated polymers. For this purpose, membranes based exclusively on polymerized protic ionic liquids were developed and studied in chapter 4. The first membrane was based on the two polymerizable ionic liquids 1-(4-sulfobutyl)-3-methylimidazolium 2-sulfoethylmethacrylate [HSO₃-BMIm][SEM] and 1-(4-sulfobutyl)-3-vinylimidazolium 2-sulfoethylmethacrylate [HSO₃-BVIIm][SEM]. In the second case, composite membranes based on the polymerizable ionic liquid 1-(4-sulfobutyl) 3-vinylimidazolium trifluoromethanesulfonate [HSO₃-BVIIm][TfO] and its analogue non-polymerizable ionic liquid 1-(4-sulfobutyl)-3-methylimidazolium trifluoromethanesulfonate [HSO₃-BMIm][TfO] were synthesized at different compositional range. The effects of water content and temperature on the ionic conductivity were analyzed for both membranes. Moreover, the fuel cell performance for triflate anion-based membranes at different compositional range is

reported in this chapter. Molecular dynamics and ion transport properties of triflate monomer and its polymerized form as well as sulfoethylmethacrylate membrane are also included in this section allowing an understanding of the proton transport mechanisms of these electrolytes.

Finally, chapter 5 deals with the development of membranes based on protic plastic crystal and electrospun nanofibers. Similar to ILs, plastic crystals (PCs) are promising solid electrolytes for fuel cell applications due to their negligible volatility and high thermal and electrochemical stability. These materials have the advantages of ionic liquids (high proton conductivity without humidification) and the benefits of a solid state electrolyte. With this aim, composite membranes based on the protic plastic crystal N,N-dimethylethylene diammonium triflate [DMEDAH][TFO] and electrospun poly(vinylidene fluoride) (PVDF) nanofibers were developed for proton exchange membrane fuel cells (PEMFCs) under non-humidified conditions. Addition of 5 mol% of triflic acid and 5 mol% of the base N,N-dimethylethylenediamine was carried out to study the effects on the ionic conductivity and thermal behavior of the material. The effects of the plastic crystal doping on the thermal behavior, ionic conductivity and fuel cell performance are analyzed in this chapter.

Overall, this work contributes to the progress of the state of the art of PEMFC and targets to the research of new electrolytes for this technology with improved properties over the most widely used perfluorosulfonic membranes. Within this objective, new membranes that incorporate protic ionic liquids and protic plastic crystals have been developed and characterized and their behavior has been tested in PEMFC devices.

Resumen

Las pilas de combustible de intercambio protónico (PEMFCs) son una prometedora tecnología para la producción energética sostenible. Esta alternativa ofrece numerosas ventajas frente a las tecnologías convencionales tales como alta eficiencia energética, bajas emisiones de contaminantes, facilidad de instalación y rápido arranque. La parte fundamental de una PEMFC es el ensamblado membrana-electrodos (MEA), el cual está compuesto por una membrana intercambiadora de protones (PEM) situada entre dos electrodos. El ionómero perfluorado conocido como Nafion es la membrana más utilizada en los dispositivos PEMFC debido a su excelente estabilidad química, alta conductividad protónica y alta resistencia mecánica. Sin embargo, esta membrana altamente costosa es muy dependiente del contenido de agua para su correcto funcionamiento, lo cual implica el uso de controladores de humedad externos. La falta de agua en estas membranas perjudica los mecanismos de transporte protónico conduciendo a electrolitos con alta resistencia iónica y deficiente rendimiento en la celda de combustible. Por esta razón, el desarrollo de electrolitos con alta conductividad iónica capaces de funcionar bajo condiciones no humidificadas constituye un interesante reto científico. Numerosos esfuerzos han sido desarrollados con el objetivo de desarrollar membranas de alto rendimiento bajo condiciones anhidras. Particularmente, los líquidos iónicos (LIs) están adquiriendo interés como electrolitos para aplicaciones electroquímicas debido a sus excepcionales propiedades como despreciable volatilidad, bajo riesgo de inflamabilidad, alta estabilidad térmica y química y altas conductividades iónicas incluso en condiciones anhidras.

En vista de estas circunstancias, esta tesis se centra en el desarrollo y aplicación de membranas poliméricas innovadoras para PEMFCs sin humidificación externa empleando líquidos iónicos como un medio favorable de transporte protónico.

En primer lugar, en el capítulo 1 se presenta una revisión de la situación energética actual, enfatizando el uso de la tecnología de pilas de combustible como una alternativa ventajosa para la producción energética sostenible. El estado del arte en el campo de las membranas de intercambio protónico ha sido incluido para asentar las bases de la presente tesis doctoral.

Los métodos y equipos usados en este trabajo han sido descritos en el capítulo 2. Los fundamentos de las técnicas usadas en la caracterización de las membranas, así como la descripción del equipo experimental incluyendo el ensamblado de la membrana y los electrodos y el protocolo de funcionamiento de la pila de combustible están incluidos en esta sección.

Con el objetivo de mejorar el bajo rendimiento en condiciones anhidras reportado para las membranas comerciales perfluoradas, en el capítulo 3 se ha realizado una impregnación con los dos líquidos iónicos próticos 1-metil-3-(4-sulfobutil)-imidazolio bis(trifluorometilsulfonyl)-imida ([HSO3-BMIIm][Tf2N]) y 1-butyl-3-(4-sulfobutil)-imidazolio trifluorometanosulfonato ([HSO3-BBIIm][TfO]). El rendimiento en la pila de combustible y la resistencia iónica de estas membranas modificadas fue estudiado y comparado con el obtenido para las membranas sin modificar a diferentes condiciones de temperatura y humedad.

Habiendo demostrado la viabilidad de los líquidos iónicos próticos como transportadores de protones bajo condiciones no humidificadas, el siguiente paso consistió en el diseño de electrolitos de alto rendimiento evitando el uso de costosos polímeros perfluorados. Con este objetivo, en el capítulo 4 membranas basadas exclusivamente en líquidos iónicos próticos polimerizados fueron. La primera membrana está basada en dos líquidos iónicos polimerizables 1-(4-sulfobutil)-3-metilimidazolio 2-sulfoetilmacrilato [HSO3-BMIIm][SEM] y 1-(4-sulfobutil)-3-vinilimidazolio 2-sulfoetilmacrilato [HSO3-BVIIm][SEM]. En el segundo caso, membranas compuestas basadas en el líquido iónico polimerizado 1-(4-sulfobutil) 3-vinilimidazolio trifluorometanosulfonato [HSO3-BVIIm][TfO] y su análogo líquido iónico no polimerizable 1-(4-sulfobutil)-3-metilimidazolio trifluorometanosulfonato [HSO3-BMIIm][TfO] fueron sintetizadas a diferentes rangos composicionales. Los

efectos del contenido de agua y de la temperatura en la conductividad iónica fueron analizados para ambas membranas. Además, en este capítulo se ha incluido el rendimiento en la pila de combustible de las membranas de anión triflato con diferente composición. Por otra parte, los estudios de la dinámica molecular del monómero basado en el anión triflato, su forma polimérica y la membrana basada en el anión sulfoetilmecrilato incluidos en este capítulo permiten una comprensión de los mecanismos de transporte protónico de estos electrolitos.

Finalmente, en el capítulo 5 se han desarrollado membranas basadas en cristales plásticos próticos y nanofibras poliméricas. Similares a los LIs, los cristales plásticos (PCs) son prometedores electrolitos sólidos para pilas de combustible debido a su baja volatilidad y alta estabilidad térmica y química. Estos materiales presentan las ventajas de los líquidos iónicos (alta conductividad protónica sin humidificación) y los beneficios de los electrolitos sólidos. Con este objetivo, membranas compuestas basadas en el cristal plástico prótico N-N-dimetil-etileno diamina triflato [DMEDAH][TFO] y nanofibras de poli(vinilideno fluorado) (PVDF) han sido desarrolladas para PEMFCs bajo condiciones sin humidificar. Con el objetivo de analizar su influencia en la conductividad iónica, comportamiento térmico y rendimiento en la celda de combustible, se ha realizado una adición de 5 mol% de ácido tríflico y de 5 mol% de base N-N-dimetil-etileno diamina.

En general, este trabajo contribuye al progreso en el estado del arte de las PEMFCs y en la investigación de nuevos electrolitos para esta tecnología con ventajas significativas frente a las ampliamente usadas membranas perfluoradas. Dentro de este objetivo, nuevas membranas con líquidos iónicos próticos y cristales plásticos próticos han sido desarrolladas, caracterizadas y testeadas en dispositivos PEMFCs.

Table of Contents

Summary/Resumen	vii
<hr/>	
Chapter 1. Introduction	1
<hr/>	
1.1. Current energy situation	2
1.2. Fuel cells	9
1.3. Proton exchange membranes for PEMFCs	13
1.4. Room temperature ionic liquids	17
1.5. Thesis scope and outline	20
1.6. References	22
2. Methods and equipment	29
<hr/>	
2.1. Analytical and characterization techniques	30
2.1.1. Electrochemical impedance spectroscopy (EIS)	30
2.1.2. Broadband dielectric spectroscopy (BDS)	34
2.1.3. Thermogravimetric analysis (TGA)	37
2.1.4. Karl-Fischer titration	38
2.1.5. Differential scanning calorimetry (DSC)	39
2.1.6. Attenuated total reflection Fourier transform infrared spectroscopy (ATR-FTIR)	40
2.2. Experimental	41
2.2.1. Set-up general description	41
2.2.2. Membrane electrode assembly (MEA)	42
2.2.3. Performance testing of the fuel cell	43
2.2.4. Verification of the experimental set-up	45
2.3. References	48
3. Polymer/ionic liquid composite membranes	53
<hr/>	
3.1. Introduction	54
3.2. Experimental methods	57
3.2.1. Materials	57
3.2.2. Design and synthesis of protic ionic liquids	57
3.2.3. Impregnation of perfluorinated membranes	59
3.2.4. Operation conditions	60
3.3. Results and discussion	60
3.3.1. Thermal characterization of ionic liquids	60
3.3.2. Influence of temperature and humidity of inlet gases on the fuel cell performance	61

3.4. Conclusions	64
3.5. References	65

4. Membranes based on polymerized ionic liquids **69**

4.1. Introduction	70
4.2. Experimental methods	74
4.2.1 Materials	74
4.2.2. Design and synthesis of the ionic liquids	75
4.2.3. Photopolymerization of ionic liquids	79
4.2.4. Operation conditions	80
4.3. Results and discussion	80
4.3.1. Characterization of membranes	81
4.3.2. Influence of temperature and water content on ex-situ ionic conductivity	88
4.3.3. Ionic conductivity mechanisms in polymerized ionic liquids: ion dynamics studies	92
4.3.4. Fuel cell performance	96
4.3.4.1. Influence of the thickness of the membrane	96
4.3.4.2. Influence of non-polymerizable ionic liquid and temperature	97
4.4. Conclusions	100
4.5. References	103

5. Membranes based on protic plastic crystal and polymers **107**

5.1. Introduction	108
5.2. Experimental methods	111
5.2.1. Materials	111
5.2.2. Fabrication of composite membranes	112
5.2.3. Membrane characterization and operation conditions	114
5.3. Results and discussion	115
5.3.1. Membrane synthesis	115
5.3.2. Thermal behavior	116
5.3.3. Ionic conductivity	118
5.3.4. Fuel cell testing	120
5.4. Conclusions	121
5.5. References	122

6. Conclusions and challenges for future research **127**

6.1. Conclusions	128
6.2. Challenges for future research	131

Chapter 1

INTRODUCTION

Abstract

This thesis aims at the development and characterization of innovative polymeric membranes for proton exchange membrane fuel cells without external humidification using ionic liquids as favorable proton exchange medium. This preface chapter introduces an overview of the current worldwide energy situation, fuel cell fundamentals and a review of the different proton exchange membranes used in this technology. An introduction to ionic liquids as alternative electrolytes is provided to set the foundations for the development of ionic liquid-based membranes for fuel cell applications. Finally, the scope and outline of the thesis are summarized.

1.1. Current energy situation

Modern lifestyle requires a steady, secure and accessible supply of energy. The global demand of energy is rapidly increasing with growing human population, urbanization and modernization [1]. Global primary energy consumption in 2015 was 13147.3 million tons of equivalent oil. This means an increase of 1.0% respect to the previous year and similar to the growth recorded in 2014 (1.1%) but below its 10-year average increase of 1.9% [2]. During the 2008-2013 period there was an important economic adjustment in developed countries, especially those belonging to the European Union, due to the economic crisis. This situation was reflected in the primary energy consumptions which declined in 2008 as it can be observed in figure 1.1. After that moment the primary energy consumption progressively increased up to the present values.

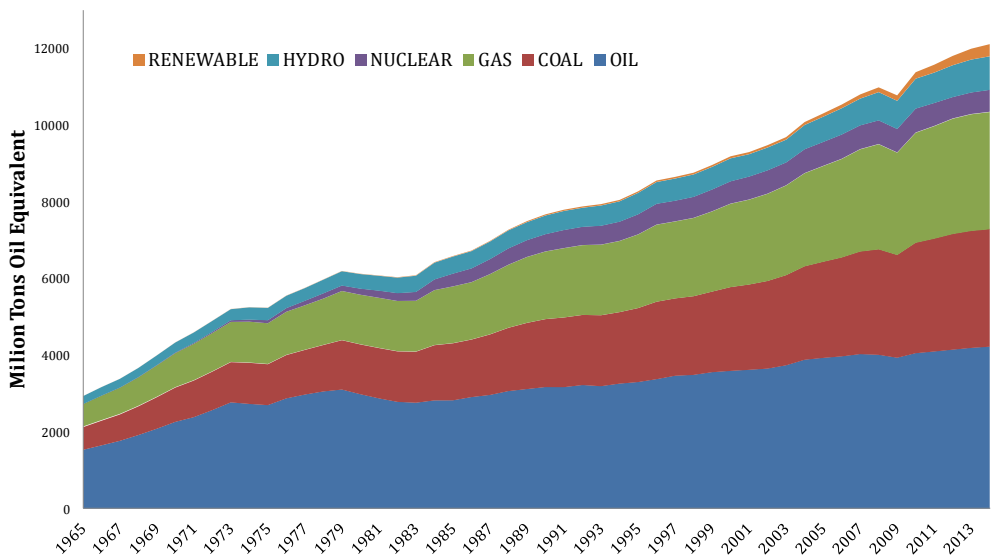


Figure 1.1. Historical evolution of primary energy consumption by fuel type

Fossil fuels such as oil, gas and coal provide almost 86% of the energy demands. Oil is the fuel mostly consumed, with 32.9% of the global energy consumption. This means an increase of 1.9% in comparison to the figures of 2014. World natural gas

consumption grew by 1.7% in 2015, a significant increase from the weak growth of 2014 but below the 10-year average increase of 2.3%. On the other hand, global coal consumption fell in 2015 by 1.8%, below the 10-year average annual growth of 2.1%. Global nuclear output grew by 1.3%, being China the country that contributed the most to this increase. Regarding renewable energy sources for power generation, they continued increasing in 2015 reaching 2.8% of the global energy consumption, 0.8% more than in the previous decade.

Figure 1.2 shows the fuel regional consumption in 2015. Oil is the dominant fuel in Africa and America, whereas natural gas is the major consumed fuel in Europe & Eurasia and the Middle East. Coal is the dominant fuel in the Asia Pacific region, which represents 51% of the regional energy consumption. The Middle East based its primary energy consumption on oil and gas, accounting for 98% of the energy consumption.

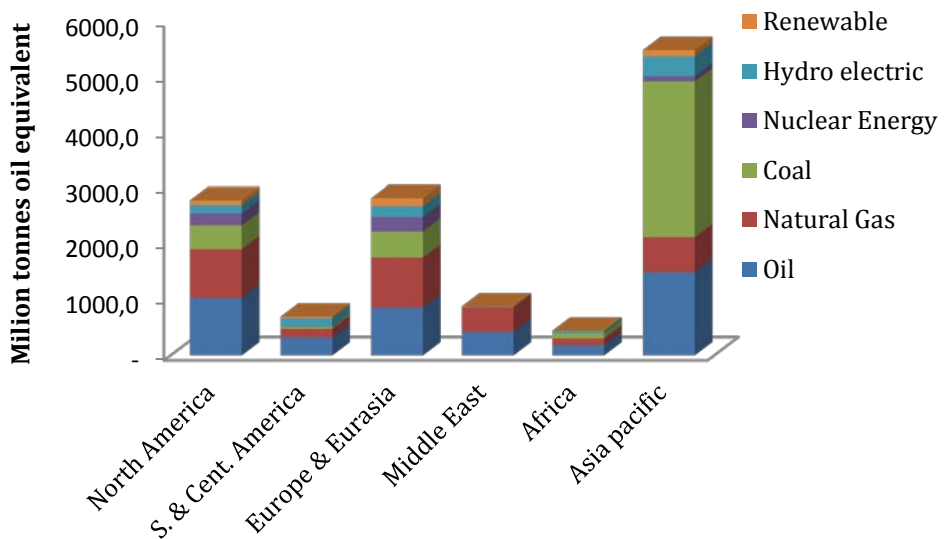


Figure 1.2. Distribution of primary energy consumption by fuel and region in 2015

The energy dependence on fossil fuel could lead to an undesirable and unsustainable situation due to the depletion of fossil fuel reserves, global warming and military conflicts.

The fossil fuel reserves are finite. If we maintain our present energy consumption trends the fossil fuel reserves will be compromised. To determine the depletion level of the fossil fuel reserves it is necessary to analyze each type of fossil fuel separately. Figure 1.3 shows the reserves-to-production (R/P) ratio of each type of fuel, which is a widely used measure to assess natural energy and mineral resources. The R/P ratio depicts the number of years that oil and mineral reserves will sustain the current level of energy consumption. The R/P ratio is calculated by dividing the proved reserves by the energy production in that year [3].

Oil is the less abundant fossil fuel, sufficient to meet 50.7 years of global energy production, being South and Central American reserves those with highest R/P ratio, 117 years. Natural gas reserves are enough to meet 52.8 years of global energy production and coal is by far the most abundant fossil fuel with world R/P ratio of 114 years. The Middle East has the highest R/P ratio for natural gas whereas Europe & Eurasia and North America have the highest R/P ratio for coal, 273 and 276 years respectively.

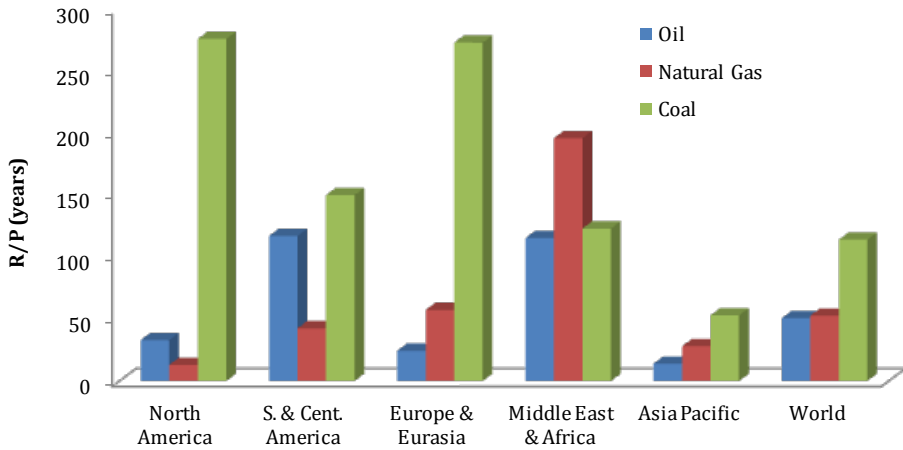


Figure 1.3. Fossil fuel reserves to production (R/P) ratio at 2015

The price of crude oil is an important concern that should be taken into account. Increasing demand especially from developing countries, geopolitical features in Middle East and extreme weather factors are factors that have played a significant role in the rapid rise of global oil prices [1]. Figure 1.4 shows the historical evolution of crude oil prices. As it can be observed, Kippur war (1973), Iranian Revolution (1979), Iran/Iraq War (1980) and First and Second Gulf Wars (1991 and 2003) have influenced oil price. However, from 2005 onwards, the price trend of the crude oil market changed significantly. After the Katrina Hurricane gasoline prices reached a top record during September of 2005 and the oil production decreased due to several political tensions in the Middle East, until it reached a price of 117 USD per barrel in 2011.

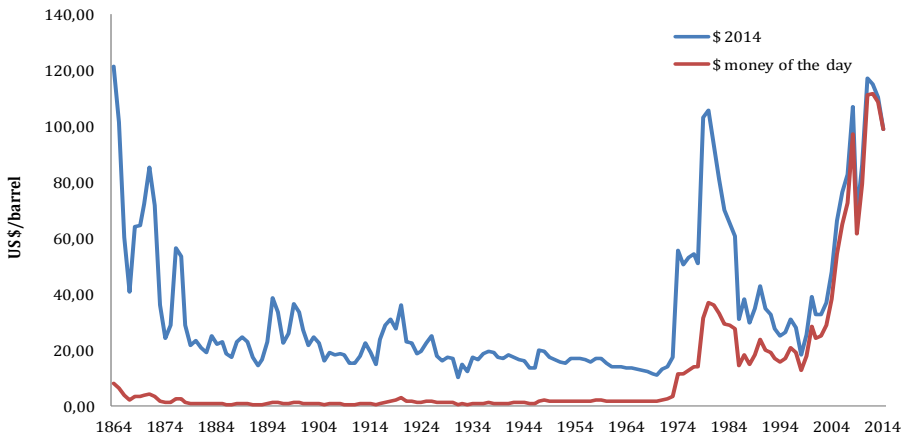


Figure 1.4. Historical evolution of crude oil prices (US \$)

Another consequence of the massive burning of fossil fuels is the environmental impact, especially the global warming caused by CO₂ emissions. Figure 1.5 suggests a discernible human influence on CO₂ emissions. The global CO₂ emissions have risen by 53.6% in the last ten years, from 23101.3 million tons in 1994 to 35498.7 million tons in 2014. With respect to 1974, the emissions have increased by 109.6%. Developing countries have the strongest influence in this increase in CO₂ emissions, being China the major contributing country, accounting for 27.5% of the global emissions in 2014 [4].

Human influence on the climate system is unquestionable due to the anthropogenic emissions of greenhouse gases. Recent climate changes have had several impacts on human and natural systems, as well as several economical consequences. The report published by the Intergovernmental Panel on Climate Change (IPCC) in 2014 points out that the globally averaged combined land and ocean surface temperature show a warming of 0.85 °C over the period 1880 to 2012. On the other hand, over the period 1901–2010, the global mean sea level increased 0.19 m [5].

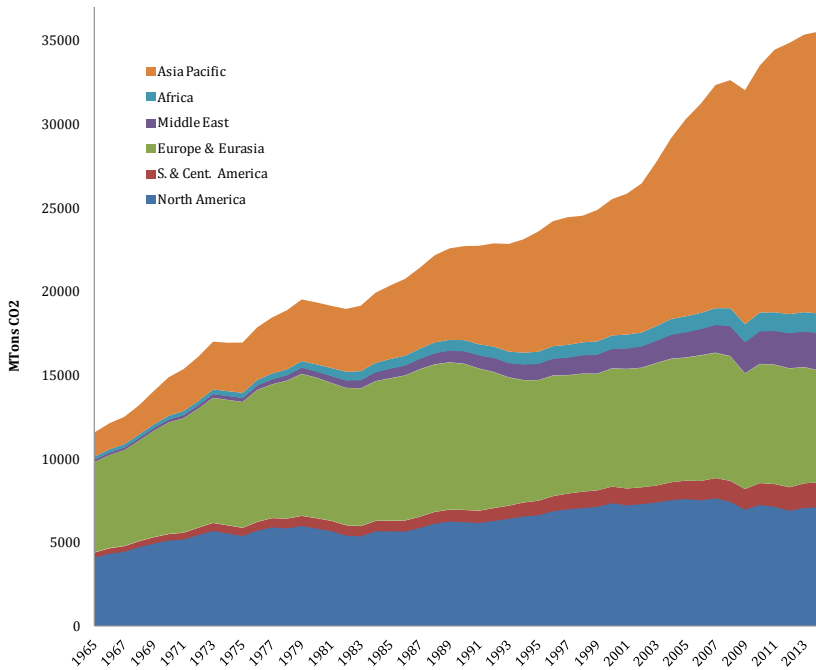


Figure 1.5. Historical evolution of CO₂ emissions (MTons) by geographic region

Global utilization of fossil fuels for energy needs is leading to critical environmental, human, political and economical concerns. This situation demands the search for alternative energy sources such as renewable energy sources.

Renewable energy sources in power generation continued to increase in 2015, reaching 2.8% of global energy consumption. Renewable power generating capacity had its largest annual increase ever in 2015, with an estimated 147 GW of renewable capacity added to the global energy capacity. The total global capacity at the end of this year was 785 GW (1849 GW including hydropower). Wind and solar photovoltaic (PV) saw record addition for the second consecutive year, together accounting for 77% of the whole renewable power capacity added in 2015. At the end of 2015 renewables constituted an estimated 28.9% of the world's power generating capacity. Figure 1.6 shows the technology distribution for renewable electric power global capacity in 2015 (not including hydropower)[6].

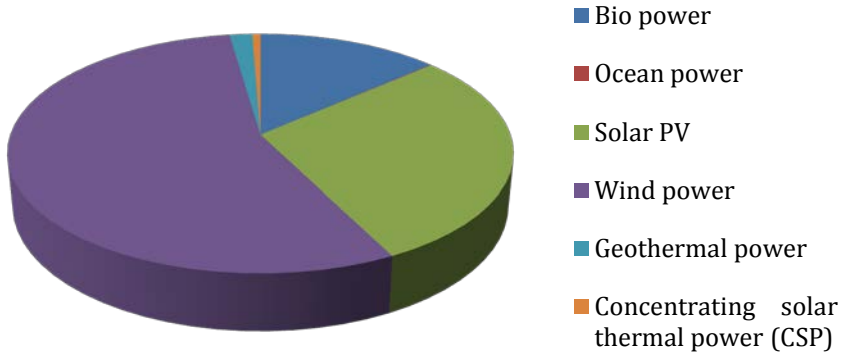


Figure 1.6. Renewable electric power global capacity

Nevertheless, it is worth mentioning that due to their intermittent character, renewable energy sources cannot be effectively used until appropriate energy storage technologies are developed. This means that it is necessary to store the energy generated by renewable technologies to use it when needed. One of the most desirable options is to convert this energy into hydrogen (renewable hydrogen production).

There are two different routes for the production of renewable hydrogen: direct and electrolytic [7]. In the electrolytic route the energy source is first converted into electricity followed by the production of hydrogen via electrolysis of water. Direct photoconversion into hydrogen can be achieved using a solar energy source through photocatalytic, photoelectrochemical, photobiological or photovoltaic technologies (figure 1.7).

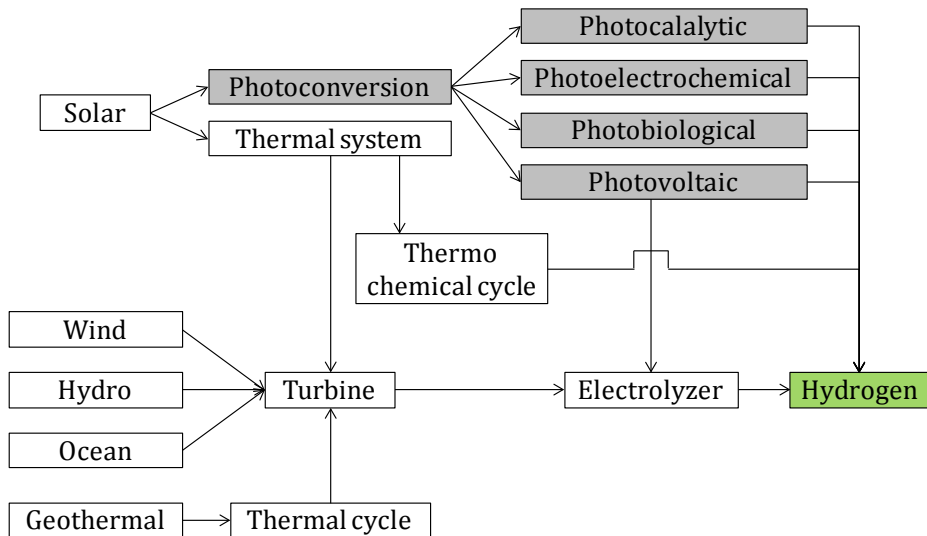


Figure 1.7. Renewable hydrogen production routes [7]

A worldwide shift from fossil fuels to renewable hydrogen technology would eliminate many of the problems associated to fossil fuels dependency [8]. As previously mentioned, hydrogen is an energy vector that is utilized to store and transport energy. Chemical energy can be transformed to electrical energy by means of electrochemical technologies such as fuel cells.

1.2. Fuel Cells

Fuel cells are electrochemical devices that convert directly chemical energy into electrical energy through oxidation and reduction reactions. There are different types of fuel cells depending on the fuel, electrolyte and operating temperature (table 1.1). However, the most studied fuel cell for transport is the Proton Exchange Membrane Fuel Cell (PEMFC) because of its adequate characteristics as fast and easy start-up and durability.

Table 1.1. Types of fuel cells

Fuel cell	AFC (Alkaline)	PEMFC (Proton exchange membrane)	PAFC (Phosphoric acid)	MCFC (Molten carbonate)	SOFC (Solid oxide)
Operating temperature (°C)	<100	60-120	160-220	600-800	500-1000
Applications	Transportation, space, military and energy storage systems		Stationary power systems	Stationary power systems and transportation	
Power	5-150 kW	5 – 250 kW	50 kW- 11 MW	100 kW – 2 MW	100 – 250 kW
Charge carrier in electrolyte	OH ⁻	H ⁺	H ⁺	CO ₃ ²⁻	O ²⁻

PEMFC typically use hydrogen as inlet fuel, which is introduced in the negative electrode (anode) where it is oxidized and dissociated into protons and electrons. In the positive electrode (cathode) oxygen is reduced and dissociated into O₂⁻. Protons pass through the proton exchange membrane (PEM) and electrons go to an external circuit generating electricity. Subsequently, electrons, protons and O₂⁻ react in the cathode forming water as the only byproduct (figure 1.8).

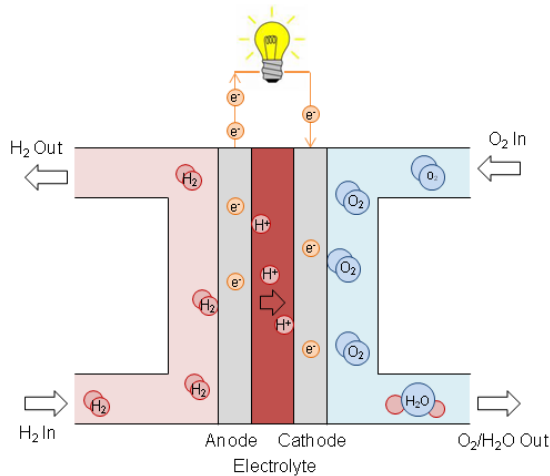


Figure 1.8. PEMFC scheme

The electrochemical reduction reaction of oxygen and the oxidation reaction of hydrogen are the following:



The core of a PEMFC is called the membrane electrode assembly (MEA) that is composed of the proton exchange membrane (PEM) placed between two electrodes. Proton exchange membranes have different functions, such as separation device of the gaseous reactants, protons transport from the anode to the cathode, to electrically insulate the electrons and as support for the catalyst [9]. Membranes must meet the following requirements to be applied in PEMFCs [10]:

- High proton conductivity
- Outstanding mechanical strength and dimensional stability
- Chemical, electrochemical and thermal stability under the operating conditions
- Low fuel and oxygen crossover
- Easy conformation to form a membrane electrode assembly (MEA)
- Competitive cost

Nafion perfluorosulfonic acid ionomer, represented in figure 1.9, is the most widely used membrane in PEMFC devices because of its excellent chemical stability, high ionic conductivity and good mechanical strength [11, 12]. However, the conductivity of Nafion drops at temperatures above 100 °C due to the evaporation of water that is critical for proton conduction.

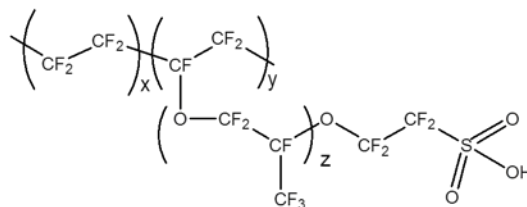


Figure 1.9. Chemical structure of Nafion

The commercial development of fuel cells has made a strong progress in recent years. The fuel cell industry grew to \$2.2 billion in 2014, up from \$1.2 billion in 2013. Moreover, more than 50000 fuel cells were shipped in 2014 (180 MW). Regards to transportation, Hyundai started in 2014 the commercial introduction of the fuel cell electric vehicle (FCEV), Toyota began FCEV sales in 2015 in the United States of America and Honda will start it in 2016. Moreover, more than 90 hydrogen fueling stations were announced worldwide [13].

Despite the fact that this technology is starting to be commercially available some technical and economic issues still need to be solved. Several authors have focused on the optimization of the stack design and the fuel cell configuration. Other aspects that require improvement include the structure and composition of the catalyst layer. For the electrolyte, many efforts have been focused to develop a PEM with high conductivity at low relative humidity. It would permit working at higher temperature helping the electrochemical process to be more efficient. Moreover, catalyst CO poisoning and water management would be avoided. Table 1.2 lists the 2020 US Department of Energy (DOE) technical targets for proton exchange membranes [14]. These targets incorporate the most important characteristics for PEMs, i.e. high conductivity, good thermal, mechanical and chemical stability, adequate durability and low cost.

Table 1.2. Targets for PEMs according to US DOE for 2020

Characteristic	Units	2015 status
Cost	\$.m ⁻²	17
Durability		
Mechanical	Cycles until >15 mA.cm ⁻² H ₂ crossover	23000
Chemical	Hours until >15 mA.cm ⁻² crossover or >20% loss in OCV	742
Maximum operating temperature	° C	120
Maximum electrical resistance	ohm.cm ²	>5600
Maximum oxygen crossover	mA.cm ⁻²	2,4
Maximum hydrogen crossover	mA.cm ⁻²	1,1
Area specific proton resistance at:		
Maximum operating temperature and water partial pressure from 40-80 kPa	ohm.cm ²	0,072 (120 °C, 40 kPa)
80 °C and water partial pressure from 25-45 kPa	ohm.cm ²	0,027 (25 kPa)
30 °C and water partial pressures up to 4 kPa	ohm.cm ²	0,027 (4 kPa)

1.3. Proton exchange membranes for PEMFCs

Conventional proton exchange membranes have been widely investigated by many researchers as electrolytes for fuel cell applications. As it was aforementioned, Nafion is the most frequent polymer in PEMFCs because of its excellent mechanical and thermal properties and outstanding conductivities when it is well hydrated. However, using Nafion is not feasible at temperatures above 80 °C because of the evaporation of water. It is indubitable that these membranes require improvements in order to achieve a real implementation of this technology. It is still necessary the development of a proton exchange membrane which satisfies all the requirements namely, proton conductivity high enough at high temperature, durability, mechanical and chemical stability and a reasonable cost. Consequently, other proton exchange membranes are being studied for fuel cells as it is shown in table 1.3 [15].

Table 1.3. Proton exchange membranes for fuel cells

Membrane	Structure	Advantages	Disadvantages
Perfluorinated membranes	-Fluorinated backbone -Fluorocarbon side chain -Ionic clusters consisting of sulfonic acid ions attached to side chains	-Excellent chemical and electrochemical stability -High proton conductivity	-Expensive -High methanol crossover -Dehydration above 80 °C
Partially fluorinated membranes	-Fluorocarbon base -Hydrocarbon aromatic side chain grafted onto the backbone or the	-Inexpensive -Low crossover -Good anti-free radical oxidation -Relatively strong compared to perfluorinated membranes	-Less durable -Low performance
Non-fluorinated membranes	-Hydrocarbon aromatic base, typically modified with polar or sulfonic groups or	-Low cost -Low crossover -Proton conductivity comparable to Nafion at a high water uptake	-High swelling -Inadequate durability
Acid-base membranes	-Incorporation of acid component into an alkaline polymer base	-High thermal, dimensional and chemical stability -Proton conductivity comparable to Nafion	-Durability
Ionic liquid membranes	-Formed from an organic cation and an organic/inorganic anion	-Tunable -High conductivity -High chemical, electrochemical and thermal stability -Non-volatile	-Difficulty constructing a solid membrane

Regarding perfluorinated membranes, several studies aim to the modification of Nafion membranes towards improving their water retention. Zeng and co-workers [16] developed Nafion membranes with silica for PEMFCs without humidification. These membranes have conductivities of approximately $1.11 \times 10^{-1} \text{ S.cm}^{-1}$ at $25 \text{ }^\circ\text{C}$, allowing an increase of approximately 30% in the fuel cell performance in comparison to unmodified Nafion membranes.

To overcome the drawbacks of perfluorinated membranes, different alternatives such as the use of partially fluorinated membranes are being studied by many authors [17-23]. This technique allows the design of new advanced materials, improving their mechanical and thermal properties relative to the individual polymers. Besides, the cost of these membranes is reduced because of the smaller amount of fluorinated polymer required due to the utilization of less expensive polymers. However, the proton conductivity can be compromised. Perfluoroalkylvinylether/polytetrafluoroethylene (PFA/PTFE) membranes were developed by Muto et al. [24]. High conductivity of $1.7 \times 10^{-1} \text{ S.cm}^{-1}$ at $60 \text{ }^\circ\text{C}$ was obtained, and peak power densities of approximately 630 mW.cm^{-2} at $60 \text{ }^\circ\text{C}$ with humidified gases were reached. However, similarly to the fluorinated membranes, these electrolytes need humidification for an optimal performance.

Non-fluorinated membranes might be alternative membranes for PEMFCs able to replace the expensive fluorinated membranes that show high fuel crossover and limited operating temperatures. However, similarly to fluorinated acid membranes, these polymers require a proton conductor for their use in fuel cell devices. Poly(arylene ether) materials are studied by many researchers because of their availability, processability, varied chemical compositions and high stability in the fuel cell environment [25-38]. Park and co-workers [39] have developed a new concept of self-humidifying membrane based on the use of a sulfonated poly(arylene ether sulfone) random polymer with a hydrophobic surface coating. The water content in this membrane is regulated through nanometre cracks located in the hydrophobic surface layer working as valves in order to retain water inside the

polymer analogous to the water retention mechanisms of the cactus plant. It has been proved that coated membranes have delayed the water desorption rate as well as enhanced fuel cell performance in comparison with uncoated membranes.

Other encouraging non-fluorinated materials as PEMs are sulphonated polyimides (SPIs) because of their excellent mechanical and thermal properties, as well as their chemical stability and low crossover [40-44]. Cross-linkable sulphonated poly(ether sulphone) showed a conductivity of $1.2 \times 10^{-1} \text{ S.cm}^{-1}$ at room temperature and power density of 900 mW.cm^{-2} at 0.6 V in a PEMFC at $70 \text{ }^\circ\text{C}$ with humidified gases [26]. SPEEK/amino-functionalised silica membranes showed $1.0 \times 10^{-1} \text{ S.cm}^{-1}$ at $120 \text{ }^\circ\text{C}$ and peak power densities of 246 mW.cm^{-2} at $120 \text{ }^\circ\text{C}$ with humidified gases [37].

Another promising alternative developed by many authors consists of blending basic polymers with strong acids. These membrane electrolytes show high proton conductivities even under non-humidified conditions. The basicity of these polymers permits the formation of hydrogen bonds with the acid. H_3PO_4 and H_2SO_4 acids show effective proton conductivity, even in their anhydrous form, due to their exceptional proton conduction mechanism; this mechanism utilises self-ionisation and self-dehydration [45, 46]. Among the basic polymers, polybenzimidazole (PBI) has received significant attention due to its excellent thermal and chemical stability [47-56]. However, high acid content results in high conductivities, but the mechanical stability is reduced. Moreover, the loss of the acid component during the operation limits the application of these membranes. PBI/ H_3PO_4 membranes were developed by Li et al. [47], showing conductivities ranging from 2.5×10^{-2} - $6.8 \times 10^{-2} \text{ S.cm}^{-1}$ at $200 \text{ }^\circ\text{C}$. These materials showed a peak power density of 1000 mW.cm^{-2} in a PEMFC at $200 \text{ }^\circ\text{C}$ without humidification.

Finally, it is worth mentioning that room temperature ionic liquids (ILs) are attracting interest as electrolytes for electrochemical applications due to their exceptional properties such as negligible volatility, non-flammability, high thermal and electrochemical stability and outstanding ionic conductivity even under anhydrous conditions.

1.4. Room temperature ionic liquids (ILs)

Room temperature ionic liquids are organic salts with melting points below or equal to room temperature. ILs are formed entirely by ions and differ from ionic solutions in that ionic liquids do not contain a solvent (figure 1.10) [15].

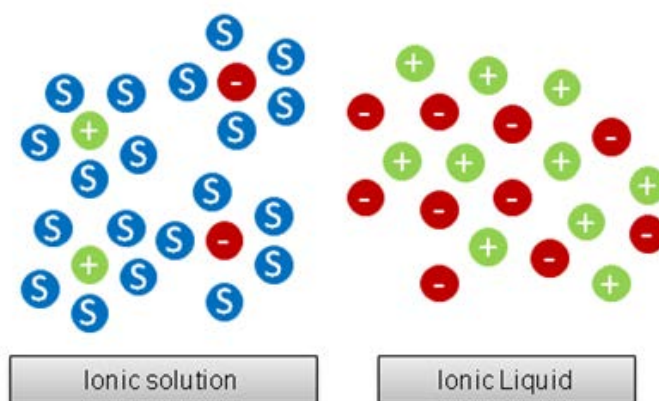


Figure 1.10. Ionic liquid vs. ionic solution

Some ions that are frequently used in ionic liquids are shown in figure 1.11. Because ionic liquids are formed entirely of ions, they can be combined to meet the desired properties for specific applications [57]. Currently, there are more than 10^3 different ionic liquids available, but it has been demonstrated that there are at least 10^6 simple ionic liquids that can be synthesized in the laboratory. There will be 10^{12} binary combinations of these and 10^{18} ternary systems possible [58-61].

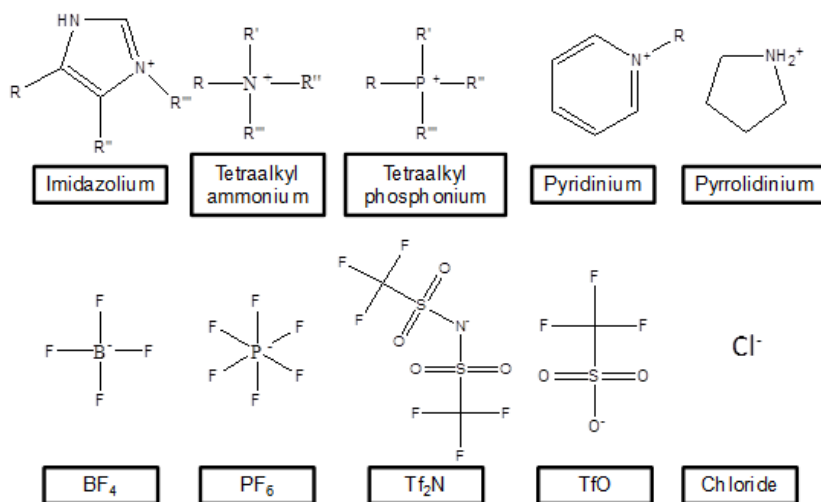


Figure 1.11. Cations and anions frequently used in ILs

The conductivities of ionic liquids at room temperature range from 1.0×10^{-4} - 1.8×10^{-2} S.cm⁻¹. Generally, conductivities of approximately 1.0×10^{-2} S.cm⁻¹ are typical of ionic liquids based on dialkyl-substituted imidazolium cations. Ionic liquids based on tetraalkylammonium, pyrrolidinium, piperidinium and pyridinium cations have lower conductivities, ranging from 1.0×10^{-4} to 5.0×10^{-3} S.cm⁻¹.

One possibility to classify these interesting compounds is into aprotic and protic ionic liquids. Protic ionic liquids can be easily obtained by a proton transfer from a Brønsted acid to a Brønsted base, leading to the presence of proton donor and acceptor sites that can be used to build a hydrogen-bonded network. A benefit of using protic ionic liquids is that cells can be operated at temperatures above 100 °C under anhydrous conditions because the proton transport is independent of the water content. The reactivity of this active and mobile proton located on the cation makes them appropriate for use as electrolytes in fuel cell applications [62]. On the other hand, aprotic ILs contain other substituent, typically alkyl groups, instead of the mobile proton located in their analogous protic ionic liquid.

To use ILs as electrolytes in PEMFCs they must be in a solid film state. One approach towards achieving this property is mixing an ordinary polymer with the ionic liquids. This technique results in an improvement of the transport properties of the polymer electrolytes because the degree of ion dissociation, concentration of ionic moieties and T_g of the membrane are modified. The mixture can be prepared by polymerising various monomers in the presence of ionic liquids or by generating a simple mixture of polymers with ionic liquids [80]. However, this technique often results in compromise between the desirable RTIL properties and the mechanical strength of the membranes [63, 64]. Another innovative technique used to generate solid polymeric electrolytes from ionic liquids is the polymerization of ionic liquids containing polymerizable groups. Polymerized ionic liquids constitute an important innovation in the field of electrolyte membranes because they can be used directly as polymeric solid membranes replacing conventional perfluorinated membranes. The tunability of ionic liquids permits the synthesis of ionic liquid polymers with different morphologies and specific properties for fuel cell applications [65-73].

Similar to ionic liquids, organic ionic plastic crystals (OIPCs) are a family of solid state electrolytes with electrochemical applications. Their negligible volatility and high thermal and electrochemical stability make them suitable solid electrolytes in many electrochemical devices, such as lithium batteries, dye-sensitised solar cells and fuel cells [74-78]. These materials have the advantages of ILs (high proton conductivity without humidification) and the benefits of a solid state electrolyte, making them promising new proton conductive electrolytes for fuel cells.

OIPCs are usually formed from a large symmetric organic cation and an inorganic anion that is normally symmetrical or has a diffusive charge. These materials have one or more solid-phase transitions before melting that are associated with the beginning of rotational or translational motions of the ions. This transition leads to a progressive transformation from an ordered crystalline phase to an increasingly disordered structure. The conductivity of these materials is attributed to the presence of defects or vacancies in the crystalline structure, the rotational and

translational disorder of the cation and anion and the conformational disorder of the ions [79]. These materials are referred to as “plastic crystals” due to their softness; they are easily deformed under stress. This deformation occurs due to the mobility of the slip planes, dislocations or vacancy migrations. These properties are beneficial for fuel cell devices because they should suffer less from any loss of contact with the electrodes due to volumetric changes [80].

1.5. Thesis scope and outline

This study focuses on the development of innovative proton exchange membranes based on ionic liquids for fuel cells without external humidification. The work covers the selection of suitable ionic liquids and describes the development, characterization and performance of different ionic liquid-based proton exchange membranes.

Chapter 2 describes the methods and equipment used in this work, including the techniques necessary for the membrane characterization. Moreover, a general description of the experimental set-up, the assembly between membrane and electrodes and the protocol for fuel cell testing are explained.

Chapter 3 reports the development of membranes based on perfluorinated polymer and protic ionic liquids for PEMFC fed with hydrogen under non-humidified conditions. The selection and synthesis of suitable ionic liquids and the development, characterization and performance of the composite membranes were described.

Chapter 4 deals with the synthesis of membranes based on polymerized ionic liquids used for the first time in this application. Two different families of ionic liquids were designed and studied for this application (triflate and sulfoethylmethacrylate anion-based ionic liquids). The synthesis of these ionic liquids, the polymerization procedure and the characterization of the membranes are explained in this chapter. Besides, triflate anion-based membranes were tested in the fuel cell set-up at different operating conditions (temperature, membrane

thickness and membrane composition through the incorporation of a non-polymerizable ionic liquid). Moreover, molecular dynamics and ions transport properties of these two membranes based on polymerized ionic liquids were studied by means of dielectric relaxation studies.

Chapter 5 describes the synthesis of membranes based on protic plastic crystals supported on polymeric nanofibers. For this purpose, a protic plastic crystal formed by an diammonium cation and triflate anion was supported on poly(vinylidene fluoride) (PVDF) nanofibers. With the aim of increasing the ionic conductivity and the fuel cell performance, the plastic crystal was doped with triflic acid and N,N-dimethylethylenediamine and its performance was compared with pure plastic crystal membranes.

Finally, chapter 6 collects the general conclusions of this thesis and an overview of the challenges and prospects for future research.

1.6. References

- [1] M. Asif, T. Muneer. Energy supply, its demand and security issues for developed and emerging economies. *Renewable Sustainable Energy Rev*, 11 (2007) 1388.
- [2] B. Dudley, BP Statistical Review of World Energy, London, 65 2016.
- [3] M. Feygin, R. Satkin. The oil reserves-to-production ratio and its proper interpretation. *Nat.Resourc.Res.*, 13 (2004) 57.
- [4] BP Statistical Review of World Energy, Data workbook. 2015.
- [5] Core Writing Team, R.K. Pachauri and L.A. Meyer, IPCC, Climate Change 2014: Synthesis Report. Contribution of Working Groups I, II and III to the Fifth Assessment Report of the Intergovernmental Panel on Climate Change, Switzerland 2016.
- [6] REN21 Secretariat, Renewables 2016. Global Status Report (2016).
- [7] T. Abbasi, S.A. Abbasi. 'Renewable' hydrogen: Prospects and challenges. *Renewable and Sustainable Energy Reviews*, 15 (2011) 3034.
- [8] M. Momirlan, T.N. Veziroglu. Current status of hydrogen energy. *Renewable Sustainable Energy Rev*, 6 (2002) 141.
- [9] H. Zhang, P.K. Shen. Recent development of polymer electrolyte membranes for fuel cells. *Chem.Rev.*, 112 (2012) 2780.
- [10] B. Smitha, S. Sridhar and A.A. Khan. Solid polymer electrolyte membranes for fuel cell applications - A review. *J.Membr.Sci.*, 259 (2005) 10.
- [11] K.M. Nouel, P.S. Fedkiw. Nafion®-based composite polymer electrolyte membranes. *Electrochim.Acta*, 43 (1998) 2381.
- [12] K. Miyatake, M. Watanabe. Recent progress in proton conducting membranes for PEFCs. *Electrochem*, 73 (2005) 12.
- [13] S. Curtin, J. Gangi, Fuel Cell Technologies Market Report, US Department of Energy, Washington D. C. 2014.

- [14] DOE technical targets for polymer electrolyte membrane fuel cell components <http://energy.gov/eere/fuelcells/doe-technical-targets-polymer-electrolyte-membrane-fuel-cell-components> 2016.
- [15] M. Díaz, A. Ortiz and I. Ortiz. Progress in the use of ionic liquids as electrolyte membranes in fuel cells. *J.Membr.Sci.*, 469 (2014) 379.
- [16] R. Zeng, Y. Wang, S. Wang and P.K. Shen. Homogeneous synthesis of PFSI/silica composite membranes for PEMFC operating at low humidity. *Electrochim.Acta*, 52 (2007) 3895.
- [17] L. Gubler, H. Kuhn, T.J. Schmidt, G.G. Scherer, H. Brack and K. Simbeck. Performance and Durability of Membrane Electrode Assemblies Based on Radiation-Grafted FEP-g-Polystyrene Membranes. *Fuel Cells*, 4 (2004) 196.
- [18] S.J. Peighambardoust, S. Rowshanzamir and M. Amjadi. Review of the proton exchange membranes for fuel cell applications. *Int J Hydrogen Energy*, 35 (2010) 9349.
- [19] D.S. Kim, Y.S. Kim, M.D. Guiver, J. Ding and B.S. Pivovar. Highly fluorinated comb-shaped copolymer as proton exchange membranes (PEMs): Fuel cell performance. *J.Power Sources*, 182 (2008) 100.
- [20] T. Sancho, J. Soler and M.P. Pina. Conductivity in zeolite-polymer composite membranes for PEMFCs. *J.Power Sources*, 169 (2007) 92.
- [21] E. Quartarone, A. Carollo, C. Tomasi, F. Belotti, S. Grandi, P. Mustarelli et al. Relationships between microstructure and transport properties of proton-conducting porous PVDF membranes. *J.Power Sources*, 168 (2007) 126.
- [22] A. Martinelli, A. Matic, P. Jacobsson, L. Börjesson, A. Fernicola, S. Panero et al. Physical properties of proton conducting membranes based on a protic ionic liquid. *J Phys Chem B*, 111 (2007) 12462.
- [23] F. Niepceron, B. Lafitte, H. Galiano, J. Bigarré, E. Nicol and J. Tassin. Composite fuel cell membranes based on an inert polymer matrix and proton-conducting hybrid silica particles. *J.Membr.Sci.*, 338 (2009) 100.
- [24] F. Muto, A. Oshima, T. Kakigi, N. Mitani, A. Matsuura, K. Fujii et al. Synthesis and characterization of PEFC membranes based on fluorinated-polymer-alloy using pre-soft-EB grafting method. *Nucl Instrum Methods Phys Res Sect B*, 265 (2007) 162.

- [25] M.A. Hickner, H. Ghassemi, Y.S. Kim, B.R. Einsla and J.E. McGrath. Alternative polymer systems for proton exchange membranes (PEMs). *Chem.Rev.*, 104 (2004) 4587.
- [26] K. Heo, H. Lee, H. Kim, B. Kim, S. Lee, E. Cho et al. Synthesis and characterization of cross-linked poly(ether sulfone) for a fuel cell membrane. *J.Power Sources*, 172 (2007) 215.
- [27] B. Bonnet, D.J. Jones, J. Rozière, L. Tchicaya, G. Alberti, M. Casciola et al. Hybrid organic-inorganic membranes for a medium temperature fuel cell. *J.New Mater.Electrochem.Syst.*, 3 (2000) 87.
- [28] S.M.J. Zaidi, S.D. Mikhailenko, G.P. Robertson, M.D. Guiver and S. Kaliaguine. Proton conducting composite membranes from polyether ether ketone and heteropolyacids for fuel cell applications. *J.Membr.Sci.*, 173 (2000) 17.
- [29] H. Cai, K. Shao, S. Zhong, C. Zhao, G. Zhang, X. Li et al. Properties of composite membranes based on sulfonated poly(ether ether ketone)s (SPEEK)/phenoxy resin (PHR) for direct methanol fuel cells usages. *J.Membr.Sci.*, 297 (2007) 162.
- [30] T. Yang. Composite membrane of sulfonated poly(ether ether ketone) and sulfated poly(vinyl alcohol) for use in direct methanol fuel cells. *J.Membr.Sci.*, 342 (2009) 221.
- [31] K.D. Kreuer. On the development of proton conducting polymer membranes for hydrogen and methanol fuel cells. *J.Membr.Sci.*, 185 (2001) 29.
- [32] J. Wang, Z. Yue and J. Economy. Preparation of proton-conducting composite membranes from sulfonated poly(ether ether ketone) and polyacrylonitrile. *J.Membr.Sci.*, 291 (2007) 210.
- [33] H.R. Allcock, M.A. Hofmann, C.M. Ambler, S.N. Lvov, X.Y. Zhou, E. Chalkova et al. Phenyl phosphonic acid functionalized poly[aryloxyphosphazenes] as proton-conducting membranes for direct methanol fuel cells. *J.Membr.Sci.*, 201 (2002) 47.
- [34] X. Yu, A. Roy, S. Dunn, A.S. Badami, J. Yang, A.S. Good et al. Synthesis and characterization of sulfonated-fluorinated, hydrophilic-hydrophobic multiblock copolymers for proton exchange membranes. *J.Polym.Sci.Part A*, 47 (2009) 1038.
- [35] G. Alberti, M. Casciola, L. Massinelli and B. Bauer. Polymeric proton conducting membranes for medium temperature fuel cells (110–160°C). *J.Membr.Sci.*, 185 (2001) 73.

- [36] I. Colicchio, F. Wen, H. Keul, U. Simon and M. Moeller. Sulfonated poly(ether ether ketone)-silica membranes doped with phosphotungstic acid. Morphology and proton conductivity. *J.Membr.Sci.*, 326 (2009) 45.
- [37] A. Carbone, R. Pedicini, A. Saccà, I. Gatto and E. Passalacqua. Composite S-PEEK membranes for medium temperature polymer electrolyte fuel cells. *J.Power Sources*, 178 (2008) 661.
- [38] W. Li, A. Manthiram and M.D. Guiver. Acid-base blend membranes consisting of sulfonated poly(ether ether ketone) and 5-amino-benzotriazole tethered polysulfone for DMFC. *J.Membr.Sci.*, 362 (2010) 289.
- [39] C.H. Park, S.Y. Lee, D.S. Hwang, D.W. Shin, D.H. Cho, K.H. Lee et al. Nanocrack-regulated self-humidifying membranes. *Nature*, 532 (2016) 480.
- [40] Y. Li, R. Jin, Z. Cui, Z. Wang, W. Xing, X. Qiu et al. Synthesis and characterization of novel sulfonated polyimides from 1,4-bis(4-aminophenoxy)-naphthyl-2,7-disulfonic acid. *Polymer*, 48 (2007) 2280.
- [41] H. Bai, W.S.W. Ho. New poly(ethylene oxide) soft segment-containing sulfonated polyimide copolymers for high temperature proton-exchange membrane fuel cells. *J.Membr.Sci.*, 313 (2008) 75.
- [42] Z. Hu, Y. Yin, K. Okamoto, Y. Moriyama and A. Morikawa. Synthesis and characterization of sulfonated polyimides derived from 2,2'-bis(4-sulfophenyl)-4,4'-oxydianiline as polymer electrolyte membranes for fuel cell applications. *J.Membr.Sci.*, 329 (2009) 146.
- [43] J. Yan, C. Liu, Z. Wang, W. Xing and M. Ding. Water resistant sulfonated polyimides based on 4,4'-binaphthyl-1,1',8,8'-tetracarboxylic dianhydride (BNTDA) for proton exchange membranes. *Polymer*, 48 (2007) 6210.
- [44] H. Bai, W.S.W. Ho. Recent developments in fuel-processing and proton-exchange membranes for fuel cells. *Polym.Int.*, 60 (2011) 26.
- [45] J.S. Lee, N.D. Quan, J.M. Hwang, S.D. Lee, H. Kim, H. Lee et al. Polymer electrolyte membranes for fuel cells. *J.Ind.Eng.Chem.*, 12 (2006) 175.
- [46] S.M.J. Zaidi, S.F. Chen, S.D. Mikhailenko and S. Kaliaguine. Proton conducting membranes based on polyoxadiazoles. *J.New Mater.Electrochem.Syst.*, 3 (2000) 27.

[47] Q. Li, R. He, J.O. Jensen and N.J. Bjerrum. PBI-based polymer membranes for high temperature fuel cells - Preparation, characterization and fuel cell demonstration. *Fuel Cells*, 4 (2004) 147.

[48] H.L. Lin, Y.S. Hsieh, C.W. Chiu, T.L. Yu and L.C. Chen. Durability and stability test of proton exchange membrane fuel cells prepared from polybenzimidazole/poly(tetrafluoro ethylene) composite membrane. *J.Power Sources*, 193 (2009) 170.

[49] L. Jörissen, V. Gogel, J. Kerres and J. Garche. New membranes for direct methanol fuel cells. *J.Power Sources*, 105 (2002) 267.

[50] Y. Zhai, H. Zhang, Y. Zhang and D. Xing. A novel H₃PO₄/Nafion-PBI composite membrane for enhanced durability of high temperature PEM fuel cells. *J.Power Sources*, 169 (2007) 259.

[51] V. Deimede, G.A. Voyiatzis, J.K. Kallitsis, L. Qingfeng and N.J. Bjerrum. Miscibility behavior of polybenzimidazole/sulfonated polysulfone blends for use in fuel cell applications. *Macromolecules*, 33 (2000) 7609.

[52] C. Hasiotis, L. Qingfeng, V. Deimede, J.K. Kallitsis, C.G. Kontoyannis and N.J. Bjerrum. Development and Characterization of Acid-Doped Polybenzimidazole/Sulfonated Polysulfone Blend Polymer Electrolytes for Fuel Cells. *J.Electrochem.Soc.*, 148 (2001).

[53] Q. Li, R. He, J.O. Jensen and N.J. Bjerrum. Approaches and Recent Development of Polymer Electrolyte Membranes for Fuel Cells Operating above 100 °C. *Chem.Mater.*, 15 (2003) 4896.

[54] J. Kerres, A. Ullrich, T. Häring, M. Baldauf, U. Gebhardt and W. Preidel. Preparation, characterization and fuel cell application of new acid-base blend membranes. *J.New Mater.Electrochem.Syst.*, 3 (2000) 229.

[55] M. Li, Z. Shao and K. Scott. A high conductivity Cs_{2.5}H_{0.5}PMo₁₂O₄₀/polybenzimidazole (PBI)/H₃PO₄ composite membrane for proton-exchange membrane fuel cells operating at high temperature. *J.Power Sources*, 183 (2008) 69.

[56] J. Wang, R.F. Savinell, J. Wainright, M. Litt and H. Yu. A H₂/O₂ fuel cell using acid doped polybenzimidazole as polymer electrolyte. *Electrochim.Acta*, 41 (1996) 193.

- [57] A. Ortiz, A. Ruiz, D. Gorri and I. Ortiz. Room temperature ionic liquid with silver salt as efficient reaction media for propylene/propane separation: Absorption equilibrium. *Sep.Purif.Technol.*, 63 (2008) 311.
- [58] M.J. Earle, K.R. Seddon. Ionic liquids. Green solvents for the future. *Pure Appl.Chem.*, 72 (2000) 1391.
- [59] J.F. Brennecke, E.J. Maginn. Ionic liquids: Innovative fluids for chemical processing. *AIChE J.*, 47 (2001) 2384.
- [60] R.D. Rogers, K.R. Seddon. Ionic Liquids - Solvents of the Future? *Science*, 302 (2003) 792.
- [61] G.W. Meindersma, M. Maase and A.B. De Haan, Ionic liquids, in Anonymous , *Ullman's Encyclopedia of Industrial Chemistry*, Wiley-VCH, 2007.
- [62] A. Fericola, B. Scrosati and H. Ohno. Potentialities of ionic liquids as new electrolyte media in advanced electrochemical devices. *Ionics*, 12 (2006) 95.
- [63] J. Le Bideau, L. Viau and A. Vioux. Ionogels, ionic liquid based hybrid materials. *Chem.Soc.Rev.*, 40 (2011) 907.
- [64] T. Yasuda, S. Nakamura, Y. Honda, K. Kinugawa, S. Lee and M. Watanabe. Effects of polymer structure on properties of sulfonated polyimide/protic ionic liquid composite membranes for nonhumidified fuel cell applications. *ACS Appl.Mater.Interfaces*, 4 (2012) 1783.
- [65] M. V. M. de Yuso, M.T. Cuberes, V. Romero, L. Neves, I. Coelho, J.G. Crespo et al. Modification of a Nafion membrane by n-dodecyltrimethylammonium cation inclusion for potential application in DMFC. *Int J Hydrogen Energy*, 39 (2014) 4023.
- [66] M. Díaz, A. Ortiz, M. Vilas, E. Tojo and I. Ortiz. Performance of PEMFC with new polyvinyl-ionic liquids based membranes as electrolytes. *Int J Hydrogen Energy*, 39 (2014) 3970.
- [67] J.S. Lee, T. Nohira and R. Hagiwara. Novel composite electrolyte membranes consisting of fluorohydrogenate ionic liquid and polymers for the unhumidified intermediate temperature fuel cell. *J.Power Sources*, 171 (2007) 535.
- [68] P.R. Jothi, S. Dharmalingam. An efficient proton conducting electrolyte membrane for high temperature fuel cell in aqueous-free medium. *J.Membr.Sci.*, 450 (2014) 389.

- [69] T. Yasuda, M. Watanabe. Protic ionic liquids: Fuel cell applications. *MRS Bull*, 38 (2013) 560.
- [70] H. Nakajima, H. Ohno. Preparation of thermally stable polymer electrolytes from imidazolium-type ionic liquid derivatives. *Polymer*, 46 (2005) 11499.
- [71] M. Yoshizawa, W. Ogihara and H. Ohno. Novel polymer electrolytes prepared by copolymerization of ionic liquid monomers. *Polym.Adv.Technol.*, 13 (2002) 589.
- [72] S. Washiro, M. Yoshizawa, H. Nakajima and H. Ohno. Highly ion conductive flexible films composed of network polymers based on polymerizable ionic liquids. *Polymer*, 45 (2004) 1577.
- [73] H. Ohno, M. Yoshizawa and W. Ogihara. Development of new class of ion conductive polymers based on ionic liquids. *Electrochim.Acta*, 50 (2004) 255.
- [74] J. Chen, T. Peng, K. Fan, R. Li and J. Xia. Optimization of plastic crystal ionic liquid electrolyte for solid-state dye-sensitized solar cell. *Electrochim.Acta*, 94 (2013) 1.
- [75] M. Anouti, L. Timperman, M. El Hilali, A. Boisset and H. Galiano. Sulfonium bis(trifluorosulfonimide) plastic crystal ionic liquid as an electrolyte at elevated temperature for high-energy supercapacitors. *J.Phys.Chem.C*, 116 (2012) 9412.
- [76] Q. Li, J. Zhao, B. Sun, B. Lin, L. Qiu, Y. Zhang et al. High-temperature solid-state dye-sensitized solar cells based on organic ionic plastic crystal electrolytes. *Adv Mater*, 24 (2012) 945.
- [77] J. Sunarso, Y. Shekibi, J. Efthimiadis, L. Jin, J.M. Pringle, A.F. Hollenkamp et al. Optimising organic ionic plastic crystal electrolyte for all solid-state and higher than ambient temperature lithium batteries. *J.Solid State Electrochem.*, 16 (2012) 1841.
- [78] C. Shi, L. Qiu, X. Chen, H. Zhang, L. Wang and F. Yan. Silica nanoparticle doped organic ionic plastic crystal electrolytes for highly efficient solid-state dye-sensitized solar cells. *ACS Appl.Mater.Interfaces*, 5 (2013) 1453.
- [79] J.M. Pringle. Recent progress in the development and use of organic ionic plastic crystal electrolytes. *Phys.Chem.Chem.Phys.*, 15 (2013) 1339.
- [80] U.A. Rana, M. Forsyth, D.R. Macfarlane and J.M. Pringle. Toward protic ionic liquid and organic ionic plastic crystal electrolytes for fuel cells. *Electrochim.Acta*, 84 (2012) 213.

Chapter 2

METHODS AND EQUIPMENT

Abstract

This chapter deals with the methods and equipment used in this work. The fundamentals of the techniques used for the membrane characterization are thoroughly explained. Moreover, a description of the experimental set-up, including the membrane-electrodes assembly and the protocol for fuel cell testing are included in this section.

2.1. Characterization techniques

2.1.1. Electrochemical Impedance Spectroscopy (EIS)

There are several methods for diagnosing and analyzing PEM fuel cells. Electrochemical impedance spectroscopy (EIS) is a suitable and powerful diagnostic testing method for fuel cells because it is non-destructive and provides useful information about the fuel cell performance and its components without perturbing the system from equilibrium [1-4]. This technique has the following advantages [5]:

- It provides microscopic information about the electrochemical system
- It allows modeling the system through an equivalent circuit
- It differentiates the individual contributions of each fuel cell component to the overall performance and each internal process

Due to the versatile capabilities of EIS, it has been applied for the optimization of the membrane electrode assembly structure and operation conditions, for the study of the effects of contaminants on the fuel cell as well as to measure the membrane resistance.

The EIS technique is used to measure the frequency dependence of the impedance of a fuel cell by applying a small sinusoidal AC potential (or current) as a perturbation signal to the fuel cell and measuring the current (or potential) response [6]. The response to this potential will be a sinusoid at the same frequency but shifted in phase.

The excitation signal expressed as a function of time is [7]:

$$E_t = E_0 \sin(\omega t) \quad (2.1)$$

E_t is the potential at time t , E_0 is the amplitude of the signal and ω is the radial frequency. ω and the frequency f are related by the following equation:

$$\omega = 2\pi f \quad (2.2)$$

In a linear system the response signal I_t is shifted in phase (φ) and has a different amplitude I_0

$$I_t = I_0 \sin(\omega t + \varphi) \quad (2.3)$$

An expression analogous to the Ohm's Law allows us to calculate the impedance of the system as:

$$Z = \frac{E_t}{I_t} = \frac{E_0 \sin(\omega t)}{I_0 \sin(\omega t + \varphi)} \quad (2.4)$$

As a result, the impedance is expressed in terms of a magnitude Z_0 and a phase shift φ .

With Euler's relationship:

$$\exp(j\varphi) = \cos \varphi + j \sin \varphi \quad (2.5)$$

It is possible to express the impedance as a complex function. The potential and the current response are described as:

$$E_t = E_0 \exp(j\omega t) \quad (2.6)$$

$$I_t = I_0 \exp(j\omega t - \varphi) \quad (2.7)$$

The impedance is represented by a complex number:

$$Z(\varphi) = \frac{E}{I} = Z_0 \exp(j\varphi) = Z_0(\cos \varphi + j \sin \varphi) \quad (2.8)$$

The two most common graphics to represent the EIS data are the Bode and Nyquist plots [8]. In the Bode graphic the impedance is plotted with log frequency on the X-axis and both the absolute values of the impedance and the phase-shift on the Y-axis. In the Nyquist plot the real part is plotted on the X-axis and the imaginary part is plotted on the Y-axis.

As it was aforementioned, EIS technique has the capacity to determine the contribution of each individual component to the overall fuel cell performance and the internal processes associated with charge transfer and mass transport [9, 10].

In the low frequency range of the spectra, for frequencies lower than 3 Hz, the mass transport process can be observed. This diffusion process is related to an oxygen concentration gradient in the cathode, including the gas diffusion layer and gas channel. The frequency range between 3 Hz to 1 kHz is controlled by the charge transfer reaction at the electrodes. The high frequency range of the spectrum, where the impedance passes through a minimum, is determined by the electrolyte resistance as it can be observed in figure 2.1.

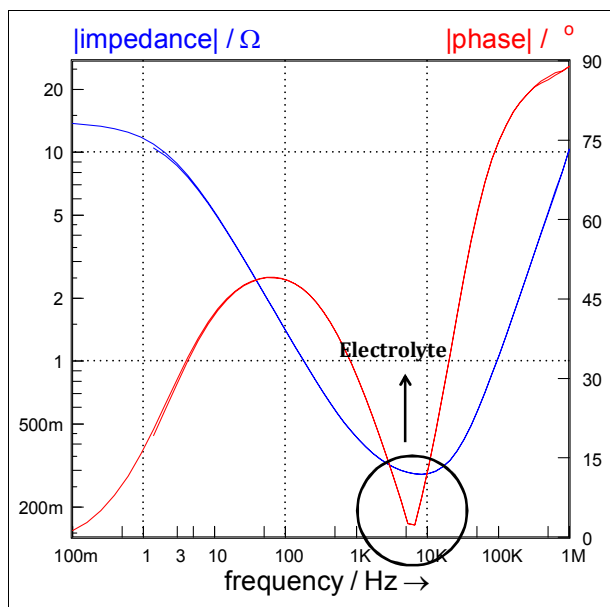


Figure 2.1. Electrolyte resistance (Bode plot)

In this work, electrochemical impedance spectroscopy was used to measure the ionic resistance exerted by ionic liquid-based membranes using the electrochemical station Zennium (Zahner). All impedance measurements were performed in potentiostatic mode with amplitude of 10 mV in a frequency range of 1 Hz to 1MHz.

The data were collected and analyzed with the “Thales” software from Zahner and presented in the Bode plot.

The Ionic conductivity was calculated with the equation:

$$\sigma = \frac{L}{R \cdot A} \quad (2.9)$$

where σ is the ionic conductivity ($\text{S}\cdot\text{cm}^{-1}$), L is the thickness of the membrane (cm), A is the active area (cm^2) and R is the membrane resistance (ohm) obtained from the EIS analysis.

Two different procedures were designed and carried out: *in-situ* and *ex-situ* measurements. *In-situ* measurements were performed following the procedure reported by Wagner et al.[10]. Impedance spectra reported were measured between the fuel cell cathode (working and sense electrode) and anode (counter and reference electrode). The anode was used as reference and as counter electrode, which is very stable and has negligible overpotential compared to the cathode. Before each experiment, the cell was prepolarized for at least 15 min at the measuring voltage to reach the steady-state operation [11].

Ex-situ procedure was selected to avoid the influence of the water produced during the fuel cell reactions on the ionic conductivity. To achieve this, ionic conductivity measurements were performed not during fuel cell tests but in an external homemade cell specifically designed to this aim, which is a modification of a conductivity cell reported in literature [12]. The design of the ionic conductivity cell is shown in figure 2.2.



Figure 2.2. Homemade conductivity cell

A stainless steel rod ($\frac{1}{2}$ " diameter, 3" long) ended by a thinner stainless steel rod (3mm diameter, 2 cm long) is fitted with a Swagelok ferrule (Swagelok SS-810-SET) and inserted into a $\frac{1}{2}$ " perfluoroalkoxy (PFA) union (Swagelok PFA-820-6). Inside the union a spring (Barnes Group, A480-029-062) is placed between the stainless steel rod and a stainless steel spacer ($\frac{1}{2}$ " diameter, 0.01" thickness). Another stainless steel rod fitted with the Swagelok ferrule is inserted into the other end of the union. The electrolyte is located between the spacer and the rod.

2.1.2. Broadband dielectric spectroscopy (BDS)

The broadband dielectric spectroscopy (BDS) is a very powerful experimental tool for understanding the molecular level dynamics in ion-containing liquids and polymers [13-16]. This technique allows the measurement of the dielectric response over 12 decades of frequency at different temperatures giving a valuable insight into molecular mobility of a polymerized ionic liquid, below as well as above its glass transition temperature (T_g)[17]. Additionally, dielectric measurements allow recognition of the type of the charge transport mechanism in ionic conductors. Namely, if conductivity of a system is controlled by the fast proton hopping through the H-bond network (Grotthuss mechanism), close to the liquid-glass transition region the examined ionic material exhibits decoupling of ionic conductivity from

the structural relaxation [18]. It means that the ionic motions are still very fast when the structural relaxation becomes frozen. This specific separation between the time scale of charge and mass diffusion in the vicinity of T_g is manifested by the characteristic crossover of the temperature dependence of conductivity (σ_{dc}) or conductivity relaxation times (τ_σ) at τ_σ faster than 10^2 s from the Vogel-Fulcher-Tammann-like (equation 2.10) at $T > T_g$ to Arrhenius behavior (equation 2.11) at $T < T_g$ [19-21].

$$\sigma = \sigma_0 \exp \left[\frac{-E_a^{VFT}}{T - T_0} \right] \quad (2.10)$$

$$\sigma = \sigma_0 \exp \left[\frac{-E_a}{K \cdot T} \right] \quad (2.11)$$

Generally, dielectric spectra can be presented in three frequency dependent complex quantities: the complex permittivity $\varepsilon^*(f) = \varepsilon'(f) - i\varepsilon''(f)$, the complex conductivity $\sigma^*(f) = \sigma'(f) + i\sigma''(f)$ and the complex electric modulus $M^*(f) = M'(f) + iM''(f)$, which are related to each other by the following equation:

$$M^*(f) = \frac{1}{\varepsilon^*(f)} = \frac{i2\pi f \varepsilon_0}{\sigma^*(f)} \quad (2.12)$$

It should be noted that all these representations emphasize different facets of the same process. Therefore, details that are not readily evident from one approach can be discriminated from the spectra in the other two representations.

To better visualize the differences between $M^*(f)$, $\sigma^*(f)$, and $\varepsilon^*(f)$ formalisms, a representative BDS spectrum of polymerized ionic liquid measured at 238 K is shown in all three representations in figure 2.3. The imaginary part of the complex modulus takes the form of a well-pronounced peak, called a conductivity relaxation peak, in contrast to the $\varepsilon''(f)$ function that suddenly increases with a decreasing frequency. On the other hand, the real part of the complex conductivity is characterized, on the low frequency side, by a plateau (the value of which directly yields the dc conductivity, σ_{dc}). In this context, it noteworthy that the dc-

conductivity, usually defined as the product of the number of ions and their mobility, is inversely proportional to the conductivity relaxation time τ_σ (or τ_M) determined from the frequency of M'' peak maximum $\tau_M = \frac{1}{2\pi f_M}$ [22].

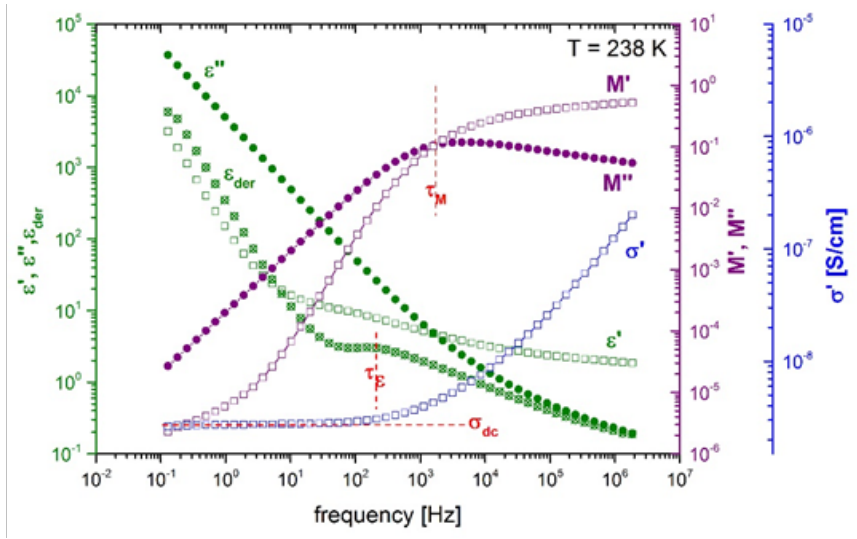


Figure 2.3. Dielectric relaxation spectrum at 238 K for polymerized ionic liquid presented in three equivalent representations: electric modulus, dielectric permittivity and conductivity

In this work, ambient pressure dielectric measurements were performed for the protic ionic liquid monomer 1-(4-sulfobutyl) 3-vinylimidazolium trifluoromethanesulfonate ([HSO₃-BVIIm][TfO]) and its polymer counterpart. Dielectric measurements under high pressure conditions were carried out for a membrane based on the two polymerizable protic ionic liquids 1-(4-sulfobutyl)-3-methylimidazolium 2-sulfoethylmethacrylate [HSO₃-BMIm][SEM] and 1-(4-sulfobutyl) 3-vinylimidazolium 2-sulfoethylmethacrylate [HSO₃-BVIIm][SEM] (50 wt%). The measurements were performed over a wide frequency range from 10⁻¹ to 10⁶ Hz using a Novo-Control GMBH Alpha dielectric spectrometer. For the isobaric measurements, the sample was placed between two stainless steel electrodes of the capacitor. The dielectric spectra were collected in a wide temperature range from 153 to 373 K. The temperature was controlled by the Novo-Control Quattro system,

with the use of a nitrogen gas cryostat. Temperature stability was better than 0.1 K. For the pressure dependent dielectric measurements the capacitor filled with the studied samples was placed in the high-pressure chamber and compressed using the silicone oil. Pressure was measured by the Nova Swiss tensiometric pressure meter with a resolution of 0.1 MPa. The temperature was controlled within 0.1 K by means of a liquid flow provided by a Weiss fridge.

2.1.3. Thermogravimetric analysis (TGA)

Thermogravimetric analysis is a technique in which the mass of a substance is monitored as a function of temperature or time in a controlled atmosphere [23]. The measurements are used primarily to determine the thermal and/or oxidative stabilities of materials as well as their compositional properties. The technique can analyze materials that exhibit either mass loss or gain due to decomposition, oxidation or loss of volatile components such as water content [24-28]. It is especially useful to characterize the behavior of polymeric materials, including thermoplastics, thermosets, elastomers, composites, films, fibers, coatings and paints [29].

In this work, special attention has been given to the degradation temperature and the water content (W_c) of the samples. W_c of polymeric membranes was determined by the weight difference between the initial weight of the membrane at room temperature and the weight of the membrane at 150 °C. On the other hand, the degradation temperature used in this work was the onset temperature (T_o) that denotes the temperature at which the weight loss begins. T_o is calculated as the temperature at the intersection of the extrapolated base line with the tangent to the curve taken at the point of maximum slope (figure 2.4)[11].

For this purpose, thermogravimetric analysis was carried out using a TGA-60H Shimadzu thermobalance under nitrogen atmosphere at temperatures ranging from room temperature to 500 °C with a heating rate of 10 °C.min⁻¹.

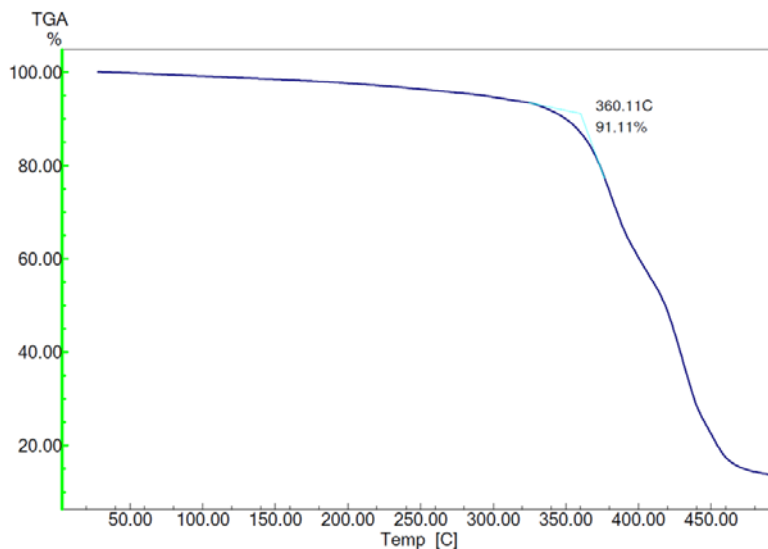


Figure 2.4. TGA curve. T_o example

2.1.4. Karl-Fischer titration

Karl-Fischer titration allows to determine the water content of a sample by adding an iodine solution as reagent until the following reaction is completed [30]:



In coulometric Karl-Fischer titration, iodine (I₂) is generated electrochemically from iodide (I⁻). When iodine comes in contact with the water in the sample, water is titrated according to equation 2.13. The amount of water in the sample is calculated by measuring the electric current needed for the electrochemical generation of iodine from iodide.

To determine the endpoint of the titration bivalentametric indication was used [31]. Using this indicator, a small current is applied between the electrodes and the voltage required to maintain this current is measured. The voltage required to maintain the current is of the order of 100 mV as long as an excess of water is

present in the sample. When the endpoint of the titration is reached, free iodine is available in the solution and the voltage drops to less than 100 mV.

In this work, the water content of ionic liquid samples was determined by Karl Fischer coulometer (Metrohm 899) employing Coulomat AG (Sigma Aldrich) as an analyte solution.

2.1.5. Differential Scanning Calorimetry (DSC)

Differential scanning calorimetry is a thermoanalytical technique in which the difference in the amount of heat required to increase the temperature of a sample and a reference sample is measured as a function of temperature. Whether less or more heat must be added to the sample depends on whether the process is exothermic or endothermic. DSC is a powerful technique to study phase transitions, such as melting, glass transitions or exothermic decompositions (figure 2.5). The result of a DSC experiment is a curve of heat flux versus temperature or versus time [32, 33].

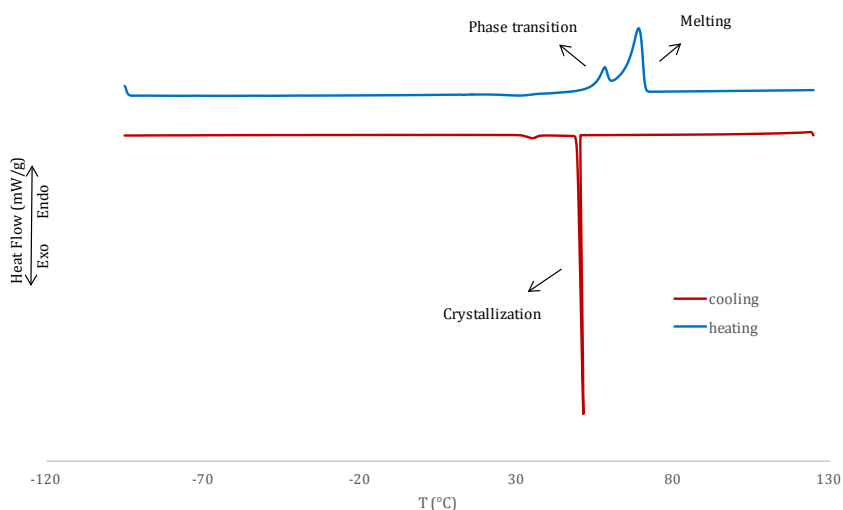


Figure 2.5. Example DSC thermal traces

In this work, DSC technique was used for determining the melting point and solid-solid phase transition of the plastic crystal N-N-dimethylethylene diammonium triflate ([DMEDAH][TFO]). A Mettler Toledo differential scanning calorimeter was used for thermal analysis between -95 °C to 120 °C at a heating rate of 5 °C.min⁻¹ and a cooling rate of -2 °C.min⁻¹. The reported traces are for the heating step. All sample preparation and sealing of the pans was conducted inside an argon glove box.

Glass transition temperature of triflate anion-based polymeric membranes was measured in a TA Instruments Q2000. The samples were first heated to 150 °C with a heating rate of 10 °C.min⁻¹ and kept isothermal for 5 min. The samples were then cooled down to -75 °C with a cooling rate of 10 °C.min⁻¹ and kept isothermal for 5 min. Second run heating cycles were taken and analyzed for the detection of the glass transition temperature of the polymers.

Using a stochastic temperature-modulated differential scanning calorimetry (TMDS) technique implemented by Mettler-Toledo, the dynamic behavior of the glass-liquid transition of the polymerized ionic liquids was analyzed in the frequency range from 4 mHz to 40 mHz in a single measurement at a heating rate of 0.5 K.min⁻¹. In these experiments, the temperature amplitude of the pulses of 0.5 K was selected. The calorimetric segmental relaxation times $\tau_{\alpha} = 1/2\pi f$ were determined from the temperature dependence of the real part of the complex heat capacity $C_p'(T)$ obtained at different frequencies in the glass transition region. The glass transition temperature T_g was determined for each frequency as the temperature at half the step height of $C_p'(T)$ [13].

2.1.6. Attenuated Total Reflection Fourier Transform Infrared Spectroscopy (ATR-FTIR)

Fourier Transform-Infrared Spectroscopy (FTIR) is an analytical technique used to identify chemical compounds. The spectrum is obtained by passing IR radiation through a sample and determining what fraction of the incident radiation is

absorbed at a particular energy. The energy at which any peak in an absorption spectrum appears corresponds to the frequency of a vibration of a part of a sample molecule. FTIR is an effective analytical instrument to detect functional groups and characterize covalent bonding information [34]. Among the FTIR techniques, Attenuated Total Reflection mode has the advantage to manage a wide variety of solid and liquid samples without a complex sample preparation [35].

In this work, polymeric samples were analyzed by Attenuated Total Reflection Fourier Transform Infrared Spectroscopy (ATR-FTIR) to confirm the success of the photopolymerization by the disappearance of the peaks or bands corresponding to the polymerizable groups. Spectra were recorded on Bruker ALPHA-P equipment from 350 cm^{-1} to 4000 cm^{-1} with a resolution of 2 cm^{-1} [11].

2.2. Experimental

2.2.1. Set-up general description

The experimental setup used for testing the fuel cell performance of the ionic liquid-based membranes is represented in figure 2.6. The core of the experimental system is the PEMFC. The cell has 5 cm^2 of active area containing serpentine channels and equipped with a pneumatic actuator that ensures good contact pressure between the internal components of the cell (quick CONNECT, Baltic Fuel Cells GmbH)[11, 36, 37]. Moreover, the cell is connected to a temperature controller. The anode is fed with pure hydrogen (99.99%) while the cathode is fed with air. Flow rates are measured by Bronkhorst High-Tech gas flow meters and controlled by IB32 Iberfluid flow controller. The gases pass through bubblers, which are filled with distilled water in the case of working in wet conditions. The temperature of the bubblers was around $10\text{ }^{\circ}\text{C}$ below the cell temperature. To prevent condensation of water on the gas streams the inlet pipes were heated. The total system pressure is controlled by micrometric valves.

The cell is connected to an external electronic load (ZS, H & H) to measure the fuel cell performance. Besides, the electrochemical station Zennium (Zahner) was used to measure the ionic resistance exerted by the electrolyte using electrochemical impedance spectroscopy.

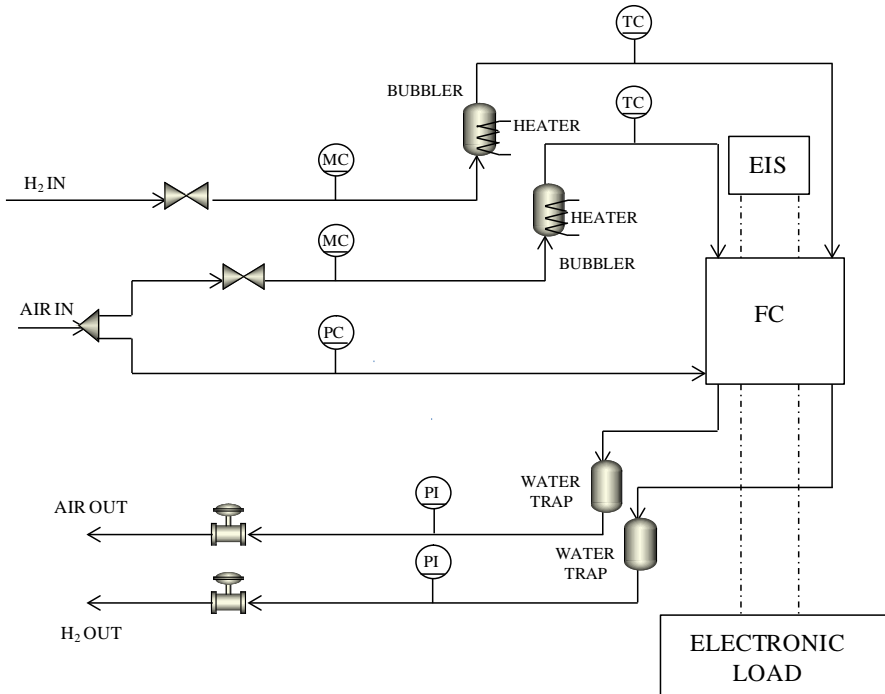


Figure 2.6. Experimental set-up

2.2.2. Membrane Electrode Assembly (MEA)

The membrane electrode assembly design is essential for the fuel cell performance. It is important to achieve a good contact between the membrane and the electrolytes in order to maximize catalyst utilization and decrease the mass transport losses.

There are different techniques to fabricate MEAs [38-40]. In this work, membrane electrode assemblies were fabricated using gas diffusion electrodes (GDEs) with 3

mg Pt.cm⁻² from Baltic Fuel Cell GmbH. To achieve this, GDEs were placed on both sides of the membrane acting as the anode and the cathode.

Nafion and plastic crystal-based membranes were hot pressed with GDEs during 3 minutes at 135 °C with a pressure of 80 bar using a commercially available Carver 4386 press. In the case of polymerized ionic liquid, hot pressing was not necessary due to the stickiness character of these membranes that improves the contact with the electrodes.

2.2.3. Performance testing of the fuel cell

The potential of the PEMFC to perform electrical work is measured by voltage or potential. The electrical work done by moving a charge Q (C) through an electrical potential difference E (V) is:

$$W_{elec} = EQ \quad (2.14)$$

If the charge is carried by electrons:

$$Q = nF \quad (2.15)$$

where n is the number of moles of electrons transferred and F is Faraday's constant.

The maximum electrical work that a system can perform in a constant temperature and pressure process is given by the negative of the Gibbs free energy difference for the process:

$$W_{elec} = -\Delta g_{rxn} \quad (2.16)$$

Combining equations (2.14), (2.15) and (2.16):

$$\Delta g = -nFE \quad (2.17)$$

The Gibbs free energy sets the magnitude of the reversible voltage for an electrochemical reaction. The hydrogen-oxygen fuel cell reaction has a Gibbs free-

energy charge of $-237 \text{ kJ}\cdot\text{mol}^{-1}$ under standard conditions for liquid water product. The reversible voltage generated by a H_2/O_2 fuel cell under standard-state conditions is:

$$E^\circ = -\frac{\Delta g^\circ_{\text{rxn}}}{nF} = -\frac{-237000\text{J/mol}}{(2\text{mol}\frac{e^-}{\text{mol}}\text{reactant})(\frac{96400\text{C}}{\text{mol}})} = +1.23 \text{ V} \quad (2.18)$$

Where E° is the standard-state reversible voltage and $\Delta g^\circ_{\text{rxn}}$ is the standard state free energy change for the reaction [41].

However, the real fuel cell potential is lower than the theoretical one because of different irreversible losses and it results in a complex function of the working current density [42]. These losses, also called polarization or overpotential, are originated primarily from activation polarization, ohmic polarization and mass transport polarization [43]. One of the most typical representations of the fuel cell performance is the polarization curve, where the cell voltage is represented versus the current density (figure 2.7) [44].

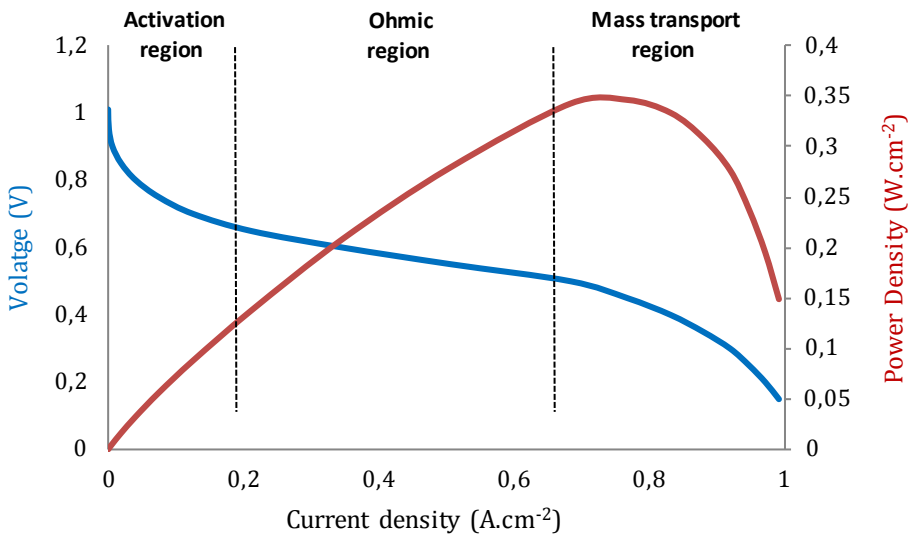


Figure 2.7. Polarization and power curves

The first region corresponds to the activation losses that occur at low current density. This potential loss is due to the slow kinetics of the electrochemical reactions at the electrode surface. The second region of the polarization curve, the ohmic region, is because of the resistance to the flow of ions in the electrolyte and the flow of electrons through the electrodes and the external electrical circuit, being the dominant ohmic loss the electrolyte. In the mass transport region there is slow transport of reactants to the electrochemical reaction and slow removal of products from the reaction sites causing concentration polarization especially at higher current densities [44].

In this work, polarization curves were performed under potentiostatic control. The system was stabilized for two hours in open circuit voltage. After this time, the voltage was reduced in steps of 0.05 V once steady state was reached.

2.2.4. Verification of the experimental set-up

In order to verify a proper operation of the installed experimental setup, a commercially available Nafion 212 membrane electrode assembly membrane with 0.3 mg Pt.cm⁻² was tested at different temperatures with humidified gases. The pressure was fixed at 1.5 bar and hydrogen and air flow rates were 320 and 500 ml.min⁻¹, respectively.

Figures 2.8 and 2.9 show the influence of temperature in the fuel cell performance through polarization and power curves with humidified inlet gases for Nafion 212 membranes. As it can be observed, the temperature improves the fuel cell performance up to 50 °C. Beyond this point, the performance is slightly lower than 25 °C because of the dehydration of the membrane. As it was aforementioned, water plays a key role in proton transport and high temperatures can compromise the fuel cell performance. The highest performance was obtained at 50 °C reaching 0.91 A.cm⁻² at 0.15 V and peak power density of 0.3 W.cm⁻².

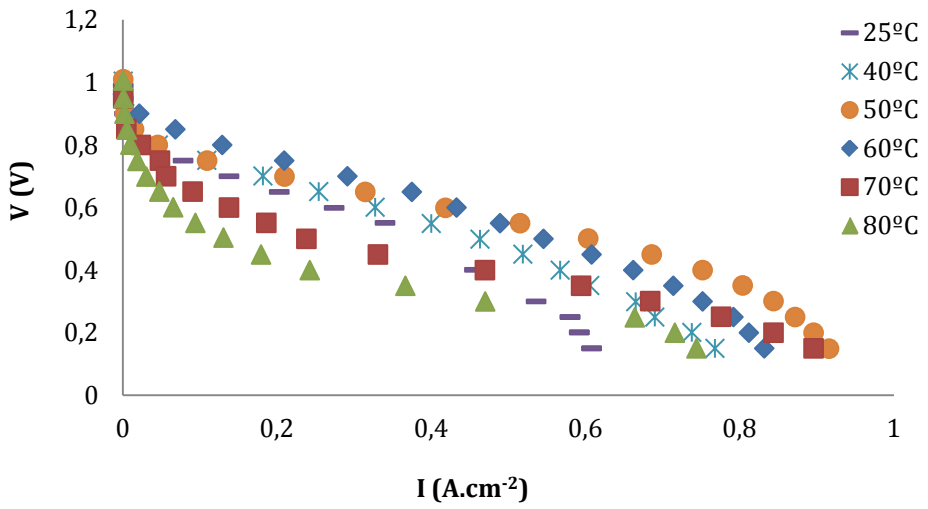


Figure 2.8. Influence of temperature in the fuel cell performance. Polarization curve

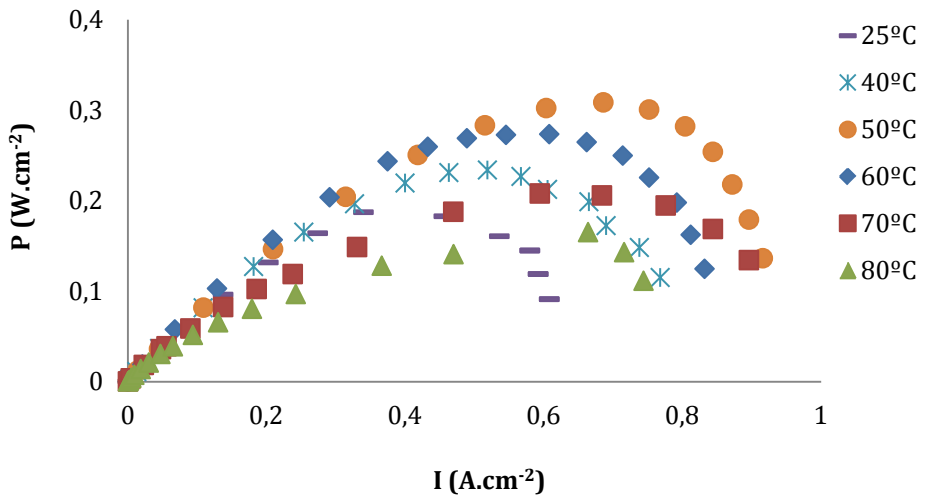


Figure 2.9. Influence of temperature in the fuel cell performance. Power curve

These results were in accordance with those reported in literature. In the work published by Liu et al. [45] the fuel cell performance increased with temperature up to 45 °C reaching peak power density about 400 mW.cm⁻² for Nafion 212 membrane. Similar results were obtained by Fernandes and Ticianelly [46]. In that work, the fuel cell performance increased with temperature up to 70 °C, reaching about 1.7 A.cm⁻² at 0.3 V. It is worth mentioning that the fuel cell performance reported is slightly higher than the results published in this chapter probably due to both higher pressure (2 atm H₂, 3 atm air) and higher catalyst loading (0.4 mg Pt.cm⁻²) used in the experiments.

2.3. References

- [1] S. Asghari, A. Mokmeli and M. Samavati. Study of PEM fuel cell performance by electrochemical impedance spectroscopy. *Int J Hydrogen Energy*, 35 (2010) 9283.
- [2] J.L. Jespersen, E. Schaltz and S.K. Kær. Electrochemical characterization of a polybenzimidazole-based high temperature proton exchange membrane unit cell. *J.Power Sources*, 191 (2009) 289.
- [3] N. Wagner, W. Schnurnberger, B. Müller and M. Lang. Electrochemical impedance spectra of solid-oxide fuel cells and polymer membrane fuel cells. *Electrochim.Acta*, 43 (1998) 3785.
- [4] X. Yuan, C. Song, H. Wang and J. Zhang, *Electrochemical Impedance Spectroscopy in PEM Fuel Cells*, London, Springer, 2010.
- [5] X. Yuan, J.C. Sun, H. Wang and J. Zhang. AC impedance diagnosis of a 500 W PEM fuel cell stack. Part II: Individual cell impedance. *J.Power Sources*, 161 (2006) 929.
- [6] X. Yuan, H. Wang, J. Colin Sun and J. Zhang. AC impedance technique in PEM fuel cell diagnosis—A review. *Int J Hydrogen Energy*, 32 (2007) 4365.
- [7] Gamry Instruments. Basics of Electrochemical Impedance Spectroscopy <http://www.gamry.com/application-notes/EIS/basics-of-electrochemical-impedance-spectroscopy/> 2016.
- [8] D. García, Estudio experimental y teórico de la gestión del agua en Pilas de Combustible Poliméricas (PEFC) bajo condiciones de deshidratación (2011).
- [9] M. Ciureanu, R. Roberge. Electrochemical impedance study of PEM fuel cells. Experimental diagnostics and modeling of air cathodes. *J Phys Chem B*, 105 (2001) 3531.
- [10] N. Wagner, T. Kaz and K.A. Friedrich. Investigation of electrode composition of polymer fuel cells by electrochemical impedance spectroscopy. *Electrochim.Acta*, 53 (2008) 7475.
- [11] M. Díaz, A. Ortiz, M. Isik, D. Mecerreyes and I. Ortiz. Highly conductive electrolytes based on poly([HSO₃-BVIm][TfO])/[HSO₃-BMIm][TfO] mixtures for fuel cell applications. *Int J Hydrogen Energy*, 40 (2015) 11294.

- [12] S.D. Beattie, D.M. Manolescu and S.L. Blair. High-capacity lithium-air cathodes. *J.Electrochem.Soc.*, 156 (2009).
- [13] Z. Wojnarowska, J. Knapik, M. Díaz, A. Ortiz, I. Ortiz and M. Paluch. Conductivity mechanism in polymerized imidazolium-based protic ionic liquid [HSO₃-BVI_m][OTf]: Dielectric relaxation studies. *Macromolecules*, 47 (2014) 4056.
- [14] Y. Yu, W. Beichel, G. Dlubek, R. Krause-Rehberg, M. Paluch, J. Pionteck et al. Free volume and phase transitions of 1-butyl-3-methylimidazolium based ionic liquids from positron lifetime spectroscopy. *Phys.Chem.Chem.Phys.*, 14 (2012) 6856.
- [15] Z. Wojnarowska, K. Grzybowska, A. Grzybowski, M. Paluch, K. Kaminski, P. Włodarczyk et al. Study of molecular dynamics of the pharmaceutically important protic ionic liquid verapamil hydrochloride. II. Test of entropic models. *J.Chem.Phys.*, 132 (2010).
- [16] A. Rivera-Calzada, K. Kaminski, C. Leon and M. Paluch. Elucidating the existence of the excess wing in an ionic liquid on applying pressure. *J Phys Condens Matter*, 20 (2008).
- [17] J. P. Runt, J. J. Fitzgerald, *Dielectric Spectroscopy of Polymeric Materials*, Washington DC, ACS, 1997.
- [18] Z. Wojnarowska, Y. Wang, J. Pionteck, K. Grzybowska, A.P. Sokolov and M. Paluch. High pressure as a key factor to identify the conductivity mechanism in protic ionic liquids. *Phys.Rev.Lett.*, 111 (2013).
- [19] Z. Wojnarowska, C.M. Roland, A. Swiety-Pospiech, K. Grzybowska and M. Paluch. Anomalous electrical conductivity behavior at elevated pressure in the protic ionic liquid procainamide hydrochloride. *Phys.Rev.Lett.*, 108 (2012).
- [20] J. Vila, P. Ginés, J.M. Pico, C. Franjo, E. Jiménez, L.M. Varela et al. Temperature dependence of the electrical conductivity in EMIM-based ionic liquids: Evidence of Vogel–Tamman–Fulcher behavior. *Fluid Phase Equilib.*, 242 (2006) 141.
- [21] S. Slgaryov. Vogel-Fulcher-Tammann behavior of ionic conductivity in KTiOPO₄. *J.Phys.D*, 26 (1993) 1326.
- [22] F. Kremer, A. Schoenhals, *Broadband Dielectric Spectroscopy*, Berlin, Springer, 2003.

[23] PerkinElmer. Thermogravimetric Analysis (TGA) https://www.perkinelmer.com/lab-solutions/resources/docs/FAQ_Beginners-Guide-to-Thermogravimetric-Analysis_009380C_01.pdf 2016.

[24] L. Guerreiro da Trindade, M. Regina Becker, F. Celso, C.L. Petzhold, E.M.A. Martini and R.F. de Souza. Modification of sulfonated poly(ether ether ketone) membranes by impregnation with the ionic liquid 1-butyl-3-methylimidazolium tetrafluoroborate for proton exchange membrane fuel cell applications. *Polym.Eng.Sci.*, 56 (2016) 1037.

[25] K. Peng, J. Lai and Y. Liu. Nanohybrids of graphene oxide chemically-bonded with Nafion: Preparation and application for proton exchange membrane fuel cells. *J.Membr.Sci.*, 514 (2016) 86.

[26] J.M. Gohil, D.G. Karamanev. Novel approach for the preparation of ionic liquid/imidazolecarboxylic acid modified poly(vinyl alcohol) polyelectrolyte membranes. *J.Membr.Sci.*, 513 (2016) 33.

[27] J. Luo, A.H. Jensen, N.R. Brooks, J. Sniekers, M. Knipper, D. Aili et al. 1,2,4-Triazolium perfluorobutanesulfonate as an archetypal pure protic organic ionic plastic crystal electrolyte for all-solid-state fuel cells. *Energy Environ.Sci.*, 8 (2015) 1276.

[28] H. Zhang, W. Wu, J. Wang, T. Zhang, B. Shi, J. Liu, et al. Enhanced anhydrous proton conductivity of polymer electrolyte membrane enabled by facile ionic liquid-based hopping pathways. *J.Membr.Sci.*, 476 (2015) 136.

[29] PerkinElmer. Characterization of Polymers Using TGA http://depts.washington.edu/mseuser/Equipment/RefNotes/TGA_Notes.pdf 2016.

[30] M. Castañeda, Assessment of the water content in several ionic liquids using the coulometric Karl Fischer technique (2015).

[31] GPS Instrumentation. Measuring Principle Karl Fischer Titration <http://www.gpsil.com/our-products/karl-fischer-titrators/measuring-principle/#affixMenu1> 2016.

[32] Differential Scanning Calorimetry (DSC) Thermal Analysis <http://www.andersonmaterials.com/dsc.html> 2016.

[33] Differential Scanning Calorimetry DSC <http://instrument-specialists.com/applications/differential-scanning-calorimetry-dsc/> 2016.

- [34] B. Stuart, *Infrared spectroscopy*, Wiley Online Library, 2005.
- [35] Bruker. Total Reflection (ATR) – a versatile tool for FT-IR spectroscopy https://www.bruker.com/fileadmin/user_upload/8-PDF-Docs/OpticalSpectroscopy/FT-IR/ALPHA/AN/AN79_ATR-Basics_EN.pdf 2016.
- [36] M. Díaz, A. Ortiz, M. Vilas, E. Tojo and I. Ortiz. Performance of PEMFC with new polyvinyl-ionic liquids based membranes as electrolytes. *Int J Hydrogen Energy*, 39 (2014) 3970.
- [37] Baltic FuelCells GmbH. Introduction qCf http://www.balticfuelcells.de/download/introductionQCF_balticfuelcells.pdf 2016.
- [38] S. Thanasilp, M. Hunsom. Effect of MEA fabrication techniques on the cell performance of Pt-Pd/C electrocatalyst for oxygen reduction in PEM fuel cell. *Fuel*, 89 (2010) 3847.
- [39] C. Liu, C. Sung. A review of the performance and analysis of proton exchange membrane fuel cell membrane electrode assemblies. *J.Power Sources*, 220 (2012) 348.
- [40] A.D. Taylor, E.Y. Kim, V.P. Humes, J. Kizuka and L.T. Thompson. Inkjet printing of carbon supported platinum 3-D catalyst layers for use in fuel cells. *J.Power Sources*, 171 (2007) 101.
- [41] R. O'Hayre, A. Cha, W. Colella and F.B. Prinz, *Fuel Cell thermodynamics*, in Anonymous, *Fuel Cell fundamentals*, Wiley, 2009.
- [42] Javier Lemus Godoy, Development of proton exchange membranes based on synergistic combination of polybenzimidazole, ionic liquids and zeolites/zeotypes for high temperature PEM fuel cells, (2015).
- [43] M. Prasanna, H.Y. Ha, E.A. Cho, S. Hong and I. Oh. Influence of cathode gas diffusion media on the performance of the PEMFCs. *J.Power Sources*, 131 (2004) 147.
- [44] I. Pilatowsky, R.J. Romero, C.A. Isaza, S.A. Gamboa, P.J. Sebastian and W. Rivera, *Thermodynamics of Fuel Cells, Cogeneration Fuel Cell-Sorption Air Conditioning Systems*, Springer, 2011.
- [45] W. Liu, Y. Xie, J. Liu, X. Jie, J. Gu and Z. Zou. Experimental study of proton exchange membrane fuel cells using Nafion 212 and Nafion 211 for portable

application at ambient pressure and temperature conditions. *Int J Hydrogen Energy*, 37 (2012) 4673.

[46] A.C. Fernandes, E.A. Ticianelli. A performance and degradation study of Nafion 212 membrane for proton exchange membrane fuel cells. *J.Power Sources*, 193 (2009) 547.

Chapter 3

POLYMER/IONIC LIQUID COMPOSITE MEMBRANES

Abstract

This chapter deals with the development of membranes based on perfluorinated polymer and protic ionic liquids as electrolytes for proton exchange membranes fuel cells fed with hydrogen (PEMFCs) without external humidification. For this purpose, a perfluorinated polymer was impregnated with two protic ionic liquids as proton carriers. Fuel cell performance and ionic resistance of these modified membranes were studied and compared with the behavior of unmodified perfluorinated membranes at different temperature and humidity conditions.

3.1. Introduction

Perfluorosulfonic acid ionomer membranes (PFSI), such as Nafion (developed by DuPont), are the most commonly used membranes in PEMFCs due to their excellent chemical and electrochemical stabilities, as well as their high proton conductivity [1-6]. Nafion has a hydrophobic fluorocarbon backbone that imparts structural integrity and perfluoroether side chains that contain pendant sulfonic acid groups to provide proton conductivity (figure 1.9). When the membrane is fully hydrated, the hydrophobic regions are separated because water fills the hydrophilic regions, forming ionic pathways in the proton exchange membrane (PEM). Protons can be transported through water molecules by a hopping or Grotthuss mechanism (protons hop from one water molecule to another forming hydronium ions H_3O^+) and a vehicular mechanism (diffusion of hydronium ions)[7, 8]. Moreover, an additional hopping mechanism, in which protons are conducted along the sulfonic acid groups hopping from one anion moiety to another, also contribute to proton transport [9]. Because water is critical for proton transport, perfluorosulfonic acid membranes are infeasible at temperatures above 100 °C due to water evaporation [10, 11]. Higher temperatures are desirable because catalyst poisoning by absorbed CO can be reduced and hydrogen with less purity can be used. Besides, increasing the temperature the kinetics of the chemical reactions is accelerated [12-15]. Other disadvantages of this type of membrane include their high fuel crossover and excessive cost.

Many efforts were made in the development of PEM with high conductivity at low relative humidity capable of working at high temperature with the aim of reducing the cost and complexity of the system. Various studies have been carried out employing hybrid inorganic-organic PEMs to overcome this issue [16]. Alternatively, sulfonated hydrocarbon polymers such as poly (ether ketone) (PEK), poly (ether ether ketone) (PEEK) and polyimide (PI), which are cheaper than the perfluorinated ionomers and can be employed over a wide temperature range, have been extensively studied as polymer electrolytes for PEMFCs. However, these polymers,

as in the case of Nafion, require humidification to maintain high proton conductivity, since water molecules play the role of proton carriers in such polymer electrolytes [11]. Other promising membranes are acid-doped PBI which do not rely on hydration for conductivity. However, the leaching out of the acid component from the membrane during the operation represents a problem that must be solved. Besides, due to the large uptake of liquid acid, these membranes display significant anisotropic swelling and the mechanical properties of these membranes may become critically poor [17].

Several studies have arisen in literature integrating the use of conventional polymers and ionic liquids for their use as electrolytes in fuel cells [18-24]. In this way, various authors have studied the modification of PFSI membranes through the incorporation of ionic liquids in their structure [25, 26]. Martínez de Yuso et al. modified Nafion 112 membranes by means of the incorporation of different ionic liquid cations for their application in fuel cells [27, 28]. It was found that depending of the cation incorporated, methanol crossover can be reduced 60-300 times compared to Nafion membranes. Moreover, gas crossover through all ionic liquid-modified membranes was lower than that obtained with the unmodified membrane. The results obtained in this work suggest that the reduction in both methanol and gas crossover is mainly related to the water structuring degree inside the membrane induced by cation incorporation [25]. In the work developed by Li and coworkers [29] a composite membrane based on the ionic liquid 1-(3-hydroxypropyl)-3-methylimidazolium tetrafluoroborate, Nafion and silica was developed by the solvent-casting method for PEMFCs. The resulting membrane has ionic conductivity of $39 \text{ mS}\cdot\text{cm}^{-1}$ and power density of $340 \text{ mW}\cdot\text{cm}^{-2}$ under anhydrous conditions at $160 \text{ }^\circ\text{C}$. Yang and coworkers developed [30] high temperature proton exchange membranes based on Nafion 115, the ionic liquid cation 1-butyl-3-methylimidazolium and phosphoric acid. These membranes were able to obtain ionic conductivity of $10.9 \text{ mS}\cdot\text{cm}^{-1}$ at $160 \text{ }^\circ\text{C}$ without humidification. In another study carried out by Schmidt and coworkers [26] Nafion 117 membranes were impregnated with different ionic liquids. It was observed that the conductivity

of dry pristine Nafion 117 decreased with temperature from 0.95 mS.cm^{-1} at $40 \text{ }^\circ\text{C}$ to 0.01 mS.cm^{-1} at $122 \text{ }^\circ\text{C}$. Nevertheless, the ionic conductivity of impregnated membranes increased with temperature and exceeded values of pure dry Nafion for temperatures higher than $80 \text{ }^\circ\text{C}$, reaching values about 1 mS.cm^{-1} at $120 \text{ }^\circ\text{C}$ for Nafion 117 impregnated with 1-hexyl-3-methylimidazolium bis(trifluoromethylsulfonyl)imide. Moreover, it was proved that ionic liquids act as plasticizers within the Nafion membrane, reducing the elastic modules and resulting in higher breaking strains. Hernández-Fernández et al. [31] developed proton exchange membranes based on polyvinylidene chloride and the ionic liquids 1-octyl-3-methylimidazolium hexafluorophosphate and methyl trioctyl ammonium chloride for microbial fuel cells. Ammonium-based ionic liquid membranes provided a maximum power of 450 mW.m^{-3} . It is worth noting that an increase in the amount of ionic liquid involved an increase of the microbial fuel cell power, demonstrating the role of ionic liquid in proton transport through the membrane.

Among ionic liquids, protic ionic liquids, which could be easily obtained through the combination of a Brønsted acid and a Brønsted base, have the ability to transfer protons from the acid to the base, leading to the presence of proton donor and acceptor sites, which can be used to build up a hydrogen-bonded network [32]. A benefit of using protic ionic liquids is that cells can be operated at temperatures above $100 \text{ }^\circ\text{C}$ under anhydrous conditions.

Due to the potential improvements that derive from the use of protic ionic liquids in fuel cells membranes, this chapter studies the performance of Nafion 112 membranes impregnated with two different types of protic imidazolium ionic liquids: 1-methyl-3-(4-sulfobutyl)-imidazolium bis(trifluoromethylsulfonyl)-imide ($[\text{HSO}_3\text{-BMIm}][\text{Tf}_2\text{N}]$) and 1-butyl-3-(4-sulfobutyl)-imidazolium trifluoromethanesulfonate ($[\text{HSO}_3\text{-BBIm}][\text{TfO}]$). These two protic ionic liquids were specifically designed due to their chemical structure, which led to the desirable properties required for this electrochemical application such as high thermal and electrochemical stability and outstanding ionic conductivity. Electrical impedance

spectroscopy (EIS) was used to determine the resistance exerted by the electrolyte under the operating conditions [33].

3.2. Experimental methods

3.2.1. Materials

Hydrogen was purchased from Air Liquid with a purity of 99.99 %. The Nafion 112 membrane was supplied by Ion Power. Gas diffusion electrodes (3 mg Pt.cm⁻²) were provided by Baltic Fuel Cells. 1-butyl-3-(4-sulfobutyl)-imidazolium trifluoromethanesulfonate ([HSO₃-BBIm][TfO]) (Sigma-Aldrich, ≥97%), 1-methylimidazole (Sigma-Aldrich, 99%), 1,4-butane sultone (Acros Organics, ≥ 99%), and bis(trifluoromethane)sulfonamide lithium salt (Sigma-Aldrich, 99%) were commercially available and used without any further pre-treatment or pre-purification, except acetonitrile (Sigma-Aldrich, ACS reagent, ≥ 99.5%), which was dried with suitable drying agents and distilled under argon prior to use. 1-methyl-3-(4-sulfobutyl)-imidazolium bis(trifluoromethylsulfonyl)-imide ([HSO₃-BMIm][Tf₂N]) was synthesized in the laboratory and it will be described in detail in section 3.2.2..

¹H and ¹³CNMR spectra of the obtained products were recorded in D₂O on a Bruker ARX at 400.1621 and 100.6314 MHz respectively. Chemical shifts are reported in parts per million (ppm, δ) and referenced to D₂O ($\delta = 4.77$). ESI mass spectra were recorded on a micrOTOF Focus spectrometer.

3.2.2. Design and synthesis of protic ionic liquids

Nafion 112 membranes were impregnated with [HSO₃-BMIm][Tf₂N] and [HSO₃-BBIm][TfO] (figure 3.1) for their application as electrolytes in PEMFC. As previously mentioned, these protic ionic liquids were designed to meet the desirable properties for fuel cell applications such as high thermal and electrochemical stability and high

ionic conductivity. The imidazolium cation was chosen because it exhibits high electrochemical stability [34]. In order to facilitate the proton transport, sulfonic groups were incorporated to the cation as side chains acting as carriers. The two anions used, Tf_2N and TfO , exhibit high ionic conductivity that makes them suitable for this application.

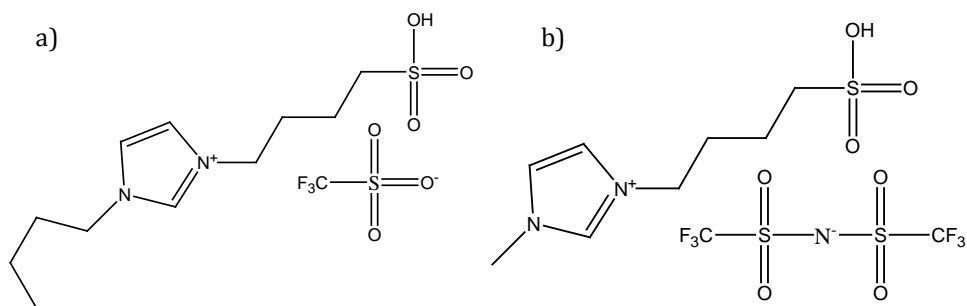


Figure 3.1. Protic ionic liquid structures: a) $[\text{HSO}_3\text{-BBIm}][\text{TfO}]$; b) $[\text{HSO}_3\text{-BMIm}][\text{Tf}_2\text{N}]$

$[\text{HSO}_3\text{-BBIm}][\text{TfO}]$ ionic liquid was commercially available (Sigma-Aldrich, $\geq 97\%$). $[\text{HSO}_3\text{-BMIm}][\text{Tf}_2\text{N}]$ ionic liquid was synthesized by the Organic Chemistry Group from the University of Vigo headed by Prof. Emilia Tojo, following the procedure previously reported in literature (figure 3.2.) [35][6].

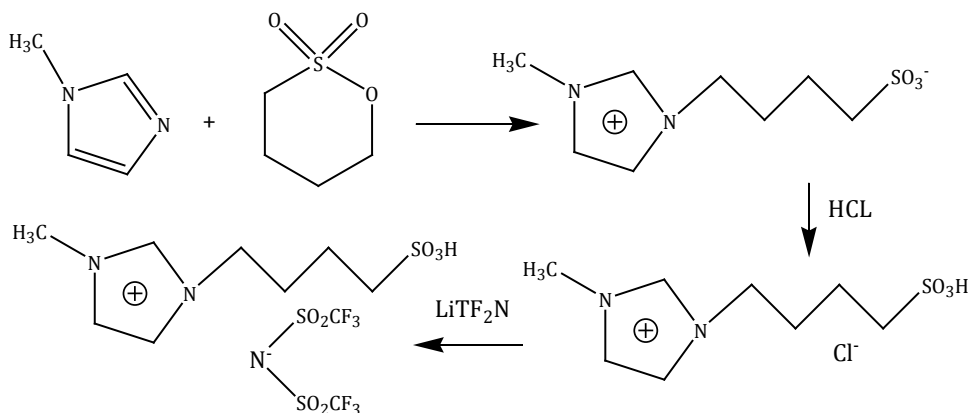


Figure 3.2. $[\text{HSO}_3\text{-BMIm}][\text{Tf}_2\text{N}]$ synthesis procedure

A solution of 1-vinylimidazole (14.3 mL, 157.7 mmol) in dry acetonitrile (75 mL) was introduced into a two-neck 250 mL round flask under inert atmosphere. The mixture was cooled at 0 °C in an ice bath and 1,4-butane sultone (16.2 mL, 157.7 mmol) was added dropwise. The mixture was stirred at 85 °C for five days to afford the corresponding zwitterion as a white precipitate that was isolated by filtration, washed with diethyl ether (3 x 25 mL) and dried under high vacuum. Zwitterion was obtained with more than 99 % purity and high yield (91%). Zwitterion (25.0 g, 114.6 mmol) was then dissolved in water (50 mL) and a stoichiometric amount of concentrated hydrochloric acid was added at 0 °C. The reaction mixture was stirred at room temperature for 12 h. The water was then removed under low pressure and the obtained residue was washed with diethyl ether (3 x 25 mL) and dried under vacuum to give $[\text{HSO}_3\text{-BMIm}][\text{Cl}]$ as a light yellow viscous liquid (yield 99%). Finally, a solution of $[\text{HSO}_3\text{-BMIm}][\text{Cl}]$ (29.2 g, 114.6 mmol) in methanol (5 mL) was added to a solution of bis(trifluoromethane)sulfonamide lithium salt (32.9 g, 114.6 mmol) in acetonitrile (25 mL) and the mixture was stirred at room temperature for 5 h. The mixture was kept at -20 °C for 12 h to afford a white precipitate that was filtered. The filtrate was concentrated by rotary evaporation and dried by heating at 50 °C under high vacuum for 12 h to yield $[\text{HSO}_3\text{-BMIm}][\text{Tf}_2\text{N}]$ as a very viscous slightly yellow liquid (93%). $[\text{HSO}_3\text{-BMIm}][\text{Tf}_2\text{N}]$ structure was confirmed by comparison of its ^1H and ^{13}C NMR data with those reported in literature [6,35].

3.2.3. Impregnation of perfluorinated membranes

Nafion 112 membranes were pretreated by immersion in hydrochloric acid at 60 °C for one hour in order to protonate the sulfonic acid groups. Once protonated they were impregnated with the ionic liquid and left under vacuum for 12 hours for a correct incorporation of the ionic liquid and removal of air bubbles. Then, the membranes were separated from the ionic liquid and the excess of the ionic liquid in the membrane surface was wiped out with a tissue [6].

3.2.4. Operation conditions

A membrane electrode assembly was fabricated sandwiching the membrane between two gas diffusion electrodes and hot-pressed (Carver 4386) during 3 minutes at 135 °C with a pressure of 80 bar. The anode is fed with hydrogen with a flow rate of 320 ml.min⁻¹, while the cathode is fed with air at a rate of 500 ml.min⁻¹. The system pressure is fixed at 1.5 bar. Two different temperatures were set for ionic-liquid modified membranes: 25 and 40 °C. In the case of perfluorinated membranes the temperature range was from 25 to 80 °C.

3.3. Results and discussion

3.3.1. Thermal characterization of ionic liquids

Figure 3.3 shows TGA curves of the ionic liquids [HSO₃-BBI_m][TfO] and [HSO₃-BBI_m][Tf₂N] used for the impregnation of Nafion membranes. As it can be observed, both ionic liquids have outstanding thermal stability. The degradation temperature of [HSO₃-BBI_m][TfO] is 359.9 °C whereas [HSO₃-BBI_m][Tf₂N] shifts its degradation temperature to 425.1 °C.

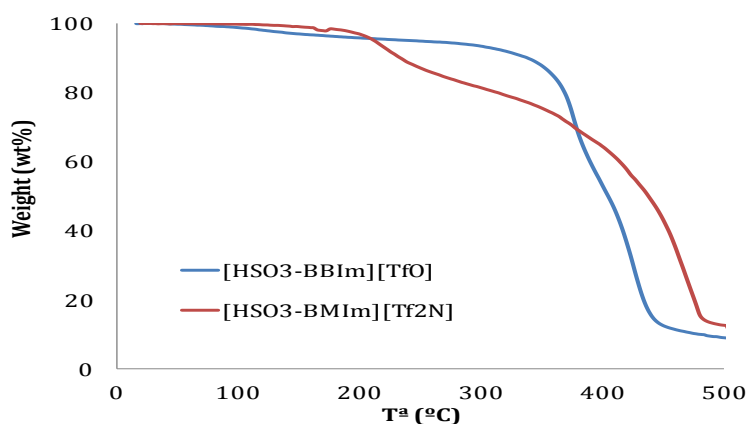


Figure 3.3. TGA curves of protic ionic liquids

The water content of the ionic liquids was determined by Karl-Fischer technique. Accordingly, $[\text{HSO}_3\text{-BBIm}][\text{TfO}]$ has an initial water content of 0.25 wt% and $[\text{HSO}_3\text{-BBIm}][\text{Tf}_2\text{N}]$ of 0.27 wt%. The ability of ionic liquids to absorb water from the atmosphere is of great interest for fuel cell applications without inlet humidification. It promotes the proton transport in the electrolyte through vehicular and Grotthuss mechanisms.

3.3.2. Influence of temperature and humidity of inlet gases on the fuel cell performance

Figures 3.4 and 3.5 show the influence of the temperature on the fuel cell performance for ionic liquid-impregnated commercial membranes with humidified and dry inlet gases, respectively.

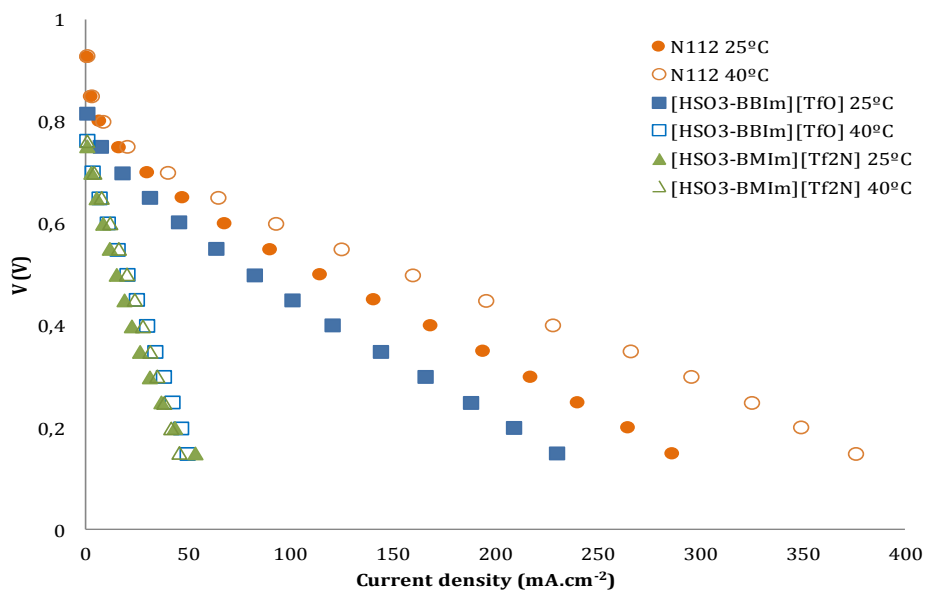


Figure 3.4. Influence of temperature. Humidified inlet gases

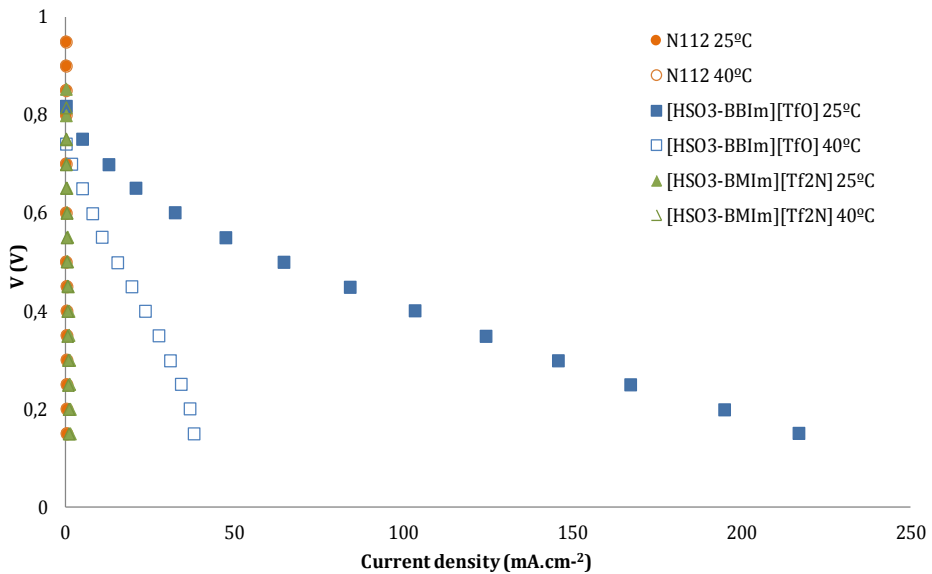


Figure 3.5. Influence of temperature. Dry inlet gases

Polarization curves of Nafion 112 membrane with dry gases could not be obtained due to the absence of moisture and therefore absence of proton transport mechanisms. However, current density of 217 mA.cm⁻² was obtained at 25 °C for Nafion 112 membranes impregnated with [HSO₃-BBIm][TfO]. Although these values are lower than the results obtained with traditional fully hydrated membranes it should be noted that they have been obtained working with dry gases (no humidification of the inlet gases). The reason why this membrane is able to generate electric current in the absence of water in the system is the ability of protic ionic liquids to conduct ions under these conditions due to the delocalization of the proton in the cation [32]. In addition, the ionic liquid [HSO₃-BBIm][TfO] is a highly hydrophilic compound, capable of capturing water from the atmosphere allowing the transport of protons across the water molecules through Vehicular and Grotthus mechanism. The influence of the inlet gas humidification on the impregnated ionic liquid membrane can be considered negligible.

On the other hand, membranes impregnated with [HSO₃-BIm][Tf₂N] led to poorer results than the membranes impregnated with [HSO₃-BIm][TfO], especially at dry conditions where current density could not be detected. The performance of the impregnated membranes is influenced by the ionic liquid uptake, the interactions between ionic liquids and polymer and the structuration of the ionic liquid in the membrane. The ionic liquid uptake was evaluated by the weight difference between the initial and the impregnated membrane. [HSO₃-BIm][TfO] and [HSO₃-BIm][Tf₂N] uptakes were 9.4 % and 1.6 % respectively. These results are in agreement with those reported by Lee and coworkers [36] where the ionic liquid with TfO anion was suitable to be used as electrolyte due to its better electrical properties.

Table 3.1. Characteristics of Nafion 112 membranes impregnated with [HSO₃-BIm][Tf₂N] and [HSO₃-BIm][TfO]

T ^o cell (°C)	Gases	Ionic liquid	OCV (V)	I (0,15V) (mA.cm ⁻²)	P max (mW.cm ⁻²)	R (0,8V) (mΩ)
25	wet	-	0,926	286	68	95
40	wet	-	0,929	376	93	94
25	dry	[HSO ₃ -BIm][Tf ₂ N]	0,853	2	0,4	>10Ω
40	dry	[HSO ₃ -BIm][Tf ₂ N]	0,851	1	0,27	>10Ω
25	wet	[HSO ₃ -BIm][Tf ₂ N]	0,752	53	9,2	306
40	wet	[HSO ₃ -BIm][Tf ₂ N]	0,762	45,2	11	336
25	dry	[HSO ₃ -BIm][TfO]	0,818	217	43,6	116
40	dry	[HSO ₃ -BIm][TfO]	0,741	38	9,7	500
25	wet	[HSO ₃ -BIm][TfO]	0,816	223	50	141
40	wet	[HSO ₃ -BIm][TfO]	0,763	49	12	447

Table 3.1 shows the resistance values of the Nafion 112 membrane impregnated with the ionic liquids [HSO₃-BIm][Tf₂N] and [HSO₃-BIm][TfO]. As it is well expected, the resistance exerted by the membrane impregnated with [HSO₃-BIm][TfO] is smaller than the resistance exerted by the membrane impregnated with [HSO₃-BIm][Tf₂N]. In addition, the resistance decreases when the

temperature decreases from 40 °C to 25 °C justifying the better performance of the membrane at the lowest temperatures mentioned above.

3.4. Conclusions

In this work, ionic liquid-impregnated membranes were developed as electrolytes in fuel cells without external humidification.

In good agreement with already reported information, the membrane electrode assembly formed by Nafion membranes and gas diffusion electrode is infeasible for PEMFCs working without inlet humidification. Dehydration of the membrane and the absence of proton transport mechanisms led to a high proton resistance that decreases the fuel cell performance. However, Nafion membranes impregnated with the ionic liquid [HSO₃-BBIm][TfO] at 25 °C with dry inlet gases exhibited similar performances to humidified Nafion 112 membranes, reaching a current density of 217 mA.cm⁻² at 0.15V. Membranes impregnated with [HSO₃-BMIm][Tf₂N] led to poorer results than the membranes impregnated with [HSO₃-BBIm][TfO], especially at dry conditions where current density could not be detected due to the lower ionic liquid uptake and the electrical properties of this ionic liquid. Temperature did not improve the fuel cell performance and the ionic resistance increased with temperature due to the evaporation of the water embedded in the structure of ionic liquids.

High performance of Nafion membranes impregnated with [HSO₃-BBIm][TfO] was obtained at 25°C without external humidification avoiding the water management systems and reducing the complexity of the fuel cell devices.

3.5. References

- [1] F. Liu, B. Yi, D. Xing, J. Yu and H. Zhang. Nafion/PTFE composite membranes for fuel cell applications. *J.Membr.Sci.*, 212 (2003) 213.
- [2] P. Staiti, A.S. Aricò, V. Baglio, F. Lufrano, E. Passalacqua and V. Antonucci. Hybrid Nafion-silica membranes doped with heteropolyacids for application in direct methanol fuel cells. *Solid State Ionics*, 145 (2001) 101.
- [3] H. Tang, S. Peikang, S.P. Jiang, F. Wang and M. Pan. A degradation study of Nafion proton exchange membrane of PEM fuel cells. *J.Power Sources*, 170 (2007) 85.
- [4] C. Yang, S. Srinivasan, A.B. Bocarsly, S. Tulyani and J.B. Benziger. A comparison of physical properties and fuel cell performance of Nafion and zirconium phosphate/Nafion composite membranes. *J.Membr.Sci.*, 237 (2004) 145.
- [5] M. Díaz, A. Ortiz and I. Ortiz. Progress in the use of ionic liquids as electrolyte membranes in fuel cells. *J.Membr.Sci.*, 469 (2014) 379.
- [6] M. Díaz, A. Ortiz, M. Vilas, E. Tojo and I. Ortiz. Performance of PEMFC with new polyvinyl-ionic liquids based membranes as electrolytes. *Int J Hydrogen Energy*, 39 (2014) 3970.
- [7] A. Z. Weber, S. Balasubramanian and P. K. Das. Proton Exchange Membrane Fuel Cells. *Advances in Chemical Engineering*, 41 (2012).
- [8] K.A. Mauritz, R.B. Moore. State of understanding of Nafion. *Chem.Rev.*, 104 (2004) 4535.
- [9] Fuller T. F., *Proton Exchange Membrane Fuel Cells 6*, New Jersey, The Electrochemical Society, 2006.
- [10] M. Cappadonia, J.W. Erning, S.M.S. Niaki and U. Stimming. Conductance of Nafion 117 membranes as a function of temperature and water content. *Solid State Ionics*, 77 (1995) 65.
- [11] S. Lee, T. Yasuda and M. Watanabe. Fabrication of protic ionic liquid/sulfonated polyimide composite membranes for non-humidified fuel cells. *J.Power Sources*, 195 (2010) 5909.
- [12] V.D. Noto, M. Piga, G.A. Giffin, S. Lavina, E.S. Smotkin, J. Sanchez et al. Influence of anions on proton-conducting membranes based on neutralized Nafion 117, triethylammonium methanesulfonate, and triethylammonium

perfluorobutanesulfonate. 1. synthesis and properties. *J.Phys.Chem.C*, 116 (2012) 1361.

[13] V. Di Noto, M. Piga, G.A. Giffin, S. Lavina, E.S. Smotkin, J. Sanchez et al. Influence of anions on proton-conducting membranes based on neutralized nafion 117, triethylammonium methanesulfonate, and triethylammonium perfluorobutanesulfonate. 2. electrical properties. *J.Phys.Chem.C*, 116 (2012) 1370.

[14] M. Díaz, A. Ortiz, M. Isik, D. Mecerreyes and I. Ortiz. Highly conductive electrolytes based on poly([HSO₃-BVIm][TfO])/[HSO₃-BMIm][TfO] mixtures for fuel cell applications. *Int J Hydrogen Energy*, 40 (2015) 11294.

[15] Z. Wojnarowska, J. Knapik, M. Díaz, A. Ortiz, I. Ortiz and M. Paluch. Conductivity mechanism in polymerized imidazolium-based protic ionic liquid [HSO₃-BVIm][OTf]: Dielectric relaxation studies. *Macromolecules*, 47 (2014) 4056.

[16] V. Di Noto, N. Boaretto, E. Negro, G.A. Giffin, S. Lavina and S. Polizzi. Inorganic-organic membranes based on Nafion, [(ZrO₂) · (HfO₂) 0.25] and [(SiO₂) · (HfO₂) 0.28]. Part I: Synthesis, thermal stability and performance in a single PEMFC. *Int J Hydrogen Energy*, 37 (2012) 6199.

[17] C. Wannek, W. Lehnert and J. Mergel. Membrane electrode assemblies for high-temperature polymer electrolyte fuel cells based on poly(2,5-benzimidazole) membranes with phosphoric acid impregnation via the catalyst layers. *J.Power Sources*, 192 (2009) 258.

[18] T. Yasuda, S. Nakamura, Y. Honda, K. Kinugawa, S. Lee and M. Watanabe. Effects of polymer structure on properties of sulfonated polyimide/protic ionic liquid composite membranes for nonhumidified fuel cell applications. *ACS Appl.Mater.Interfaces*, 4 (2012) 1783.

[19] A. Fericola, B. Scrosati and H. Ohno. Potentialities of ionic liquids as new electrolyte media in advanced electrochemical devices. *Ionics*, 12 (2006) 95.

[20] U.A. Rana, M. Forsyth, D.R. Macfarlane and J.M. Pringle. Toward protic ionic liquid and organic ionic plastic crystal electrolytes for fuel cells. *Electrochim.Acta*, 84 (2012) 213.

[21] L.A. Neves, J. Benavente, I.M. Coelho and J.G. Crespo. Design and characterisation of Nafion membranes with incorporated ionic liquids cations. *J.Membr.Sci.*, 347 (2010) 42.

- [22] A. Eguizábal, J. Lemus, V. Roda, M. Urbiztondo, F. Barreras and M.P. Pina. Nanostructured electrolyte membranes based on zeotypes, protic ionic liquids and porous PBI membranes: Preparation, characterization and MEA testing. *Int J Hydrogen Energy*, 37 (2012) 7221.
- [23] A. Eguizábal, J. Lemus and M.P. Pina. On the incorporation of protic ionic liquids imbibed in large pore zeolites to polybenzimidazole membranes for high temperature proton exchange membrane fuel cells. *J. Power Sources*, 222 (2013) 483.
- [24] A. Eguizábal, J. Lemus, M. Urbiztondo, A.M. Moschovi, S. Ntais, J. Soler et al. Ammonium based ionic liquids immobilized in large pore zeolites: Encapsulation procedures and proton conduction performance. *J. Power Sources*, 196 (2011) 4314.
- [25] L.A. Neves, I.M. Coelho and J.G. Crespo. Methanol and gas crossover through modified Nafion membranes by incorporation of ionic liquid cations. *J. Membr. Sci.*, 360 (2010) 363.
- [26] C. Schmidt, T. Glück and G. Schmidt-Naake. Modification of Nafion membranes by impregnation with ionic liquids. *Chem. Eng. Technol.*, 31 (2008) 13.
- [27] M.D.V.M. De Yuso, M.T. Cuberes, V. Romero, L. Neves, I. Coelho, J.G. Crespo et al. Modification of a Nafion membrane by n-dodecyltrimethylammonium cation inclusion for potential application in DMFC. *Int J Hydrogen Energy*, 39 (2014) 4023.
- [28] M.V. Martínez De Yuso, L.A. Neves, I.M. Coelho, J.G. Crespo, J. Benavente and E. Rodríguez-Castellón. A study of chemical modifications of a nafion membrane by incorporation of different room temperature ionic liquids. *Fuel Cells*, 12 (2012) 606.
- [29] Y. Li, Y. Shi, N. Mehio, M. Tan, Z. Wang, X. Hu et al. More sustainable electricity generation in hot and dry fuel cells with a novel hybrid membrane of Nafion/nano-silica/hydroxyl ionic liquid. *Appl. Energy*, 175 (2016) 451.
- [30] J. Yang, Q. Che, L. Zhou, R. He and R.F. Savinell. Studies of a high temperature proton exchange membrane based on incorporating an ionic liquid cation 1-butyl-3-methylimidazolium into a Nafion matrix. *Electrochim. Acta*, 56 (2011) 5940.
- [31] F.J. Hernández-Fernández, A.P. De Los Ríos, F. Mateo-Ramírez, M.D. Juárez, L.J. Lozano-Blanco and C. Godínez. New application of polymer inclusion membrane based on ionic liquids as proton exchange membrane in microbial fuel cell. *Sep. Purif. Technol.*, 160 (2016) 51.

[32] T.L. Greaves, C.J. Drummond. Protic ionic liquids: Properties and applications. *Chem.Rev.*, 108 (2008) 206.

[33] N. Wagner, K.A. Friedrich. Application of electrochemical impedance spectroscopy for fuel cell characterization: PEFC and oxygen reduction reaction in alkaline solution. *Fuel Cells*, 9 (2009) 237.

[34] H.L. Ngo, K. LeCompte, L. Hargens and A.B. McEwen. Thermal properties of imidazolium ionic liquids. *Thermochimica Acta*, 357–358 (2000) 97.

[35] N. Yan, Yuan, R. Dykeman, Y. Kou and P.J. Dyson. Hydrodeoxygenation of lignin-derived phenols into alkanes by using nanoparticle catalysts combined with Brønsted acidic ionic liquids. *Angew.Chem.Int.Ed.*, 49 (2010) 5549.

[36] S. Lee, A. Ogawa, M. Kanno, H. Nakamoto, T. Yasuda and M. Watanabe. Nonhumidified intermediate temperature fuel cells using protic ionic liquids. *J.Am.Chem.Soc.*, 132 (2010) 9764.

Chapter 4

MEMBRANES BASED ON POLYMERIZED IONIC LIQUIDS

Abstract

Polymeric ionic liquids are gaining interest as proton exchange membranes for anhydrous fuel cell applications. In this chapter, two different membranes based on polymerizable ionic liquids are developed. The first membrane is based on the use of two ionic liquid monomers 1-(4-sulfobutyl)-3-methylimidazolium 2-sulfoethylmethacrylate [HSO₃-BMIm][SEM] and 1-(4-sulfobutyl) 3-vinylimidazolium 2-sulfoethylmethacrylate [HSO₃-BVIIm][SEM] (50/50 wt%). In the second studied membrane, composite membranes based on the polymerizable ionic liquid 1-(4-sulfobutyl) 3-vinylimidazolium trifluoromethanesulfonate [HSO₃-BVIIm][TfO] and its analogue non-polymerizable ionic liquid 1-(4-sulfobutyl)-3-methylimidazolium trifluoromethanesulfonate [HSO₃-BMIm][TfO] are synthesized at different compositional range. The effects of water content and temperature on the ionic conductivity are analyzed for both membranes. Moreover, the fuel cell performance for triflate anion-based membranes at different compositional range is reported in this chapter. Molecular dynamics and ion transport properties of triflate monomer and its polymerized form as well as sulfoethylmethacrylate membrane are also included in this section.

4.1. Introduction

As discussed in the previous chapter, there is a real need for developing innovative electrolytes for proton exchange membrane fuel cells able to operate under non-humidified conditions. Several recently published works deal with the use of ionic liquids (ILs) as electrolytes in these electrochemical systems due to their interesting characteristics. However, despite the promising properties of ionic liquids, the use of these compounds in electrochemical devices is limited due to their liquid state.

There are different approaches to form solid membranes based on ionic liquids. One strategy is the use of polymer networks containing ILs [1]. This technique results in the improvement of the transport properties of the composite membrane because the degree of ion dissociation, concentration of ionic moieties and glass transition temperature (T_g) of the membrane are modified [2]. However, this technique often results in a compromise between the desirable ionic liquid properties and the mechanical strength of the membrane [3, 4]. In the study carried out by Lee and co-workers [5] composite membranes based on sulfonated polyimide (SPI) and the protic ionic liquid diethylmethylammonium trifluoromethanesulfonate [dema][TfO] were synthesized for H_2/O_2 fuel cell applications under non-humidified conditions. The composite membranes up to 80 wt% [dema][TfO] exhibited good thermal stability, high ionic conductivity and good mechanical strength. At 120 °C a current density of 250 mA.cm⁻² was obtained with a peak power density of 63 mW.cm⁻² and open circuit voltage (OCV) of 0.75 V.

In general, vinyl monomers are soluble in common ILs and they can be polymerized via free radical polymerization. Therefore, the polymerization of methylmethacrylate ($CH_2=C(CH_3)COOCH_3$) in 1-ethyl-3-methyl imidazolium bis(trifluoromethanesulfone)imide ([C₂mim][Tf₂N]) with a small amount of crosslinker generated self-standing, flexible and transparent polymer gels in a wide [C₂mim][Tf₂N] compositional range. These membranes showed ionic conductivity at high IL content about 1.0×10^{-2} S.cm⁻¹ at room temperature [6]. Van de Ven and co-workers [7] developed a composite membrane based on PBI filled with 1-H-3-

methylimidazolium bis(trifluoromethanesulfonyl)imide. Proton conductivity of $1.86 \times 10^{-3} \text{ S.cm}^{-1}$ was obtained at $190 \text{ }^\circ\text{C}$. The performance of these membranes exceeded that of Nafion 117 at temperatures above $90 \text{ }^\circ\text{C}$, reaching power densities of 39 mW.cm^{-2} at $150 \text{ }^\circ\text{C}$ with H_2/O_2 .

Another innovative approach to generate solid polymeric electrolytes from ionic liquids is the polymerization of ionic liquid monomers. For this purpose, one simple, energy efficient and intuitive method used to prepare polymerized ionic liquids is photopolymerization [8-11]. Polymeric ionic liquids can be designed to form different systems, such as polycationic ILs, polyanionic ILs, copolymers and poly(zwitterion)s [12]. The most commonly used IL monomers have (meth)acryloyl, styrenic and N-vinylimidazolium groups. Lemus et al. [13] have photopolymerized different ionic liquids for their application in high temperature PEM fuel cells. The polymerization of 1-H-3-vinylimidazolium bis(trifluoromethanesulfonyl) imide ionic liquid in presence of 2.5 mol% divinylbenzene as reinforcement agent was the trade-off between ion transport and mechanical properties. This polymer registered an ionic conductivity value about 371 mS.cm^{-1} at $200 \text{ }^\circ\text{C}$ under anhydrous conditions. Bui and co-workers [14] developed a polymeric ionic liquid composed of a methacrylate polymerizable group, a polar tri(ethylene oxide) spacer, a trifluoromethane sulfonic anion and a free imidazolium cation for its use in dye-sensitized solar cells (DSSCs). This electrolyte was thermally stable up to $290 \text{ }^\circ\text{C}$ and registered ionic conductivity about $2.7 \times 10^{-3} \text{ S.cm}^{-1}$ at 70°C , being very promising to be used as electrolyte in DSSCs. Polymerized ionic liquids are also interesting electrolytes for battery systems. In the work carried out by Hwang et al. [15] a polypropylene (PP) membrane coated with polymerized ionic liquid was developed as separator for Zinc-Air batteries. The anionic exchange polymer was synthesized copolymerizing 1-[(4-ethenylphenyl)methyl]-3- butylimidazolium hydroxide (EBIH) and butyl methacrylate (BMA) monomers by free radical polymerization and coating the resulting copolymer on a commercially available PP membrane. Battery test results revealed an increase of 281% in lifetime and 1.4% higher initial energy efficiency.

Polymerized ionic liquid block polymers are a new promising class of polymers that combine the advantages of polymeric ionic liquids and block copolymers. They can be synthesized from a variety of polymerization techniques. This versatility in their synthesis permits the inclusion of several cations and anions, as well as a broad range of molecular weights and compositions. The selection of these parameters results in polymeric ionic liquid block copolymers in which the morphology and ionic conductivity can be specifically designed depending on their final application [16]. Thus, in the work developed by Meek and co-workers [17] a new sulfonated polymerized ionic liquid diblock copolymer, formed by covalently attached butylimidazolium cations (BIm^+) in one block and covalently attached sulfonated anions (SO_3^-) in the other block with both mobile counter bis(trifluoromethylsulfonyl)imide anions (Tf_2N^-) and mobile counter lithium cations (Li^+) was synthesized and characterized. The sulfonated block copolymer, cast with a solution of 1 M lithium bis(trifluoromethanesulfonyl)imide/1-ethyl-3-methylimidazolium bis(trifluoromethylsulfonyl) imide, possessed a high anhydrous ionic conductivity 1.5 mS.cm^{-1} at 70°C , demonstrating its suitability for a variety of applications such as solid-state capacitors or electro dialysis.

It is worth noting that ionic conductivities of ILs are usually in the order of $1.0 \times 10^{-2} \text{ S.cm}^{-1}$ depending on their chemical nature. However, after polymerization conductivities decrease down to $1.0 \times 10^{-6} \text{ S.cm}^{-1}$ due to the increase in glass transition temperature and the decrease in the number of mobile ions and their mobility [18-22]. In order to improve the ionic conductivity it is important to maintain the fluidity of the electrolyte which can be reached by the incorporation of non-polymerizable ionic liquid (also called free ionic liquid) in the polymeric structure. In the study developed by Pöhako-Esko et al. [23] the non-polymerizable ionic liquid 1-ethyl-3-methyl imidazolium tetrafluoroborate ($[\text{EMIM}][\text{BF}_4]$) was added to different methacrylate-types polymeric ionic liquids. An increase in $[\text{EMIM}][\text{BF}_4]$ content led to an increase in the ionic conductivity of the materials. The 40% vol/vol composites had conductivities of approximately $1.0 \times 10^{-4} \text{ S.cm}^{-1}$ compared to the conductivities of $1.0 \times 10^{-5} \text{ S.cm}^{-1}$ for the corresponding neat

polymeric ionic liquid. Above this [EMIM][BF₄] content the materials were sticky gels. Marcilla and co-workers [24] synthesized a new type of tailor-made polymer electrolyte based on ionic liquids and polymeric ionic liquids analogues by mixing 1-butyl-3-methylimidazolium bis(trifluoromethanesulfonimide) [bmim][Tf₂N], 1-butyl-3-methylimidazolium tetrafluoroborate [bmim][BF₄] and 1-butyl-3-methylimidazolium bromide [bmim][Br⁻] with poly(1-vinyl-ethyl-imidazolium) bearing [Tf₂N],[BF₄] and [Br⁻] as counter-anions. The chemical affinity between polymerized ionic liquids and ionic liquids result in stable polymer electrolytes. The ionic conductivity of all these electrolytes varied between 1.0 x 10⁻² S.cm⁻¹ and 1.0 x 10⁻⁵ S.cm⁻¹ at room temperature. At high IL contents the ionic conductivity reached values close to the values of the IL compounds although the mechanical stability was compromised. In the work developed by Zarca et al. [25] composite poly(ionic liquid)-ionic liquid membranes based on an IL monomer, 1-vinyl-3-butylimidazolium bistrifluoroimide ([C₄vim][Tf₂N]), copper (I) chloride (CuCl) and a non-polymerizable IL, 1-butyl-3-methylimidazolium chloride ([C₄mim][Cl]) were fabricated for gas separation applications. An enhancement of both gas permeability and ideal gas pair selectivity were observed for CO₂/N₂ and H₂/N₂ separations in the Cu-containing composite membranes with respect to the neat poly([C₄vim][Tf₂N]). Chung and co-workers [26] developed composite membranes based on 1-vinyl-3-butylimidazolium bis-(trifluoromethylsulfonyl)imide ([vbim][Tf₂N]) and 1-butyl-3-methylimidazolium bis-(trifluoromethylsulfonyl)imide ([bmim][Tf₂N]) up to 60 wt% of the non-polymerizable ionic liquid for CO₂ separation from flue gas. It was found that the incorporation of [bmim][Tf₂N] led to a decrease in the T_g and an increase in the gas solubility, diffusivity and permeability but maintains the CO₂/N₂ permeability selectivity compared with the pristine poly([vbim][Tf₂N]).

In this chapter, electrolytes consisting in polymerized ionic liquids are developed for PEMFC applications without external humidification. For this purpose, two different membrane structures are studied. The first membrane is based on the two polymerizable ionic liquids 1-(4-sulfobutyl)-3-methylimidazolium 2-sulfoethylmethacrylate [HSO₃-BMIm][SEM] (50wt%) and 1-(4-sulfobutyl)-3-

vinylimidazolium 2-sulfoethylmethacrylate [HSO₃-BVIm][SEM] (50/50 wt%). The effects of temperature and water content on the ionic conductivity are analyzed. Moreover, ion dynamics studies under high pressure conditions are developed to investigate the charge transport mechanism in this electrolyte. On the other hand, in the second studied membrane, the ionic liquid monomer 1-(4-sulfobutyl)-3-vinylimidazolium trifluoromethanesulfonate [HSO₃-BVIm][TfO] and its analogue non-polymerizable ionic liquid 1-(4-sulfobutyl)-3-methylimidazolium trifluoromethanesulfonate [HSO₃-BMIm][TfO] are mixed at different compositional range and photopolymerized. The effects of the addition of the non-polymerizable ionic liquid, water content and temperature on the ionic conductivity and fuel cell performance are reported. Molecular dynamics and ions transport properties of [HSO₃-BVIm][TfO] monomer and its polymerized form are also analyzed in this section.

4.2. Experimental methods

4.2.1. Materials

Hydrogen was purchased from Air Liquid with a purity of 99.99 %. Gas diffusion electrodes (3 mg Pt.cm⁻²) were provided by Baltic Fuel Cells. 2-hydroxy-2-methyl propiophenone (Sigma-Aldrich, 97%), 1-methylimidazole (Sigma-Aldrich, 99%), 1-vinylimidazole (Sigma-Aldrich, ≥99%), 1,4-butane sultone (Sigma-Aldrich, 99%), glycerol dimethacrylate (Sigma-Aldrich, 85%), 2-sulfoethyl methacrylate (polysciences, > 90%) and trifluoromethanesulfonic acid (Sigma-Aldrich, 98%) were commercially available and used without any further treatment. Acetonitrile was dried and distilled prior to use. [HSO₃-BVIm][TfO], [HSO₃-BMIm][TfO], [HSO₃-BMIm][SEM] and [HSO₃-BVIm][SEM] ionic liquids were synthesized in the laboratory and the procedure will be described in detail in section 4.2.2..

¹H and ¹³CNMR spectra of the obtained products were recorded in D₂O on a Bruker ARX at 400.1621 and 100.6314 MHz respectively. Chemical shifts are reported in

parts per million (ppm, δ) and referenced to D₂O ($\delta = 4.77$). ESI mass spectra were recorded on a micrOTOF Focus spectrometer.

4.2.2. Design and synthesis of the ionic liquids

The protic ionic liquids [HSO₃-BVIm][TfO], [HSO₃-BMIm][TfO], [HSO₃-BMIm][SEM] and [HSO₃-BVIm][SEM] were designed for their use as electrolytes in PEMFCs. Imidazolium cation was selected because it exhibits high electrochemical stability. In order to facilitate proton transport, sulfonic groups were incorporated to the cation. [HSO₃-BVIm][TfO] and [HSO₃-BVIm][SEM] contain a vinyl group located in the cation for the polymerization reaction. TfO anion exhibits high ionic conductivity. On the other hand, SEM anion was chosen for comparison with TfO because of its ability to polymerize resulting in a complex poly(cation)-poly(anion) membrane. Both ionic liquids forming each membrane have similar chemical structures in order to achieve a good chemical compatibility (figure 4.1). The synthesis of the protic ionic liquids was carried out in collaboration with the Organic Chemistry Group of the University of Vigo, headed by Prof. Emilia Tojo.

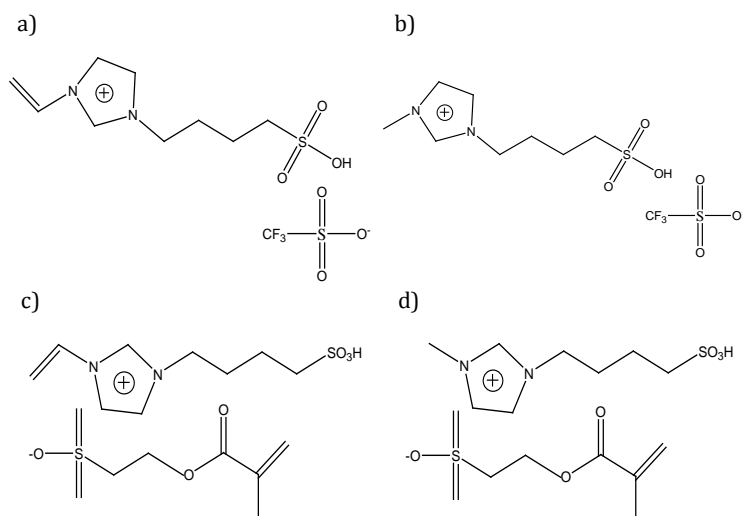


Figure 4.1. Chemical structures of ionic liquids. a) [HSO₃-BVIm][TfO]; b) [HSO₃-BMIm][TfO]; c) [HSO₃-BVIm][SEM]; d) [HSO₃-BMIm][SEM]

Synthesis [HSO₃-BMIm][TfO] and [HSO₃-BVIIm][TfO]

[HSO₃-BVIIm][TfO] and [HSO₃-BMIm][TfO] were synthesized following the procedure showed in figure 4.2.

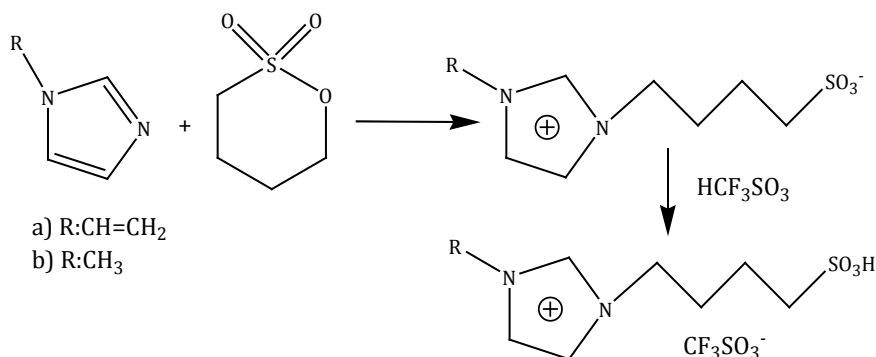


Figure 4.2. Synthesis [HSO₃-BVIIm][TfO] (a) and [HSO₃-BMIm][TfO] (b)

A solution of 1-vinylimidazole (or 1-methylimidazole) (157.7 mmol) in dry acetonitrile (75 mL) was introduced into a two-neck 250 mL round flask under inert atmosphere. The mixture was cooled at 0 °C in an ice bath and 1,4-butane sultone (157.7 mmol) was added dropwise. The mixture was stirred at 85 °C for five days to afford the corresponding zwitterion as a white precipitate that was isolated by filtration, washed with diethyl ether (3 x 25 mL) and dried under high vacuum. Zwitterion was obtained with more than 99 % purity and high yield (94%). Under inert atmosphere a stoichiometric amount of trifluoromethanesulfonic acid was added drop wise over a suspension of zwitterion (147.0 mmol) in acetonitrile (50 mL) at 0 °C and the mixture was stirred for 5 h at room temperature. The solvent was removed at low pressure and the obtained IL was washed with diethyl ether and dried by heating at 50 °C under high vacuum for 12 h. Ionic liquids were obtained in quantitative yield (99 %) as a pale-yellow viscous liquids. ¹H NMR (400 MHz, D₂O, ppm): δ 1.69 [m, 2H, NCH₂CH₂], 1.97 [m, 2H, N(CH₂)₂CH₂], 2.88 [t, 2H, J= 7.7 Hz, N(CH₂)₃CH₂], 4.22 [t, 2H, J= 7.1 Hz, NCH₂], 5.34 [dd, 1H, J₁= 2.8 Hz, J₂= 8.7 Hz, NCH=CH₂], 5.72 [dd, 1H, J₁= 2.8 Hz, J₂= 15.6 Hz, NCH=CH₂], 7.05 [dd, 1H, J₁= 8.7 Hz,

$J_2 = 15.6$ Hz, $NCH=CH_2$], 7.52 [m, 1H, Ar], 7.70 [m, 1H, Ar], 8.99 [s, 1H, H-2]. ^{13}C NMR (100.6 MHz, D_2O , ppm): δ 20.6, 27.7, 49.0, 49.8, 109.0, 119.3, 119.4 [q, $J_{CF} = 317.4$ Hz], 122.5, 127.9, 134.0. Electrospray MS (microTOF Focus) m/z (%) 232.1 $[(C_9H_{15}N_2O_3S) + 1]^+$ (4), 231.07964 $[(C_9H_{15}N_2O_3S)]^+$ requires 231.07979, 100) [27][28].

Synthesis of $[HSO_3-BMIm][SEM]$ and $[HSO_3-BVIm][SEM]$

$[HSO_3-BMIm][SEM]$ and $[HSO_3-BVIm][SEM]$ were synthesized following the procedure showed in figure 4.3.

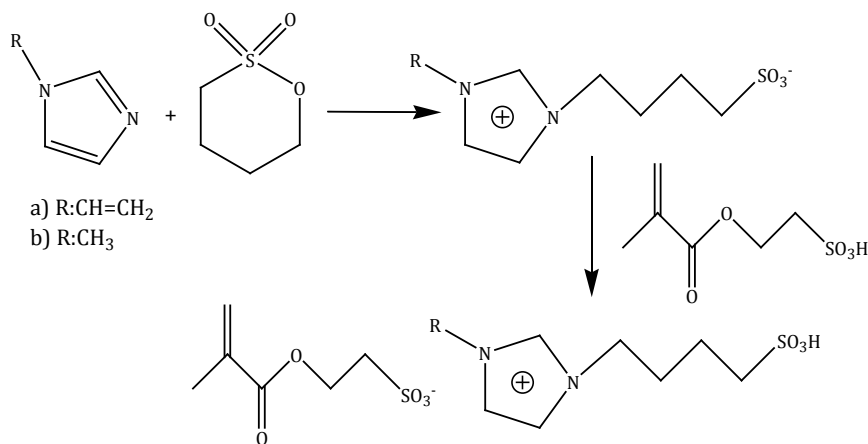


Figure 4.3. Synthesis of $[HSO_3-BVIm][SEM]$ (a) $[HSO_3-BMIm][SEM]$ (b)

1-methylimidazole (12.5 mmol, 1.00 eq.) was dissolved in CH_3CN (8 mL) and cooled down to $0^\circ C$ with an ice bath. 1,4-butanedithione (12.5 mmol, 1.00 eq.) was added dropwise and the mixture was stirred at $0^\circ C$ for 10 minutes. Then, it was stirred at $85^\circ C$ under reflux for 3 days. It was then cooled down to $-20^\circ C$ and the resulting precipitate was filtered and dried under high vacuum. 1-(4-sulfobutyl)-3-methylimidazolium was obtained as a white solid (84% yield). 2-sulfoethyl methacrylate (9.5 mmol, 1.00 eq.) was dissolved in CH_3CN and added over 1-butylsulfonate-3-methylimidazolium (10.5 mmol, 1.10 eq.). The mixture was stirred at room temperature overnight and filtered to remove the unreacted excess of the

zwitterion. The organic phase was collected and the solvent was evaporated under reduced pressure at room temperature, in order to avoid product decomposition. The resulting ionic liquid was dried under high vacuum to obtain 1-(4-sulfobutyl)-3-methylimidazolium 2-sulfoethylmethacrylate as a viscous ionic liquid (99% yield). ^1H NMR (400 MHz, D_2O) δ 8.59 (s, 1H, H-2), 7.35 (d, $J = 1.5$ Hz, 1H, H-4*), 7.29 (d, $J = 1.2$ Hz, 1H, H-5*), 6.01 (d, $J = 0.9$ Hz, 1H, $\text{CH}_3\text{C}(\text{CHH})\text{CO}_2\text{CH}_2\text{CH}_2\text{SO}_3$), 5.57 (d, $J = 1.4$ Hz, 1H, $\text{CH}_3\text{C}(\text{CHH})\text{CO}_2\text{CH}_2\text{CH}_2\text{SO}_3$), 4.37 (t, $J = 6.1$ Hz, 2H, $\text{CH}_3\text{C}(\text{CH}_2)\text{CO}_2\text{CH}_2\text{CH}_2\text{SO}_3$), 4.10 (t, $J = 7.0$ Hz, 2H, NCH_2), 3.74 (s, 3H, NCH_3), 3.16 (t, $J = 6.1$ Hz, 2H, $\text{CH}_3\text{C}(\text{CH}_2)\text{CO}_2\text{CH}_2\text{CH}_2\text{SO}_3$), 2.85 – 2.75 (m, 2H, $\text{N}(\text{CH}_2)_3\text{CH}_2\text{SO}_3\text{H}$), 1.94 – 1.82 (m, 2H, $\text{N}(\text{CH}_2)_2\text{CH}_2\text{CH}_2\text{SO}_3\text{H}$), 1.77 (d, $J = 0.9$ Hz, 3H, $\text{CH}_3\text{C}(\text{CH}_2)\text{CO}_2\text{CH}_2\text{CH}_2\text{SO}_3$), 1.65 – 1.54 (m, 2H, $\text{NCH}_2\text{CH}_2\text{CH}_2\text{CH}_2\text{SO}_3\text{H}$); ^{13}C NMR (101 MHz, D_2O) δ 169.3 ($\text{CH}_3\text{C}(\text{CH}_2)\text{CO}_2\text{CH}_2\text{CH}_2\text{SO}_3$), 135.9 (C-2), 135.6 ($\text{CH}_3\text{C}(\text{CH}_2)\text{CO}_2\text{CH}_2\text{CH}_2\text{SO}_3$), 127.0 ($\text{CH}_3\text{C}(\text{CH}_2)\text{CO}_2\text{CH}_2\text{CH}_2\text{SO}_3$), 123.6 (C-5*), 122.1 (C-4*), 60.0 ($\text{CH}_3\text{C}(\text{CH}_2)\text{CO}_2\text{CH}_2\text{CH}_2\text{SO}_3$), 50.0 ($\text{N}(\text{CH}_2)_3\text{CH}_2\text{SO}_3$), 49.5 ($\text{CH}_3\text{C}(\text{CH}_2)\text{CO}_2\text{CH}_2\text{CH}_2\text{SO}_3$), 48.8 (NCH_2), 35.6 (NCH_3), 28.0 (NCH_2CH_2), 20.8 ($\text{N}(\text{CH}_2)_2\text{CH}_2$), 17.2 ($\text{CH}_3\text{C}(\text{CH}_2)\text{CO}_2\text{CH}_2\text{CH}_2\text{SO}_3$); ESI-MS m/z (%) 219.07986 [$[\text{C}_8\text{H}_{15}\text{N}_2\text{SO}_3]^+$, calcd. for $\text{C}_8\text{H}_{15}\text{N}_2\text{SO}_3 = 219.08001$, 17), 437.15242 [$[(\text{C}_8\text{H}_{15}\text{N}_2\text{SO}_3)(\text{C}_8\text{H}_{14}\text{N}_2\text{SO}_3)]^+$, calcd. for $\text{C}_{16}\text{H}_{29}\text{N}_4\text{O}_6\text{S}_2 = 437.15230$, 100), 438.15587 [$[(\text{C}_8\text{H}_{15}\text{N}_2\text{SO}_3)(\text{C}_8\text{H}_{14}\text{N}_2\text{SO}_3) + 1]^+$, 17) 655.22503 [$[(\text{C}_8\text{H}_{15}\text{N}_2\text{SO}_3)(\text{C}_8\text{H}_{14}\text{N}_2\text{SO}_3)_2]^+$, 33), 656.22876 [$[(\text{C}_8\text{H}_{15}\text{N}_2\text{SO}_3)(\text{C}_8\text{H}_{14}\text{N}_2\text{SO}_3)_2 + 1]^+$, 8][29].

1-(4-sulfobutyl)-3-vinylimidazolium was prepared employing the same general synthetic method described for the synthesis of 1-(4-sulfobutyl)-3-methylimidazolium, employing 1-vinylimidazole instead of 1-methylimidazole, and obtained as a white solid (63% yield). 2-sulfoethylmethacrylate (12.6 mmol) was dissolved in CH_3CN and added over 1-(4-sulfobutyl)-3-vinylimidazolium (14 mmol). The mixture was stirred at room temperature overnight. Then, it was filtered. The organic phase was collected and the solvent was evaporated under reduced pressure at room temperature, in order to avoid product decomposition. The resulting IL was dried under high vacuum to obtain 1-(4-sulfobutyl)-3-vinylimidazolium 2-sulfoethylmethacrylate as a viscous ionic liquid (91% yield). ^1H

NMR (400 MHz, D₂O) δ 8.96 (s, 1H, , H-2), 7.67 (s, 1H, H-5*), 7.49 (s, 1H, , H-4*), 7.03 (dd, J = 15.6, 8.7 Hz, 1H, , NCH=CH₂), 6.04 (s, 1H, CH₃C(CHH)CO₂CH₂CH₂SO₃), 5.69 (d, J = 15.6 Hz, 1H, NCH=CHH), 5.61 (s, 1H, CH₃C(CHH)CO₂CH₂CH₂SO₃), 5.31 (d, J = 8.7 Hz, 1H, NCH=CHH), 4.40 (t, J = 5.9 Hz, 2H, CH₃C(CH₂)CO₂CH₂CH₂SO₃), 4.18 (t, J = 7.0 Hz, 2H, NCH₂), 3.19 (t, J = 5.9 Hz, 2H, CH₃C(CH₂)CO₂CH₂CH₂SO₃), 2.84 (t, J = 7.5 Hz, 2H, N(CH₂)₃CH₂SO₃H), 2.01 – 1.89 (m, 2H, N(CH₂)₂CH₂CH₂SO₃H), 1.81 (s, 3H, CH₃C(CH₂)CO₂CH₂CH₂SO₃), 1.72 – 1.59 (m, 2H, NCH₂CH₂CH₂CH₂SO₃H); ¹³C NMR (101 MHz, D₂O) δ 169.3 (CH₃C(CH₂)CO₂CH₂CH₂SO₃), 135.6 (C-2), 134.4 (CH₃C(CH₂)CO₂CH₂CH₂SO₃), 128.2 (C-5*), 127.0 (CH₃C(CH₂)CO₂CH₂CH₂SO₃), 122.8 (C-4*), 119.5 (NCH=CH₂), 109.3 (NCH=CH₂), 60.0 (CH₃C(CH₂)CO₂CH₂CH₂SO₃), 50.0 (N(CH₂)₃CH₂SO₃), 49.5(CH₃C(CH₂)CO₂CH₂CH₂SO₃), 49.2 (NCH₂), 27.9 (NCH₂CH₂), 20.8 (N(CH₂)₂CH₂), 17.2 (CH₃C(CH₂)CO₂CH₂CH₂SO₃); ESI-MS *m/z* (%) 231.08 ([C₉H₁₅N₂SO₃]⁺, 8), 461.15 ([C₉H₁₅N₂SO₃)(C₉H₁₄N₂SO₃)]⁺, 100), 462.15 ([C₉H₁₅N₂SO₃)(C₉H₁₄N₂SO₃) + 1]⁺, 17), 463.15 ([C₉H₁₅N₂SO₃)(C₉H₁₄N₂SO₃) + 2]⁺, 8), 691.22 ([C₉H₁₅N₂SO₃)(C₉H₁₄N₂SO₃)₂]⁺, 19), 692.22 ([C₉H₁₅N₂SO₃)(C₉H₁₄N₂SO₃)₂ + 1]⁺, 5) [30].

4.2.3. Photopolymerization of ionic liquids

Five different proton exchange membranes based on polymerized ionic liquids were synthesized under ultraviolet light. Four of them were triflate anion-based membranes, corresponding to mixtures between the monomer [HSO₃-BVIIm][TfO] and its analogue non-polymerizable ionic liquid [HSO₃-BMIm][TfO] ([HSO₃-BVIIm][TfO] + x wt% [HSO₃-BMIm][TfO], x=0, 10, 20, 30). The synthesis of these triflate anion-based membranes was developed in the Innovative Polymers Group at the Basque Center for Macromolecular Design & Engineering (Donostia, Spain) under the supervision of Prof. David Mecerreyes.

The other membrane, with sulfoethylmethacrylate anion, was formed by the mixture between the two polymerizable ionic liquids [HSO₃-BMIm][SEM] and [HSO₃-BVIIm][SEM] (50/50 wt%). It is worth mentioning that polymerized [HSO₃-

BMIIm][SEM] and [HSO₃-BVIIm][SEM] were not included independently in this work due to the poor mechanical stability of the resulting individual polymers.

Ionic liquids used in each type of membrane were mixed at the corresponding ratio. Afterwards, 2 wt% of the photoinitiator 2-hydroxy-2-methyl propiophenone and 5 wt% of the crosslinker glycerol dimethacrylate were added. The mixture was extended over a flat and flexible surface and exposed to 354 nm UV light (KAIS) for 30 min. After polymerization, the free-standing membrane was removed from the surface using a razor blade. The membrane thickness was measured with a micrometer (Mitutoyo 369-250) which was purchased from Mitutoyo Asia Pacific Pte. Ltd. (Japan) with an accuracy of 0.001mm (1 μ m). For every measurement at least 5 points from different positions of each film were measured and the average value was considered.

4.2.4. Operation conditions

Gas diffusion electrodes (GDEs) (Pt 3 mg.cm⁻², Baltic Fuel Cell GmbH) were placed at both sides of the polymerized membrane forming the membrane electrode assembly (MEA). The anode was fed with hydrogen while the cathode was fed with air with flow rates ranging from 10-125 and 30-500 ml.min⁻¹, respectively. The system pressure was fixed at 1.0-1.2 bar and the experiments were carried out at 25 and 40 °C. Polarization curves of cell voltage versus the electric current were performed under potentiostatic control.

4.3. Results and discussion

In this section, the main results regarding the characterization and performance of the different polymeric ionic liquid membranes are analyzed. For this purpose, the thermal behavior, ionic conductivity, ion dynamics and fuel cell performance are reported.

4.3.1. Characterization of membranes

Triflate anion-based membranes based on the polymerizable ionic liquid [HSO₃-BVIIm][TfO] with different quantities of the non-polymerizable ionic liquid [HSO₃-BMIIm][TfO] (0-30 wt%) and sulfoethylmethacrylate anion-based membrane (50 wt%) were prepared by photopolymerization. The obtained membranes were flexible, transparent and the thickness ranged from 200 to 350 microns. However, in the case of triflate anion-based membranes, at high non-polymerizable ionic liquid content the membranes were sticky gels and the mechanical stability was compromised. Figure 4.4 and 4.5 show the chemical structure and a photograph of the two membranes studied in this chapter.

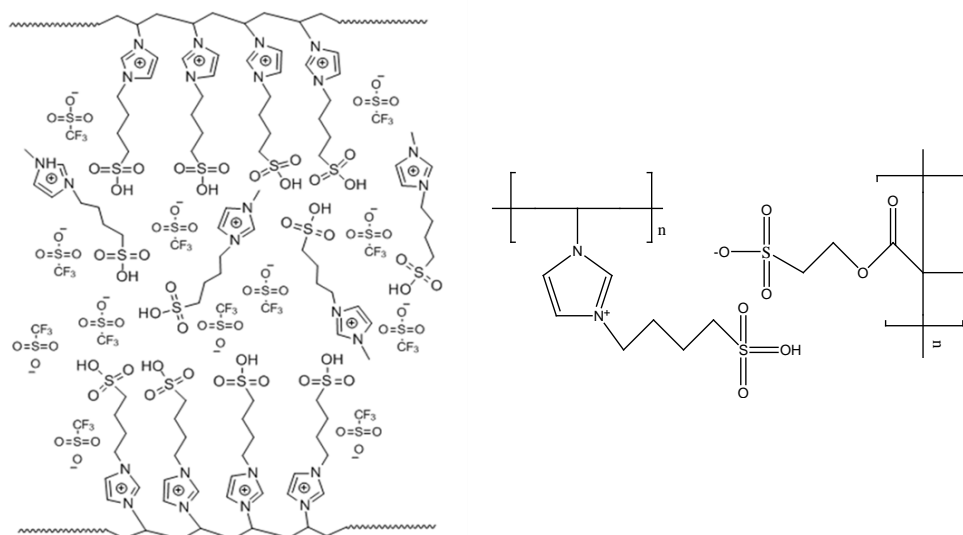


Figure 4.4. Chemical structure of triflate (left) and sulfoethylmethacrylate (right) membranes



Figure 4.5. Photograph of poly([HSO₃-BVIm][TfO]) with 20 wt% [HSO₃-BMIm][TfO] (left) and [HSO₃-BVIm][SEM]/[HSO₃-BMIm][SEM] (50 wt%) (right)

ATR-FTIR

The success of the polymerization reaction of the ionic liquid membranes can be easily monitored by analyzing the materials with ATR-FTIR spectra. Figure 4.6 provides the ATR-FTIR spectra of the monomer [HSO₃-BVIm][TfO], poly(ionic liquid)/ionic liquid triflate membranes and the crosslinker.

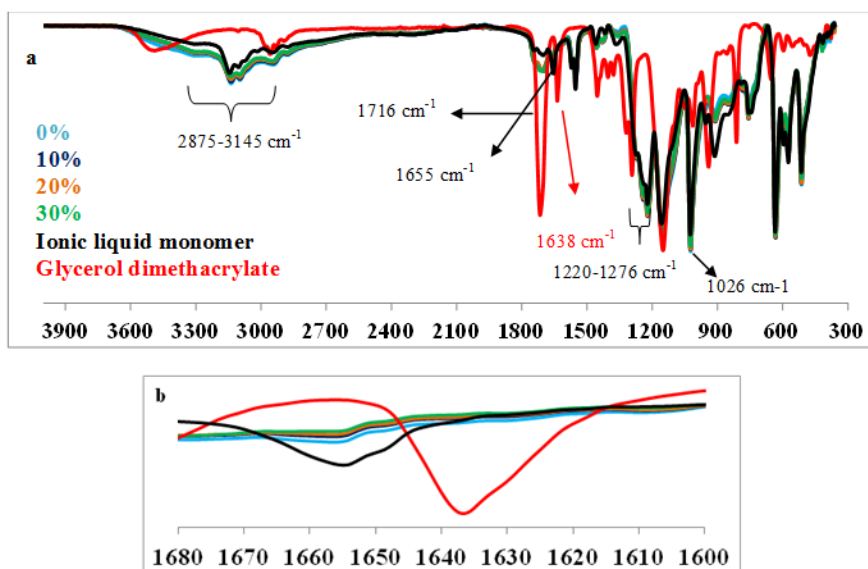


Figure 4.6. ATR-FTIR spectra of triflate membranes

The C=C vibration bands arising from the ionic liquid monomer and the crosslinker at 1655 and 1638 cm^{-1} , respectively, disappear as they are consumed upon exposure to UV light in the presence of the initiator. As it is seen in figure 4.6, the two bands decrease in the final membranes indicating that the monomers are successfully polymerized.

One important aspect worth mentioning is that the ionic liquid monomer conversion is proportional to the amount of free ionic liquid inside the mixture. As it is seen in figure 4.6b at 1655 cm^{-1} signal, there is little residual monomer left inside the membrane for the sample containing 0% free ionic liquid. The intensity of that peak at 1655 cm^{-1} from the ionic liquid monomer gradually decreases with increasing amount of free ionic liquid due to the fact that the mobility of the monomer molecules is enhanced inside the ionic liquid resulting in higher conversion to polymer. Namely, the monomer to polymer conversion increases with increasing free ionic liquid content acting as a diluent to the system.

Other characteristic peaks originating from the membranes are observed in the spectra as well. In general, the peaks between 2875-3145 cm^{-1} arise due to C-H and O-H stretching motions, the band at 1716 cm^{-1} is attributed to C=O stretching motion, the peaks between 1220-1276 cm^{-1} originate from asymmetric SO_3 and symmetric CF_3 stretching vibrations and the peaks at 1026 cm^{-1} originate from symmetric SO_3 stretching.

Figure 4.7 shows the ATR-FTIR spectra of sulfoethylmethacrylate anion-based membrane.

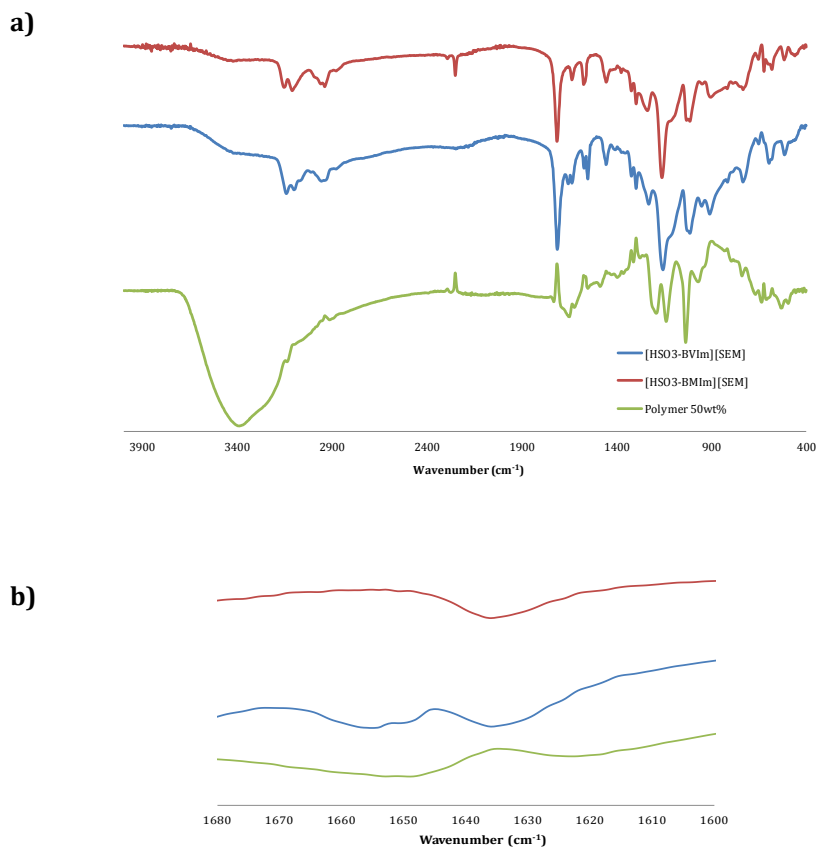


Figure 4.7. a) ATR-FTIR spectra of the polymerizable sulfoethylmethacrylate anion-based ionic liquids and the membrane from 400 to 4000 cm⁻¹ b) 1600-1680 cm⁻¹ region of the spectra

The C=C vibration band corresponding to the vinyl group located in the ionic liquid monomer [HSO₃-BIm][SEM] at 1655 cm⁻¹ attenuates as it is consumed upon exposure to UV light in the presence of the initiator. In the same way, the C=C vibration bands corresponding to the methacrylate groups of both ionic liquids and

the crosslinker at 1638 cm^{-1} disappear. As it is seen in figure 4.7, the two bands decrease in the final membrane indicating the success of the photopolymerization.

TGA-DSC measurements

In general, ionic liquids are very hygroscopic compounds able to absorb water from the atmosphere. It is crucial to identify the water content of polymerizable ionic liquids as it affects the ion transport properties of the membranes. For this reason, a thermogravimetric analysis was carried out in order to determine the onset degradation temperature (T_o) and the water content (W_c) of the polymerized membranes. W_c was determined by the weight difference between the initial weight of the membrane at room temperature and the weight of the membrane at $150\text{ }^\circ\text{C}$. The onset degradation temperature is the temperature at the intersection of the extrapolated base line with the tangent to the curve taken at the point of maximum slope. W_c of ionic liquid samples was determined using Karl-Fischer technique.

Thermogravimetric analysis (TGA) of the triflate and sulfoethylmethacrylate anion-based membranes are shown in figures 4.8 and 4.9, respectively.

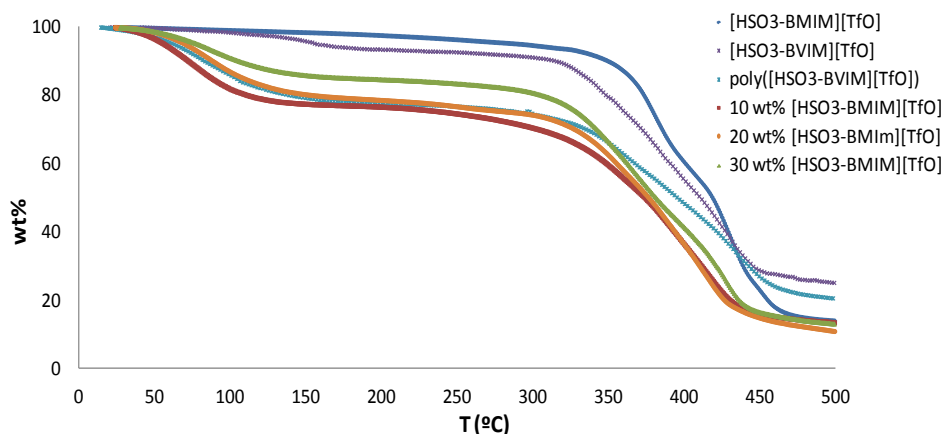


Figure 4.8. TGA curves of triflate ionic liquids and their polymer blends

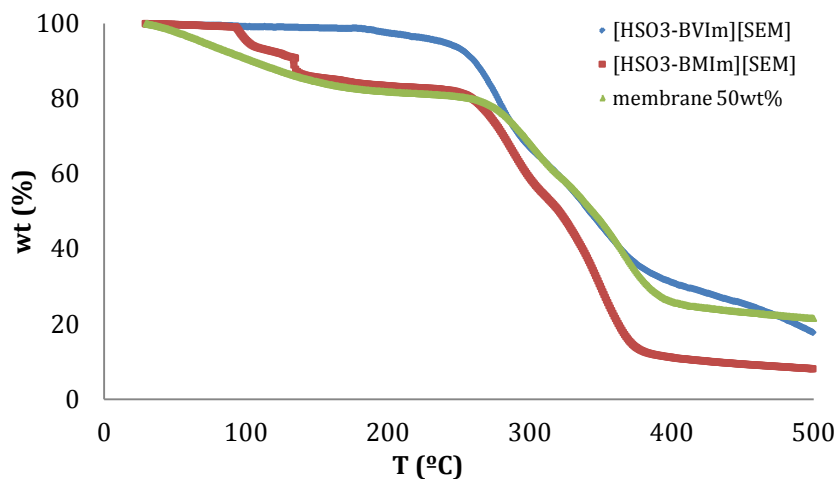


Figure 4.9. TGA curves of sulfoethylmethacrylate ionic liquids and their polymer blend

All polymeric membranes show two-step degradation. The first weight loss occurring at $T < 150$ °C is associated to the water inside the structure of the ionic liquid and between polymer chains. The water content (W_c) and the onset temperature (T_o) for each electrolyte are shown in tables 4.1 and 4.2.

Table 4.1. T_o onset and water content of triflate ionic liquids and their polymeric forms

	ILs		Poly([HSO ₃ -BVIm][TfO])/[HSO ₃ -BMIm][TfO] x wt% [HSO ₃ -BMIm][TfO]			
	[HSO ₃ -BVIm][TfO]	[HSO ₃ -BMIm][TfO]	0	10	20	30
Wc (wt%)	0.97	0.63	20.7	22.5	19.7	14.1
To (°C)	336.3	353.6	329.6	332.4	329.9	325.3

Table 4.2. T onset and water content of sulfoethylmethacrylate ionic liquids and their polymeric form

	[HSO ₃ -BVIIm][SEM]	[HSO ₃ -BMIm][SEM]	poly[HSO ₃ -BVIIm][SEM]/ poly[HSO ₃ -BMIm][SEM] (50 wt%)
Wc (wt%)	1.7	0.13	15.4
To (°C)	256.5	259.9	274.1

The information collected in the two tables shows that polymeric ionic liquid-based electrolytes are able to retain high quantities of atmospheric water inside their structure. Regarding triflate anion-based membranes, in the case of the sample with 10 wt% free ionic liquid nearly a quarter of the weight was due to retained water. However, the non-polymerizable ionic liquid and the monomer retain less water inside their structure, 0.63 wt% and 0.97 wt% respectively. With respect to sulfoethylmethacrylate anion-based ionic liquids, the water content of the polymeric membrane based on [HSO₃-BVIIm][SEM]/[HSO₃-BMIm][SEM] (50/50 wt%) was 15.4 wt%, whereas the water content of [HSO₃-BVIIm][SEM] and [HSO₃-BMIm][SEM] was 1.7 and 0.13 wt%, respectively. The reason behind the fact that polymeric electrolytes take up more water than ionic liquids is that they have a well-organized structure with nanometer-size hydrophilic domains capable of retaining water inside [31].

Ionic liquids are compounds with high thermal stability. This property is reflected in the calculated onset temperature which has a value higher than 250 °C for all the studied samples. The thermal stability of triflate anion-based membrane was slightly higher than sulfoethylmethacrylate membranes, demonstrating their suitability for fuel cells working at temperatures higher than 300 °C.

Differential scanning calorimetry experiments were performed to triflate anion-based membranes in order to determine the thermal properties of the polymer blends. All the materials were found to be amorphous and displayed glass transition temperatures (T_g). Fairly broad glass transitions were observed for all the

materials; therefore the midpoint of the transition region was taken and reported as the T_g of the material. Figure 4.10 shows that the material that does not contain any free ionic liquid displayed a T_g around 10 °C. When free ionic liquid is introduced, the T_g dropped down to -10 °C followed by a gradual decrease as the amount of free ionic liquid increases in the membrane. T_g s were recorded as -22 °C and -32 °C for the membranes containing 20 wt% and 30 wt% free ionic liquid, respectively. This behaviour is a clear evidence of the highest flexibility of the resulting polymer when a non-polymerizable ionic liquid is introduced in the structure.

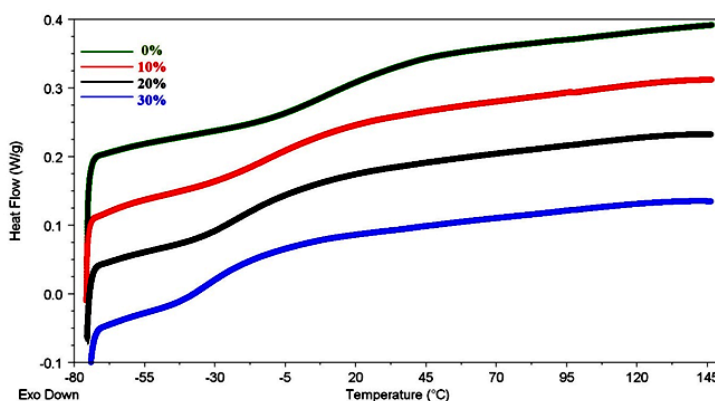


Figure 4.10. DSC traces of triflate membranes

4.3.2. Influence of temperature and water content on ex-situ ionic conductivity

One of the aims of this thesis is the development of membranes based on ionic liquids for proton exchange membrane fuel cells capable of working without external humidification. However, it is well-known that water has a key role in proton transport by Grotthuss and vehicular mechanisms. It is worth noting that despite working without inlet humidification, water is the only byproduct of the electrochemical reactions taking place at the fuel cell electrodes. Moreover, ionic liquids are very hygroscopic compounds able to absorb water from the atmosphere as it was previously demonstrated.

The herein studied ionic liquids contain SO_3H groups which in presence of water dissociate into immobile SO_3^- anions and free protons that move through the hydrogen-bonded network and thereby they are responsible for the expected higher ionic conductivity of polymeric membranes with high water contents [32].

In order to analyze the effect of the water content on the ionic conductivity, ex-situ ionic conductivity measurements were carried out. For this purpose, ionic liquid membranes were synthesized and their ionic conductivity was measured using the homemade ionic conductivity cell. Once measured, membranes were dried under vacuum (3 mbar) at 60 °C for 24 hours and their ionic conductivity was measured again.

Ex-situ ionic conductivities at different temperatures for the triflate anion-based blends are compared with those obtained with dry membranes in figure 4.11.

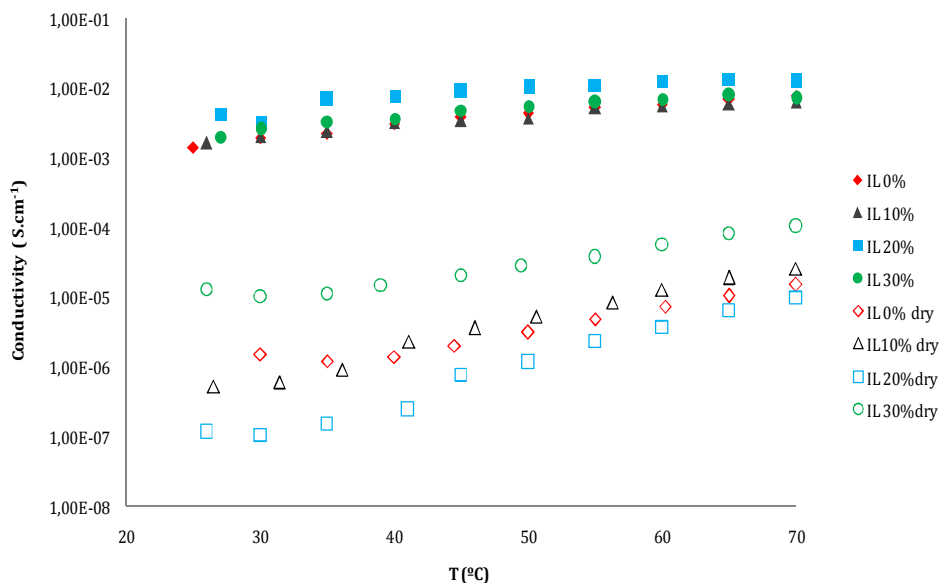


Figure 4.11. Ionic conductivity of triflate poly(ionic liquid)/ionic liquid membranes. Influence of temperature and water content

As it can be observed in figure 4.11, dry membranes have noticeable lower ionic conductivity than membranes without drying. As it was previously mentioned, the high conductivity of the polymeric ionic liquid membranes with high water content is mainly due to the mobile protons produced in the dissociation of HSO_3 groups in presence of water. As TGA results showed that these composite membranes contain high amounts of retained water inside their chemical structure, there are plenty of mobile protons that can easily jump through the H-bonded network formed by ions and water molecules [32].

As expected, the external ionic conductivity increased with temperature for all membranes. The influence of temperature is more noticeable in the case of dried membranes. In the case with 10 wt% of non-polymerizable ionic liquid, ionic conductivity increased 90 times when temperature increased from 25 to 70 °C. The temperature dependence of polymeric ionic liquid-based electrolytes suggests two competing trends, in agreement with the results reported by Zaidi et al.[33]. It is generally expected that ionic conductivity increases with temperature because it is a thermally activated phenomenon. However, at high temperature the evaporation of the retained atmospheric water takes place and the conductivity decrease. Thus, the resulting ionic conductivity is a compromise between these two trends.

Among dried membranes, the highest conductivity was obtained for the membrane with 30 % free ionic liquid, $1.05 \times 10^{-4} \text{ S.cm}^{-1}$ at 70 °C. The high non-polymerizable ionic liquid content inside its structure gives fluidity and enhances the ionic conductivity of this electrolyte. Membranes with lower ratios of non-polymerizable ionic liquid content have similar ionic conductivity values, especially at high temperatures reaching values around $1.5 \times 10^{-5} \text{ S.cm}^{-1}$ at 70 °C. In the case of membranes with high water content, there is no influence of the non-polymerizable ionic liquid ratio on the ionic conductivity. All the electrolytes show similar ionic conductivities, ranging from $10^{-3} \text{ S.cm}^{-1}$ at 25 °C to $10^{-2} \text{ S.cm}^{-1}$ at 70°C.

Figure 4.12 shows ex-situ ionic conductivities at different temperatures for sulfoethylmethacrylate membranes.

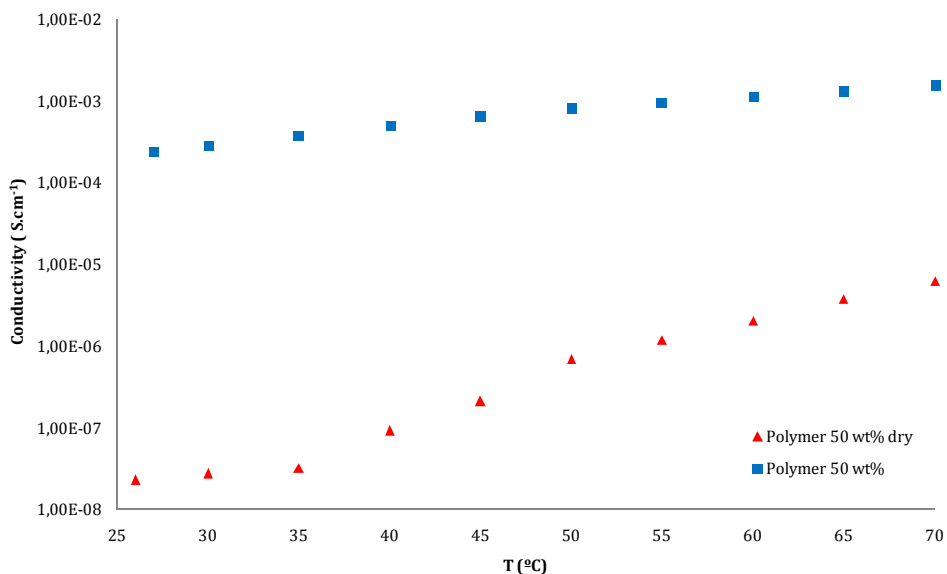


Figure 4.12. External ionic conductivity of sulfoethylmethacrylate anion-based membranes (50wt%)

Similar to triflate electrolytes, membranes with high water content have noticeable higher ionic conductivity compared to dry membranes, especially at low temperature. The dried membrane has ionic conductivity of $2.3 \times 10^{-8} \text{ S.cm}^{-1}$ at 25 °C whereas the membrane with high water content shows ionic conductivity of $2.37 \times 10^{-4} \text{ S.cm}^{-1}$ at the same temperature. At 70 °C, the dried membrane has ionic conductivity about $6.24 \times 10^{-6} \text{ S.cm}^{-1}$ whereas the membrane with high water content has ionic conductivity of $1.5 \times 10^{-2} \text{ S.cm}^{-1}$ at the same temperature.

Increasing temperature improved the external ionic conductivity, especially for membranes with low water content as it was discussed for triflate anion-based membranes. For these dried membranes, ionic conductivity was increased by 2 orders of magnitude, from $2.3 \times 10^{-8} \text{ S.cm}^{-1}$ at 25 °C to $6.24 \times 10^{-6} \text{ S.cm}^{-1}$ at 70 °C.

4.3.3. Ionic conductivity mechanisms in polymerized ionic liquids: ion dynamics studies

Ion dynamics studies were carried out to study the proton transport mechanisms of the [HSO₃-BVIIm][TfO] ionic liquid and its polymerized form as well as [HSO₃-BVIIm][SEM]/[HSO₃-BMIm][SEM] (50wt%) polymeric membrane. These measurements were performed in the Institute of Physics at the University of Silesia (Poland) headed by Prof. M. Paluch.

According to Wojnarowska and Paluch [34], in protic ionic liquids the proton transport is governed by the Grotthuss mechanism if at glass transition temperature (T_g) the temperature dependence of the conductivity relaxation time (τ_σ) reveals a well-defined shift from non-Arrhenius (T>T_g) to Arrhenius behavior (T<T_g) at τ_σ faster than 10² s. The difference between conductivity relaxation time (τ_σ) and segmental relaxation time (τ_α) at T_g is called decoupling, which is a consequence of the fast proton migration typical for the Grotthuss mechanism. It means that the ionic motions are still very fast when the structural relaxation becomes frozen [35, 36].

Ionic dynamics of [HSO₃-BVIIm][TfO] ionic liquid and its polymerized form were investigated. As it can be observed in figure 4.13, only in the case of the polymer there is a significant decoupling between the time scale of conductivity and segmental relaxation in the vicinity of the T_g. This indicates that H⁺ might still diffuse when the segmental dynamics is very slow or even completely frozen at T_g.

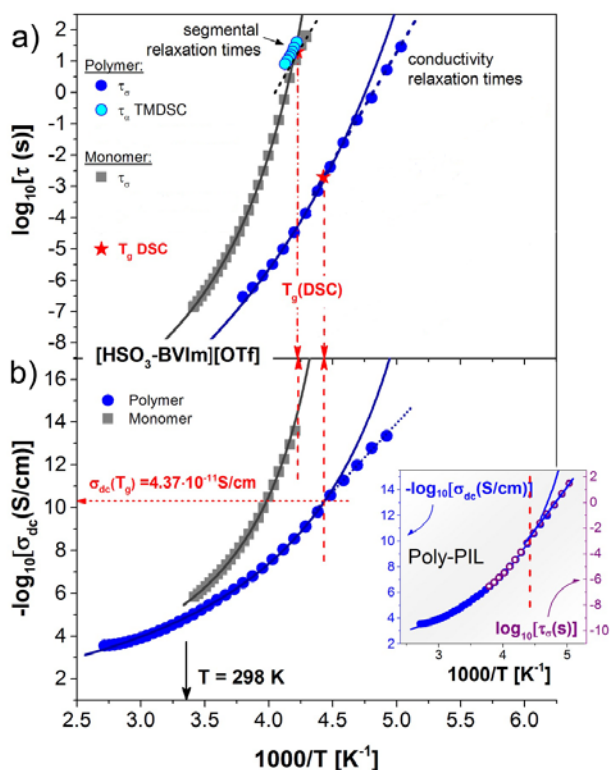


Figure 4.13. Temperature dependence of τ_{σ} (a) and conductivity (b) for the polymerized $[\text{HSO}_3\text{-BVIm}][\text{TfO}]$ and its monomer. The inset panel presents the $\log \sigma_{dc}(1/T)$ and $\log \tau_{\sigma}(1/T)$ data recorded for polymerized ILs.

Moreover, the conductivity of the polymer exceeds the value obtained for the monomer in the whole explored temperature range. Consequently, it can be assumed that different mechanisms are responsible for the conducting properties of the ionic liquid monomer and its polymerized counterpart.

As previously indicated, there are two types of charge transport mechanisms in protic ionic conductors: vehicle and Grotthuss-type. In the vehicle mechanism the charge transfer is connected with the molecular diffusion. Consequently, the conductivity is controlled by the viscosity of the system. On the other hand, in the Grotthuss mechanism, the charge transport is realized through the proton hopping via the hydrogen bonding network in addition to the translational diffusion of ions.

Intuitively, the proton migration in the H-bonded systems is much faster than the typical ionic diffusion. Therefore, the Grotthuss mechanism can be considered the reason for both the excess conductivity of polymerized ionic liquid as well as the decoupling phenomenon between τ_α and τ_σ . As a consequence, it can be assumed that in the case of the monomer the conductivity is controlled mainly by vehicular mechanism in contrast to the polymer where the proton hopping is much more relevant.

To provide a deeper understanding of the charge transport mechanism in polymerized [HSO₃-BVIm][TfO] its chemical structure was analyzed. As it was previously mentioned, when sulfonate groups are exposed to water, they dissociate into immobile SO₃⁻ residing on the side chains of the polymer and free mobile protons. As it was proved before, the synthesized poly[HSO₃- BVIm][TfO] is a highly water-saturated macromolecular system. Therefore, in the polymer matrix there are plenty of mobile protons that can easily jump through the dense H-bonded network formed by ions and water molecules. Therefore, the high conductivity of the examined polymerized protic ionic liquid is mainly due to the mobile protons that are released during dissociation of HSO₃ groups. Consequently, the σ_{dc} value is expected to decrease when the amount of water is limited as it was proved in section 4.3.2.3.

To explore the effect of water presence on the ion transport properties of the dried poly[HSO₃-BVIm][OTf] sample, the temperature dependences of conductivity and conductivity relaxation times were determined. As it can be easily seen in Figure 4.14b, evaporation of water from the polymer matrix results in a dramatic decrease of σ_{dc} . Additionally, in the whole examined temperature range, it is lower than the conductivity of non-polymerized IL, which is now in agreement with literature. However, at T_g the values of σ_{dc} are also the same. Interestingly, the kink of $\tau_\sigma(T)$ dependence from VFT-like to Arrhenius behavior determined for dried poly IL occurs at practically the same conductivity relaxation times as for the hydrated sample ($\tau_\sigma \sim 0.005$ s) (Figure 4.14a). It means that the charge transport in the

annealed poly[HSO₃-BVIIm][TfO] is still governed by the fast proton hopping through the H-bond network due to the delocalization of proton in the imidazolium cation. Consequently, using protic ionic liquids as a polyelectrolyte one can avoid the serious problem of water management observed for commercial membranes for low temperature fuel cell applications.

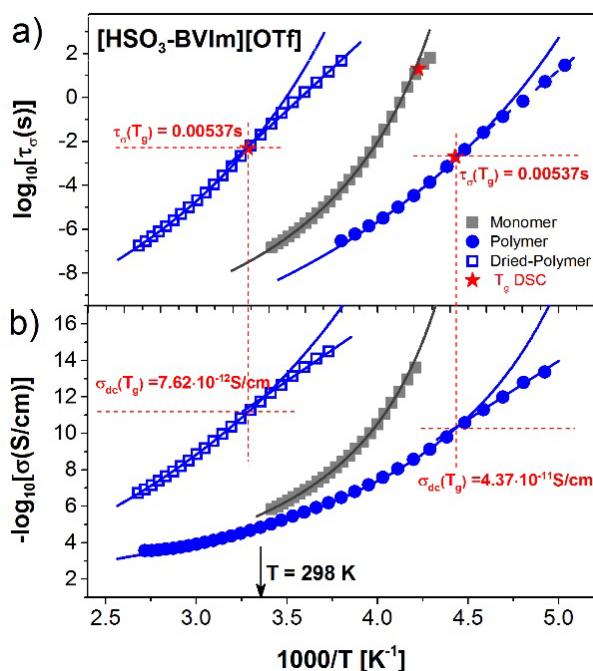


Figure 4.14. Temperature dependence of τ_σ (a) and conductivity (b) for the hydrated polymerized protic ionic liquids (solid circles), dried polymer membrane (open squares) and monomer (solid squares). Red stars denote the T_g values determined from DSC measurements.

The charge transport mechanism of [HSO₃-BVIIm][SEM]/[HSO₃-BVIIm][SEM] (50/50 wt%) membrane was also studied by means of high pressure conductivity measurements. High pressure conditions were selected because the compression of a sample not only reduces interatomic distances and free volume required for ions motions, but also reinforces the H-bonded network, consequently affecting both vehicle transport and proton hopping.

For these measurements, all polymerized ionic liquids were compressed isothermally at different temperatures above T_g . It was observed that the value of the conductivity relaxation time (τ_σ) at glass transition pressure (P_g) is faster with pressure. Due to the fact that the structural relaxation time (τ_α) is ≈ 100 s regardless of T-P conditions, compression strongly affects the decoupling between τ_σ and τ_α . This behavior demonstrates that an effective proton hopping is involved in charge transport of these membranes, because only the proton transport is accelerated when inter ionic distances are reduced and the H-bonded network becomes reinforced, both taking place under high pressure conditions.

4.3.4. Fuel cell performance

This section shows the fuel cell performance obtained for ionic polymeric liquid-based membranes. It is worth noting that the following studies included in this chapter are focused on triflate anion-based membranes. Sulfoethylmethacrylate membranes are not included due to the fact that their ionic conductivity values were slightly lower than that obtained for triflate membranes. Moreover, the mechanical stability of these membranes is not adequate enough for their testing in the fuel cell system.

4.3.4.1. Influence of the thickness of the membrane

The influence of polymerized $[\text{HSO}_3\text{-BVIIm}][\text{TfO}]$ membranes thickness was analyzed. For this purpose, membranes with different thickness (240 and 310 μm) were synthesized. The experiments were carried out under non-humidified conditions at 25 °C and 1.2 bar. The hydrogen and air flow rates were fixed at 125 $\text{ml}\cdot\text{min}^{-1}$ and 500 $\text{ml}\cdot\text{min}^{-1}$, respectively.

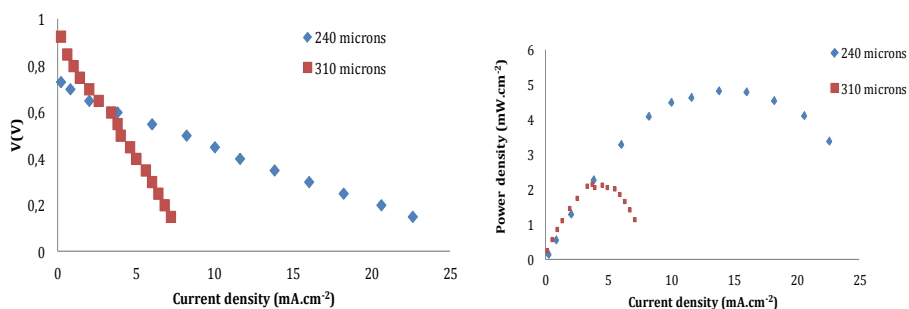


Figure 4.15. Influence of membrane thickness. Polarization and power curves

As it can be observed in figure 4.15, thinner membranes generate higher current density, 22.6 mA.cm⁻² at 0.15V, than thicker membranes, 7.2 mA.cm⁻², because of their lower proton transport resistance. However, these membranes show a value of open circuit voltage (OCV) around 0.73 V, lower than the value reached with the thicker membrane, 0.93 V due to fuel crossover. Using a thin membrane the resistance to fuel crossover through the membrane is lower causing a decrease in the voltage due to a more pronounced effect of a mixed potential [37,38].

4.3.4.2. Influence of non-polymerizable ionic liquid and temperature

Figures 4.16 and 4.17 report the fuel cell performance of the electrolytes based on polymerized ionic liquid and ionic liquid blends at 25 and 40 °C, respectively. The maximum current density obtained with poly([HSO₃-BVIIm][TfO]) is 43 mA.cm⁻², while the peak power density is approximately 14 mW.cm⁻². As it can be seen in the figures, the addition of free ionic liquid improves the fuel cell performance. Thus, the addition of 10 wt% of free ionic liquid leads to an increase in the peak power density of 30 mW.cm⁻² and in the maximum current density of 131 mA.cm⁻² at 25 °C when it is compared with the membrane with 0 wt% free IL. Additionally, an increase in the open circuit voltage is also observed. However, this improvement is less pronounced at higher quantities of free ionic liquid due to the poor mechanical stability of the electrolyte. In the case of 20 wt% free ionic liquid, the peak power

density increases to 26 mW.cm^{-2} and at 30 wt%, the peak power density is slightly lower than in the membrane with 0 wt% free IL.

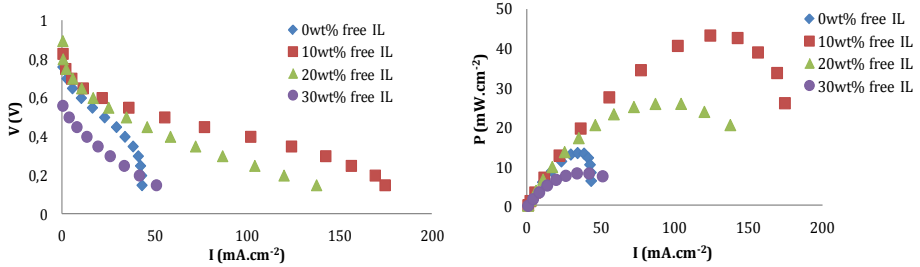


Figure 4.16. Polarization and power curves at 25 °C

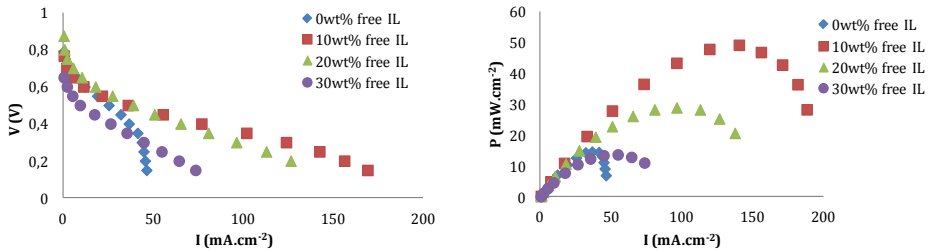


Figure 4.17. Polarization and power curves at 40 °C

It is worth mentioning that increasing temperature improves fuel cell performance, especially in the case of 30 wt% free ionic liquid in which the maximum current density reaches the value of 73 mA.cm^{-2} and the peak power density of 13.6 mW.cm^{-2} when the temperature rises from 25 to 40 °C. At lower free ionic liquid content, the effect of temperature is less marked and electrolyte with 20 wt% free ionic liquid content reaches practically the same performance at both temperatures.

Despite the fact that an increase in temperature improves the fuel cell performance especially at high free ionic liquid contents, the poor mechanical stability of the membrane hinders the application at temperatures above 40 °C. It was observed that at high temperatures the membrane penetrates into the GDEs and obstructs the gas supply to the reaction zone resulting in a poorer fuel cell performance. This

mechanical stability could be improved by adding higher quantities of crosslinker. Nevertheless, the ionic conductivity could be compromised. Further work is needed in order to develop polymeric membranes based on ionic liquids able to provide high fuel cell performance at high temperature.

Table 4.3 shows the *in-situ* ionic conductivity of the electrolyte membranes with different quantities of [HSO₃-BMIm][TfO]. All samples report high conductivities in the same order of magnitude, 10⁻¹ S.cm⁻¹, except for the electrolyte with 30 wt% [HSO₃-BMIm][TfO] which is in the order of 10⁻² S.cm⁻¹. It is worth noting that conductivities are in agreement with the fuel cell performance and membranes with highest conductivities are those that provide higher fuel cell performance.

Table 4.3. *In-situ* ionic conductivity at 25 and 40 °C (x 10⁻¹ S.cm⁻¹)

IL(wt%)	25 °C	40 °C
0	1.231	1.249
10	2.090	2.925
20	1.272	1.274
30	0.619	0.767

The addition of small quantities of [HSO₃-BMIm][TfO] improves noticeably the ionic conductivity. The addition of 10 wt% of free ionic liquid improves the ionic conductivity by 69% at 25 °C and by 134% at 40 °C. However, this tendency does not continue at higher quantities of free ionic liquid probably due to the poor mechanical stability of the electrolyte as it was aforementioned. Moreover, it is well-known that the ionic conductivity depends on the hydration of the electrolyte because water facilitates the proton transport and it has been demonstrated that electrolytes with high free ionic liquid amount retain less water. Thus, the addition of 20 wt% of free ionic liquid slightly improves ionic conductivity by 3% at 25 °C and by 2% at 40°C. Nevertheless, with 30 wt% free ionic liquid the conductivity is lower than that of the membrane without free ionic liquid. Moreover, the fact that hydration enhances ionic conductivity justifies the higher conductivity reported for

in-situ experiments compared with that obtained during *ex-situ* conductivity measurements. In-situ measurements were carried out during fuel cell experiments being water the only byproduct of the electrochemical reactions.

As it is shown in table 4.3, the temperature improves the ionic conductivity. However, due to the fact that the ionic conductivity values were measured during fuel cell experiments, the poor mechanical stability of the composite membranes hindered the ionic conductivity measurements at temperatures above 40 °C.

The ionic conductivities obtained with these composite membranes are in the same order of magnitude as other well-hydrated membranes reported in literature. In the study developed by Zeng et al. [39] silica was added to a Nafion membrane in order to increase humidification of the membrane. Conductivities of $1.11 \times 10^{-1} \text{ S.cm}^{-1}$ were obtained at 25 °C with 15 wt% silica. In another study published by Costamagna and coworkers [40] zirconium phosphate was incorporated in a recast Nafion membrane in order to enhance water retention. Conductivities about $1.2 \times 10^{-1} \text{ S.cm}^{-1}$ were obtained at 100 °C.

It is worth mentioning that ionic conductivities are in the same order of magnitude than that for Nafion when the membrane is properly hydrated. However, the fuel cell performance is lower when it is compared with this case. Thus, differences in fuel cell performance cannot be explained exclusively on the basis of ionic conductivity since there are additional key parameters such as mechanical stability and the influence of the catalyst activity [41].

4.4. Conclusions

Proton exchange membranes based on polymerized ionic liquids were developed for PEMFC applications without external humidification. For this purpose, two different membrane structures were studied.

The first membrane was based on the two polymerizable ionic liquids 1-(4-sulfobutyl)-3-methylimidazolium 2-sulfoethylmethacrylate [HSO₃-BMIm][SEM] and 1-(4-sulfobutyl)-3-vinylimidazolium 2-sulfoethylmethacrylate [HSO₃-BVIIm][SEM] (50 wt%). The effects of temperature and water content on ionic conductivity were studied. Membranes with high water content had noticeable higher ionic conductivity compared with dry membranes, especially at low temperature. The dried membrane showed ionic conductivity of $6.24 \times 10^{-6} \text{ S.cm}^{-1}$ at 70 °C whereas the membrane with high water content had ionic conductivity of $1.5 \times 10^{-3} \text{ S.cm}^{-1}$ at same temperature.

In the second structure studied in this chapter, 1-(4-sulfobutyl) 3-vinylimidazolium trifluoromethanesulfonate [HSO₃-BVIIm][TfO] ionic liquid was polymerized with different quantities of the non-polymerizable ionic liquid 1-(4-sulfobutyl) 3-methylimidazolium trifluoromethanesulfonate [HSO₃-BMIm][TfO]. Poly([HSO₃-BVIIm][TfO])/[HSO₃-BMIm][TfO] mixtures showed high *in-situ* ionic conductivities, in the order of 10^{-1} – $10^{-2} \text{ S.cm}^{-1}$. The addition of small quantities of [HSO₃-BMIm][TfO] and temperature improved ionic conductivity. It is worth mentioning that conductivities were in accordance with fuel cell performance. Thus, the membrane with 10 wt% [HSO₃-BMIm][TfO] showed the highest conductivity, $2.92 \times 10^{-1} \text{ S.cm}^{-1}$ and the best fuel cell performance, 189 mA.cm⁻² at 0.15 V and peak power density of 49 mW.cm⁻² at 40 °C.

In both membranes studied in this chapter, the high conductivity of the membranes with high water content was mainly due to the mobile protons produced in the dissociation of HSO₃ groups when they are in presence of water. Temperature improved the ionic conductivity because it produces faster movement of ions and consequently an increase in ionic conductivity. However, in the case of membranes with higher water content, the effect of temperature in the ionic conductivity was less pronounced because of the evaporation of the water which plays a key role in proton transport.

Broadband dielectric spectroscopy combined with temperature-modulated differential scanning calorimetry were used in order to analyze the molecular dynamics and ions transport properties of polymerized ionic liquid-based membranes.

The high pressure dielectric technique has demonstrated that in sulfoethylmethacrylate anion-based membrane the proton transport is governed by the Grotthuss mechanism. It has been proved that the decoupling between charge transport and structure reorganization increased with pressure in the case of protic ionic liquid polymers. The explanation for this tendency is due to the fact that the H-bonded network becomes reinforced when interionic distances are reduced by compression.

The large decoupling between the conductivity relaxation times (τ_{σ}) and segmental dynamics (τ_{α}) observed for [HSO₃-BVIm][TfO] polymer membrane in the vicinity of T_g is an evidence that the conductivity of the studied polymer is controlled by the Grotthuss mechanism, in contrast to the monomer controlled by vehicular mechanism. Evaporation of water from the polymer matrix resulted in a noticeable decrease of σ_{dc} . Interestingly, despite the drop in the water content, the kink of $\tau_{\sigma}(T)$ dependence from VFT-like to Arrhenius behavior occurred at practically the same conductivity relaxation times. Furthermore, the value of $\sigma_{dc}(T_g)$ also remained unchanged. These facts suggest that regardless of the amount of water present in the sample, the charge transport mechanism of the polymeric membrane is permanently governed by fast proton hopping. Consequently, using protic ionic liquids as polyelectrolyte one can avoid the serious problem of water management observed with commercial membranes for low temperature fuel cell applications.

4.5. References

- [1] S. Imaizumi, H. Kokubo and M. Watanabe. Polymer actuators using ion-gel electrolytes prepared by self-assembly of ABA-triblock copolymers. *Macromolecules*, 45 (2012) 401.
- [2] M. Díaz, A. Ortiz and I. Ortiz. Progress in the use of ionic liquids as electrolyte membranes in fuel cells. *J.Membr.Sci.*, 469 (2014) 379.
- [3] J. Le Bideau, L. Viau and A. Vioux. Ionogels, ionic liquid based hybrid materials. *Chem.Soc.Rev.*, 40 (2011) 907.
- [4] T. Yasuda, S. Nakamura, Y. Honda, K. Kinugawa, S. Lee and M. Watanabe. Effects of polymer structure on properties of sulfonated polyimide/protic ionic liquid composite membranes for nonhumidified fuel cell applications. *ACS Appl.Mater.Interfaces*, 4 (2012) 1783.
- [5] S. Lee, A. Ogawa, M. Kanno, H. Nakamoto, T. Yasuda and M. Watanabe. Nonhumidified intermediate temperature fuel cells using protic ionic liquids. *J.Am.Chem.Soc.*, 132 (2010) 9764.
- [6] T. Ueki, M. Watanabe. *Macromolecules in ionic liquids: Progress, challenges, and opportunities*. *Macromolecules*, 41 (2008) 3739.
- [7] E. Van De Ven, A. Chairuna, G. Merle, S.P. Benito, Z. Borneman and K. Nijmeijer. Ionic liquid doped polybenzimidazole membranes for high temperature Proton Exchange Membrane fuel cell applications. *J.Power Sources*, 222 (2013) 202.
- [8] J.E. Bara, D.L. Gin and R.D. Noble. Effect of anion on gas separation performance of polymer-room-temperature ionic liquid composite membranes. *Ind Eng Chem Res*, 47 (2008) 9919.
- [9] J.E. Bara, E.S. Hatakeyama, C.J. Gabriel, X. Zeng, S. Lessmann, D.L. Gin et al. Synthesis and light gas separations in cross-linked gemini room temperature ionic liquid polymer membranes. *J.Membr.Sci.*, 316 (2008) 186.
- [10] J.E. Bara, E.S. Hatakeyama, D.L. Gin and R.D. Noble. Improving CO₂ permeability in polymerized room-temperature ionic liquid gas separation membranes through the formation of a solid composite with a room-temperature ionic liquid. *Polym.Adv.Technol.*, 19 (2008) 1415.

- [11] K. Simons, K. Nijmeijer, J.E. Bara, R.D. Noble and M. Wessling. How do polymerized room-temperature ionic liquid membranes plasticize during high pressure CO₂ permeation? *J.Membr.Sci.*, 360 (2010) 202.
- [12] H. Ohno. Design of ion conductive polymers based on ionic liquids. *Macromol.Sympos.*, 249-250 (2007) 551.
- [13] J. Lemus, A. Eguizábal and M.P. Pina. UV polymerization of room temperature ionic liquids for high temperature PEMs: Study of ionic moieties and crosslinking effects. *Int J Hydrogen Energy*, 40 (2015) 5416.
- [14] T. Bui. Solid state dye-sensitized solar cells based on polymeric ionic liquid with free imidazolium cation. *ELECTRONIC MATERIALS LETTERS*, 10 (01) 209; 209.
- [15] H.J. Hwang. Selective Ion Transporting Polymerized Ionic Liquid Membrane Separator for Enhancing Cycle Stability and Durability in Secondary Zinc-Air Battery Systems. *ACS applied materials & interfaces*, 8 (05) 26298; 26298.
- [16] K.M. Meek, Y.A. Elabd. Polymerized ionic liquid block copolymers for electrochemical energy. *J.Mater.Chem.A*, 3 (2015) 24187.
- [17] K.M. Meek, Y.A. Elabd. Sulfonated Polymerized Ionic Liquid Block Copolymers. *Macromol.Rapid Commun.*, 37 (2016) 1200.
- [18] D. Mecerreyes. Polymeric ionic liquids: Broadening the properties and applications of polyelectrolytes. *Prog Polym Sci (Oxford)*, 36 (2011) 1629.
- [19] J. Yuan, D. Mecerreyes and M. Antonietti. Poly(ionic liquid)s: An update. *Prog.Polym.Sci.*, 38 (2013) 1009.
- [20] M. Yoshizawa, W. Ogihara and H. Ohno. Novel polymer electrolytes prepared by copolymerization of ionic liquid monomers. *Polym.Adv.Technol.*, 13 (2002) 589.
- [21] H. Ohno, M. Yoshizawa and W. Ogihara. Development of new class of ion conductive polymers based on ionic liquids. *Electrochim.Acta*, 50 (2004) 255.
- [22] H. Ohno. Molten salt type polymer electrolytes. *Electrochim.Acta*, 46 (2001) 1407.
- [23] K. Pähako-Esko, M. Timusk, K. Saal, R. Lähmus, I. Kink and U. Mäeorg. Increased conductivity of polymerized ionic liquids through the use of a nonpolymerizable ionic liquid additive. *J.Mater.Res.*, 28 (2013) 3086.

- [24] R. Marcilla, F. Alcaide, H. Sardon, J.A. Pomposo, C. Pozo-Gonzalo and D. Mecerreyes. Tailor-made polymer electrolytes based upon ionic liquids and their application in all-plastic electrochromic devices. *Electrochem.Commun.*, 8 (2006) 482.
- [25] G. Zarca, W.J. Horne, I. Ortiz, A. Urtiaga and J.E. Bara. Synthesis and gas separation properties of poly(ionic liquid)-ionic liquid composite membranes containing a copper salt. *J.Membr.Sci.*, 515 (2016) 109.
- [26] P. Li, K.P. Pramoda and T. Chung. CO₂ separation from flue gas using polyvinyl-(room temperature ionic liquid)-room temperature ionic liquid composite membranes. *Ind Eng Chem Res*, 50 (2011) 9344.
- [27] M. Díaz, A. Ortiz, M. Isik, D. Mecerreyes and I. Ortiz. Highly conductive electrolytes based on poly([HSO₃-BVIm][TfO])/[HSO₃-BMIm][TfO] mixtures for fuel cell applications. *Int J Hydrogen Energy*, 40 (2015) 11294.
- [28] M. Díaz, A. Ortiz, M. Vilas, E. Tojo and I. Ortiz. Performance of PEMFC with new polyvinyl-ionic liquids based membranes as electrolytes. *Int J Hydrogen Energy*, 39 (2014) 3970.
- [29] Y. Jeong, D. Kim, Y. Choi and J. Ryu. Intramolecular hydroalkoxylation in Brønsted acidic ionic liquids and its application to the synthesis of (±)-centrolobine. *Org.Biomol.Chem.*, 9 (2011) 374.
- [30] H. Zhou, J. Song, X. Kang, J. Hu, Y. Yang, H. Fan et al. One-pot conversion of carbohydrates into gamma-valerolactone catalyzed by highly cross-linked ionic liquid polymer and Co/TiO₂. *RSC Adv.*, 5 (2015) 15267.
- [31] M. Rikukawa, K. Sanui. Proton-conducting polymer electrolyte membranes based on hydrocarbon polymers. *Progress in Polymer Science*, 25 (2000) 1463.
- [32] Z. Wojnarowska, J. Knapik, M. Díaz, A. Ortiz, I. Ortiz and M. Paluch. Conductivity mechanism in polymerized imidazolium-based protic ionic liquid [HSO₃-BVIm][OTf]: Dielectric relaxation studies. *Macromolecules*, 47 (2014) 4056.
- [33] S.M.J. Zaidi, S.D. Mikhailenko, G.P. Robertson, M.D. Guiver and S. Kaliaguine. Proton conducting composite membranes from polyether ether ketone and heteropolyacids for fuel cell applications. *J.Membr.Sci.*, 173 (2000) 17.
- [34] Z. Wojnarowska, M. Paluch. Recent progress on dielectric properties of protic ionic liquids. *Journal of Physics: Condensed Matter*, 27 (2015) 073202.

[35] J. Vila, P. Ginés, J.M. Pico, C. Franjo, E. Jiménez, L.M. Varela et al. Temperature dependence of the electrical conductivity in EMIM-based ionic liquids: Evidence of Vogel-Tamman-Fulcher behavior. *Fluid Phase Equilib.*, 242 (2006) 141.

[36] S. Slgaryov. Vogel-Fulcher-Tammann behavior of ionic conductivity in KTiOPO_4 . *J.Phys.D*, 26 (1993) 1326.

[37] F. Seland, T. Berning, B. Børresen and R. Tunold. Improving the performance of high-temperature PEM fuel cells based on PBI electrolyte. *J.Power Sources*, 160 (2006) 27.

[38] M. Yoshizawa-Fujita, N. Byrne, M. Forsyth, D.R. MacFarlane and H. Ohno. Proton transport properties in zwitterion blends with Brønsted acids. *J Phys Chem B*, 114 (2010) 16373.

[39] R. Zeng, Y. Wang, S. Wang and P.K. Shen. Homogeneous synthesis of PFSI/silica composite membranes for PEMFC operating at low humidity. *Electrochim.Acta*, 52 (2007) 3895.

[40] P. Costamagna, C. Yang, A.B. Bocarsly and S. Srinivasan. Nafion® 115/zirconium phosphate composite membranes for operation of PEMFCs above 100 °C. *Electrochim.Acta*, 47 (2002) 1023.

[41] J. Gao, Y. Guo, B. Wu, L. Qi, B. Li, J. Liu et al. Impact of cation selection on proton exchange membrane fuel cell performance with trimethylethyl amide, ethylpyridinium and ethylmethyl imidazolium ionic liquid carried by poly(vinylidene fluoride) membrane as electrolyte. *J.Power Sources*, 251 (2014) 432.

Chapter 5

MEMBRANES BASED ON PROTIC PLASTIC CRYSTAL AND POLYMERS

Abstract

This chapter deals with the development of composite membranes based on the protic plastic crystal N-N-dimethylethylene diammonium triflate [DMEDAH][TFO] and poly(vinylidene fluoride) (PVDF) nanofibers for proton exchange membrane fuel cells (PEMFCs) under non-humidified conditions.

An addition of 5 mol% of triflic acid and 5 mol% of the base N,N-dimethylethylenediamine is carried out to study the effects on the ionic conductivity and thermal behavior of the material. Composite membranes based on PVDF nanofibers and [DMEDAH][TFO] are tested in a single PEMFC. The effects of the plastic crystal doping on the thermal behavior, ionic conductivity and fuel cell performance are analyzed in this chapter.

5.1. Introduction

Plastic crystals (PCs) are promising solid electrolytes for fuel cell applications due to their unique properties. Their negligible volatility and high thermal and electrochemical stability make them suitable for electrochemical devices [1-3]. These materials have the advantages of ionic liquids (high proton conductivity without humidification) and the benefits of a solid state electrolyte [4, 5].

PCs are usually formed from a large symmetric organic cation and an inorganic anion that is normally symmetrical or has a diffusive charge. These materials have one or more solid-phase transitions before melting that are associated with the beginning of rotational or translational motions of the ions. This transition leads to a progressive transformation from an ordered crystalline phase to an increasingly disordered structure. The highest temperature solid phase is denoted phase I; the lower temperature phases are phases II, III, etc [6]. The conductivity of these materials is attributed to the presence of defects or vacancies in the crystalline structure, the rotational and translational disorder of the cation and anion and the conformational disorder of the ions [7]. These materials are referred to as “plastic crystals” due to their softness; they are easily deformed under stress. This deformation occurs due to the mobility of the slip planes, dislocations or vacancy migrations. These properties are beneficial for fuel cell devices because they should suffer less from any loss of contact with the electrodes due to volumetric changes [8].

Plastic crystals are usually used as matrix materials for adding dopant ions, such as Li^+ for lithium batteries or I^-/I_3^- for dye-sensitized solar cells, significantly increasing the ion conductivity [9-12]. Different PCs systems have been studied for their use as electrolytes in fuel cells. Choline dihydrogenphosphate [choline][DHP] was studied for the excellent proton conductivities of the phosphoric acid base materials. The proton transport of this material might be facilitated by a triple rotation of the dihydrogenphosphate anion. High proton diffusivities can be obtained after doping with acid. The thermal stability of [choline][DHP] doped with phosphoric acid is good, with minimal weight loss up to 200 °C. However, this PC with 18 mol%

phosphoric acid presents an amorphous phase. In contrast, using 4 wt% triflic acid or Tf₂N acid improves the conductivity without deforming the crystalline structure. Moreover, [choline][DHP] doped with 4 mol% triflic acid generated significant proton reduction currents, which is an important feature for fuel cells [7]. Yoshizawa-Fujita et al. [13] synthesized choline dihydrogen phosphate [choline][DHP] and 1-butyl-3-methylimidazolium dihydrogen phosphate [C₄mim][DHP] as new proton-conducting ionic plastic crystals. [C₄mim][DHP] showed solid-solid phase transitions and a melting point at 23 and 119 °C, whereas [choline][DHP] displayed solid-solid phase transitions and melting points at 45, 71 and 167 °C. Ionic conductivities ranging from 1.0 x 10⁻⁶ to 1.0 x 10⁻³ S.cm⁻¹ for choline dihydrogen phosphate and to 1.0 x 10⁻⁵ S.cm⁻¹ for 1-butyl-3-methylimidazolium dihydrogen phosphate were achieved in the plastic crystalline phase. [choline][DHP] showed one order of magnitude higher ionic conductivity than [C₄mim][DHP] in phase I, revealing that the hydroxyl group is suitable for fast proton transport in the solid state.

Among the different types of PCs, protic plastic crystals are being studied as promising electrolytes for fuel cells [14]. Thus, the proton transport behavior in the guanidinium triflate (GTf) solid and its mixtures with triflic acid was studied by Zhu and co-workers [15]. Both the pure GTf and 1 mol% doped samples showed relatively low conductivity and strong temperature dependency. Nevertheless, for the samples containing 2 mol% acid or more, the conductivities are high (1.0 x 10⁻³ S.cm⁻¹) and relatively independent of temperature. For all the measured temperatures, an increase in the conductivity can be found between the acid contents of 1-2 mol%. This behavior is a strong indication of percolation-dominated conducting mechanisms of the system. However, at high temperatures the GTf matrix also becomes conductive and contributes to the conductivity of the composites. Guanidinium-based protic plastic crystal was also studied by Chen et al. [16]. In this work, guanidinium nonaflate was reported as a new plastic crystal with significant ionic conductivity in phase I (1.0 x 10⁻⁴ S.cm⁻¹ at 176 °C) and high thermal stability (408 °C). On the other hand, in the work developed by Luo et al. [17] 1,2,4-

triazolium perfluorobutanesulfonate was studied as anhydrous proton conductor for high temperature fuel cells. The ionic conductivity dependence with temperature is correlated with the phase transitions observed in the material, reaching $1.27 \times 10^{-6} \text{ S.cm}^{-1}$ in phase I (155 °C). During fuel cell testing at 150 °C without humidity, high open circuit values (OCV) of 1.05 V and a current density around $17 \mu\text{A.cm}^{-2}$ at 0.2 V were obtained.

To improve the mechanical stability of the electrolytes, PCs are usually combined with a commercial polymer acting as support [18-21]. Thus, proton conducting membranes based on impregnated cellulose acetate supports with mixtures of choline dihydrogen phosphate and various acids were synthesized by Rana et al. for fuel cell applications [22]. A membrane doped with 4 mol% HNTf₂ containing up to 50 wt% water showed an OCV of approximately 0.78 V at 125 °C. The impedance of the cell was approximately 3 Ω under operational conditions.

Electrospun nanofibers acting as supports are being investigated for a wide range of applications, including tissue engineering, photocatalysis and energy applications [23-29]. These materials offer high degree of compositional and morphological control using relatively simple equipment [30-34]. In the work published by Howlett et al. [35] a composite membrane based on PVDF electrospun nanofibers and the plastic crystal N-methyl-N-ethyl pyrrolidinium tetrafluoroborate [C₂mpyr][BF₄] was synthesized for electrochemical devices using the solvent-casting method. The new composite materials exhibit enhanced conductivity compared to the bulk plastic crystal and excellent thermal, mechanical and electrochemical stability making them suitable for application in different electrochemical devices. Wang and coworkers synthesized composite nanofiber based on the same plastic crystal and polymer [C₂mpyr][BF₄]/PVDF by co-electrospinning. The incorporation of the plastic crystal in electrospun fibers improves the ionic conductivity. Thus, the composite with 5 wt% [C₂mpyr][BF₄] has a conductivity 2 orders of magnitude higher than that of the pure PVDF fibers and it increases further as more plastic crystal is added before decreasing in the 20 wt % [C₂mpyr][BF₄]/PVDF fiber composite, which might be a result of the discontinuous

and agglomerated microstructure. The increased ionic conductivity of these composites is beneficial for their use as solid state electrolyte for batteries [36].

Due to the attractive advantages of protic plastic crystal and electrospun nanofibers, the aim of this work is the development of composite membranes based on the protic plastic crystal N,N-dimethylethylene diammonium triflate [DMEDAH][TFO] and poly(vinylidene fluoride) (PVDF) electrospun nanofibers for PEMFCs under non-humidified conditions.

The effects of the addition of 5 mol% of triflic acid and 5 mol% of the base N,N-dimethylethylenediamine to the pure plastic crystal on the ionic conductivity and thermal behavior are analyzed.

In order to measure the fuel cell performance of the pure and doped plastic crystal, composite membranes based on PVDF nanofibers and [DMEDAH][TFO] are synthesized and tested in a single proton exchange membrane fuel cell (PEMFC). Thermal behavior and ionic conductivity of doped [DMEDAH][TFO]/PVDF composite membranes are also reported in this work.

5.2. Experimental methods

This section describes the synthesis and the characterization of the pure and doped plastic crystal N,N-dimethylethylenediammonium triflate [DMEDAH][Tfo] as well as the composite membranes based on [DMEDAH][Tfo] and electrospun PVDF nanofibers. This work was developed at the Institute of Frontier Material of Deakin University in Melbourne (Australia) under the supervision of Dr. Jenny Pringle.

5.2.1. Materials

PVDF powder (MW 534000), N,N- Dimethylethylenediamine (99.5%) and triflic acid (98%) were purchased from Sigma-Aldrich and used as received. Dimethylformamide (DMF) and acetone were supplied by VWR.

5.2.2. Fabrication of composite membranes

Synthesis of [DMEDAH][TfO]

N,N-dimethylethylenediammonium triflate ([DMEDAH][TfO]) was made by the proton transfer reaction between triflic acid and N,N-dimethylethylenediamine. The synthesis involves a drop wise addition of aqueous solution of triflic acid (42 mmoles) to N,N-dimethylethylenediamine (42 mmoles) in an ice bath and the reactants were stirred for about 2 hours at room temperature. Then water was removed by distillation and the final solid product was dried under vacuum at 70 °C for two days. The yield was found to be 98 %. The stoichiometry of the acid–base reaction was verified by an aqueous titration method and the IL samples were tested for correct pH after dilution into water (0.1 M). This is a sensitive, routine test of the final stoichiometry for these materials. The pH of 0.1 M aqueous solution was found to be 8.0.

Electrospray mass spectroscopy analysis, (cone $\pm 25V$): [DMEDAH][TfO], m/z (relative intensity, %): ES⁺, 89.2 ($(CH_3)_2N^+CH_2CH_2NH_3$ 100); ES⁻, 149.0 ($CF_3SO_3^-$, 100). The 5 mol % triflic acid doped sample was made by adding 2.26 g (95 mol %) of aqueous [DMEDAH][TfO] to 0.075 g (5 mol%) of aqueous solution of triflic acid. The reactants were stirred to get clear liquid and then distilled at 70 °C to remove water under reduced pressure. The solid was dried under vacuum at room temperature and the yield was found to be 98 %. The pH of 0.1 M aqueous solution was found to be 7.4.

The 5 mol % doped N,N-Dimethylethylenediamine doped sample was synthesized by adding 2.26 g (95 mol%) of aqueous [DMEDAH][TfO] to 0.04 g (5 mol%) of aqueous solution of N,N-Dimethylethylenediamine. The reactants were stirred and then distilled at 70 °C to remove water under reduced pressure. The solid was dried under vacuum at room temperature and the yield was found to be 98 %. The pH of 0.1 M aqueous solution was found to be 7.9.

Electrospinning of nanofibers

1.5 g PVDF was dissolved in a mixture of 3 mL of DMF and 7 mL of acetone and heated at 60 °C for 30 min until the solution was homogeneous. The solution was transferred into a plastic syringe and discharged at 1 mL.h⁻¹ using a syringe pump (KD Scientific) into a 15 kV electric field between the syringe needle (21G) and a grounded metal collector (distance 15 cm). The fibers were accumulated randomly on the collector.

Fabrication of composite membranes

[DMEDAH][TFO] and nanofibers were dried overnight at 40 °C on a vacuum line (Schlenk line). Composite membranes were synthesized by the melting casting procedure. Plastic crystal (90 wt%) was spread on the nanofibers surface (10wt%) and melted at 70 °C in a hot plate. Composite membranes were kept in a vacuum oven at 80 °C overnight in order to completely melt the plastic crystal. Then, the membrane was pressed to ensure a homogeneous distribution of the plastic crystal between fibers. Fuel cell testing and ionic conductivity measurements require different dimensions of the sample. For this reason, in the case of ionic conductivity measurements the membrane (10 mm diameter) was pressed between two Teflon disk in a KBr cell at 1 ton pressure whereas for fuel cell experiments the composite membrane (5 cm²) was pressed at 1100 psi during 3 minutes using a Carver 4386 press.

Figure 5.1 shows the chemical structure of [DMEDAH][TFO] and the PVDF polymeric nanofiber used in this work.

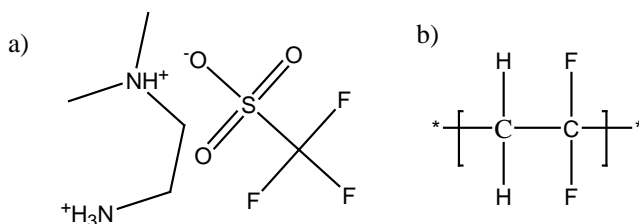


Figure 5.1. Chemical structures: a) [DMEDAH][TFO]; b) PVDF

5.2.3. Membrane characterization and operation conditions

Scanning electron microscope (SEM)

The morphology of the electrospun membranes was characterized using a JCM-5000, NeoScope, JEOL Benchtop SEM. SEM images were collected using the JCM-5000 software, with accelerating voltage of 10 kV.

Differential scanning calorimetry (DSC)

Mettler Toledo DSC instrument was used for DSC measurements. All samples were prepared and sealed in a glove box under argon atmosphere. In order to obtain accurate data, a calibration procedure using cyclohexane as reference was carried out. Temperature range from -95°C to 120°C was used to study the thermal behavior of the materials, with a heating and a cooling rates of 5 and -2 °C.min⁻¹, respectively. Two temperature scans were run; the second heating scan is reported in this chapter. DSC curves were normalized with respect to the pure plastic crystal weight.

Ionic conductivity

Solid-state ionic conductivity of the materials was evaluated using electrochemical impedance spectroscopy on a Solartron potentiostat. The samples were sandwiched between pre-polished and dried circular stainless steel electrodes located inside hermetically-sealed barrel cells (Advanced Industrial Services, Moorabbin, Australia). Pellets of pure and doped plastic crystal were obtained pressing the material at 1 ton pressure inside a KBr die (10 mm diameter). All material handling was carried out inside an argon glove box. A tubular Helios furnace (28 V/32 W) with a flexible ceramic heater was used to apply the temperature ramp. A Eurotherm 3504 temperature controller interfaced to the potentiostats, allowed impedance data to be acquired automatically throughout a programmed temperature profile. A T type thermocouple with an accuracy of ± 1 °C was used for the temperature measurements. The temperature stabilization time between measurements was 30 min, at 5 °C intervals. Data were collected at each

temperature by applying a sinusoidal signal with amplitude of 100 mV over a frequency range of 1 MHz to 1 Hz. Conductivity values were calculated from Nyquist plots in which the touchdown point of the semicircle corresponds to the bulk resistance of the ionic conducting media.

Fuel cell testing

Gas diffusion electrodes (GDEs) (Pt 3.0 mg Pt.cm⁻², Baltic Fuel Cell GmbH) were placed at both sides of the membrane forming the membrane electrode assembly (MEA). The membrane performance was tested in a fuel cell of 5 cm² containing serpentine channels and equipped with a piston that ensures good contact between the internal components of the cell (quick CONNECT, Baltic Fuel Cells GmbH). The anode was fed with hydrogen with a flow rate of 50 ml.min⁻¹ while the cathode was fed with air at a rate of 100 ml.min⁻¹. The system pressure was fixed at 1.0 bar and the experiments were carried out at 25 °C. Polarization curves of cell voltage versus the electric current were performed using an external load (ZS, H&H) under potentiostatic control at non-humidified conditions.

5.3 Results and discussion

The main results obtained in this work are reported and analyzed. Thermal characterization, SEM images, ionic conductivity and fuel cell performance of composite membranes based on PVDF nanofibers and pure, acid-doped and base-doped [DMEDAH][TFO] are included in this section.

5.3.1. Membrane synthesis

The obtained membranes were flexible and homogeneous. The average thickness was about 70 microns. A photograph of a membrane based on pure [DMEDAH][TFO]/PVDF is illustrated in figure 5.2.



Figure 5.2. PVDF/[DMEDAH][TFO] membrane photograph

In order to confirm the homogeneous distribution of the plastic crystal within the polymer nanofibers, SEM images of the composite membranes based on PVDF/[DMEDAH][TFO] are provided in figure 5.3.

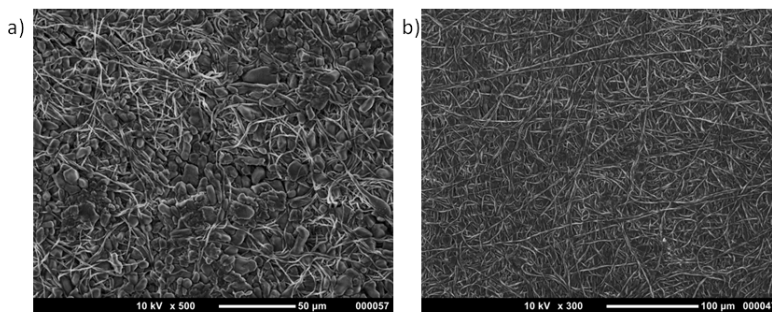


Figure 5.3. PVDF/[DMEDAH][TFO] SEM image: a) front side; b) back side

It can be observed that the PC is well distributed within the fiber matrix which is filled with PC and free of voids. Due to the synthesis procedure, both sides of each membrane have been analyzed demonstrating the feasibility of the melting-casting technique.

5.3.2. Thermal behavior

Figure 5.4 shows thermal traces obtained from DSC measurements of pure, 5 mol% acid doped and 5 mol% base doped [DMEDAH][TFO]. The PC shows a solid-solid phase transition at 55 °C and stays in the solid-state plastic phase I up to its melting temperature around 70 °C. In the acid doped [DMEDAH][TFO], the peak

corresponding to the solid-solid phase transition increased. However, when base the is added to [DMEDAH][TFO] the peak diminishes.

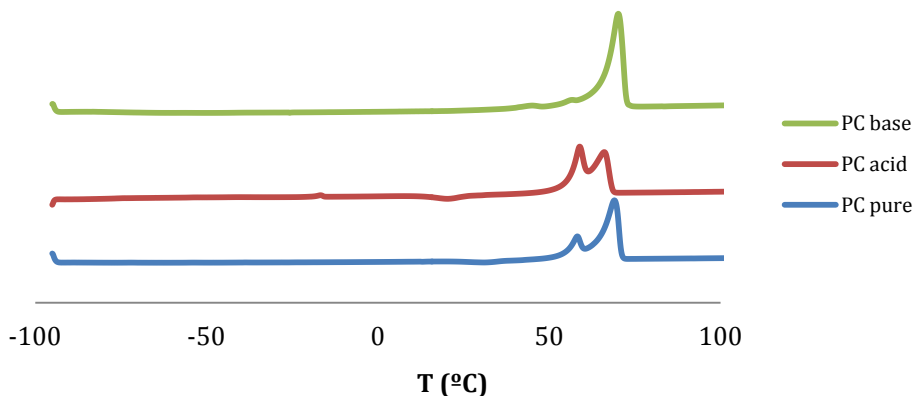


Figure 5.4. DSC thermal traces of pure [DMEDAH][TFO], 5 mol% acid doped [DMEDAH][TFO] and 5 mol% base doped [DMEDAH][TFO]

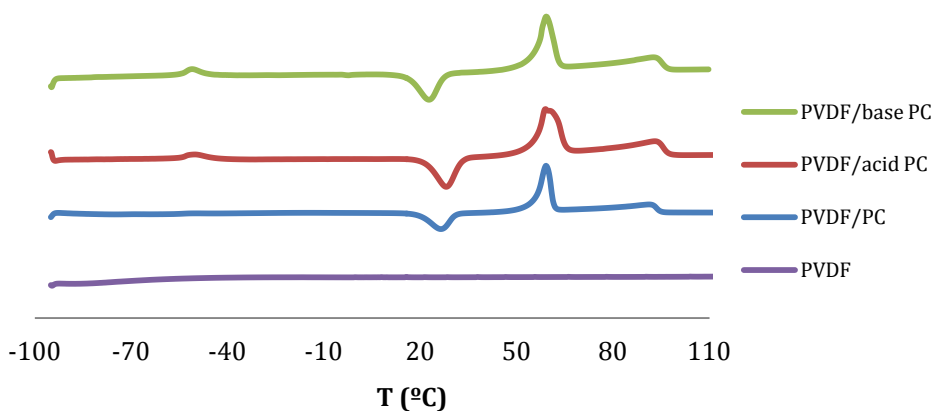


Figure 5.5. DSC thermal traces of PVDF/ [DMEDAH][TFO], PVDF/5 mol% acid doped [DMEDAH][TFO] and PVDF/5 mol% base doped [DMEDAH][TFO] composite membranes

In order to analyze the influence of the nanofibers in the plastic crystal structure, DSC measurements of PVDF composite membranes were carried out (figure 5.5). As it can be observed, the peak corresponding to the melting point of the plastic crystal appeared at 70 °C approximately. However, the solid-solid phase transition is not clearly observed in the DSC traces possibly due to its proximity to the melting point. A peak around 100 °C is observed associated with the melting point of PVDF fibers, which is lower than its normal melting point (≈ 165 °C [37]) probably due to some interactions with the plastic crystal and/or the acid and base doping agents. In addition, an exothermic peak around 25 °C appears corresponding to the recrystallization of the samples during the heating scan.

5.3.3. Ionic conductivity

Ionic conductivities of the materials as a function of temperature are illustrated in figures 5.6 and 5.7.

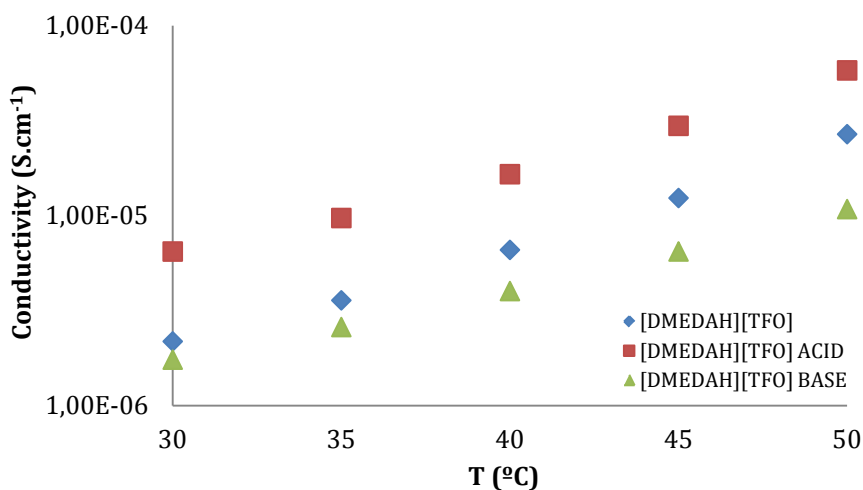


Figure 5.6. Ionic conductivity of pure and doped plastic crystal

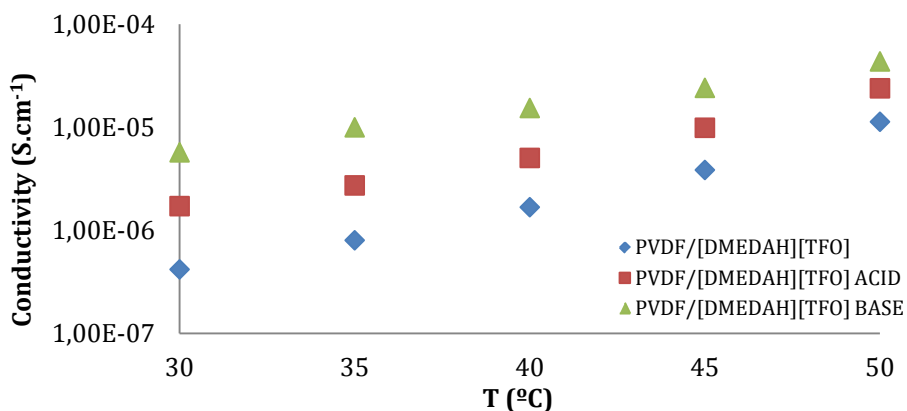


Figure 5.7. Ionic conductivity of PVDF/plastic crystal composite membrane

The conductivity of all samples increases gradually with increasing temperature, reaching $2.7 \times 10^{-5} \text{ S.cm}^{-1}$ at $50 \text{ }^\circ\text{C}$ for pure [DMEDAH][TFO]. It can be observed that the addition of 5 mol% of triflic acid to the pure PC increases the conductivity more than twice. This enhancement in conductivity can be associated to an increase in the number of dissociable protons from the doping acid [38]. Zhu et al. [15] have demonstrated by means of H NMR spectra the fast mobility of the triflic acid protons affecting the molecular dynamics of the [DMEDAH][TFO] and therefore its conductivity. However, the incorporation of the base decreases the ionic conductivity, especially at higher temperatures. Despite the fact that N,N-dimethylethylenediamine has several dissociable protons per molecule it could be possible that these protons are strongly coupled with each other leading to low mobility and negligible effect on the ionic conductivity of the material.

In the case of PVDF based membranes, surprisingly the highest ionic conductivity was obtained with base doped [DMEDAH][TFO], $4.3 \times 10^{-5} \text{ S.cm}^{-1}$ at $50 \text{ }^\circ\text{C}$ compared to $1.1 \times 10^{-5} \text{ S.cm}^{-1}$ obtained with pure [DMEDAH][TFO]. At lower temperatures the difference in ionic conductivity is more noticeable, increasing more than one order of magnitude when 5 mol% base is added ($4.1 \times 10^{-7} \text{ S.cm}^{-1}$ to $5.7 \times 10^{-6} \text{ S.cm}^{-1}$ at $30 \text{ }^\circ\text{C}$). The addition of acid also improves the ionic conductivity, $2.4 \times 10^{-5} \text{ S.cm}^{-1}$ at $50 \text{ }^\circ\text{C}$.

5.3.4. Fuel cell testing

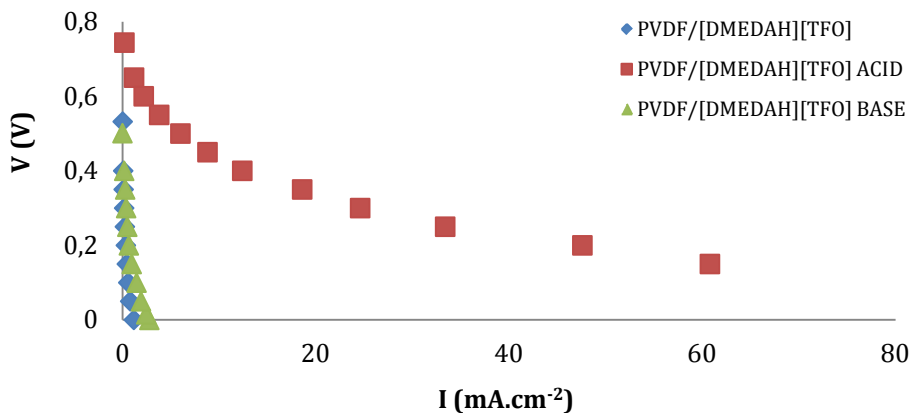


Figure 5.8. Polarization curves PVDF-based membranes

Figure 5.8 shows polarization curves obtained with PVDF-based membranes with pure [DMEDAH][TFO], 5 mol% acid doped [DMEDAH][TFO] and 5 mol% base doped [DMEDAH][TFO]. Pure [DMEDAH][TFO]/PVDF composite membranes has poor fuel cell performance, obtaining an open circuit voltage (OCV) about 0.53 V and current density of 0.45 mA.cm⁻² at 0.15 V and 25 °C. The addition of 5 mol% N,N-dimethylethylenediamine did not have noteworthy influence on the fuel cell performance compared to pure [DMEDAH][TFO], possibly due to the lower conductivity of the base-doped [DMEDAH][TFO] as previously mentioned.

However, when 5 mol% of triflic acid is added to the plastic crystal the performance improves significantly, reaching OCV of 0.74 V and current density of 61 mA.cm⁻² at 0.15 V and 25 °C. This behavior is in accordance with the highest conductivity reported for the acid doped-plastic crystal. The high mobility of the dissociable protons from the triflic acids promotes the proton transport mechanism across the composite membrane, which enhances the fuel cell performance. On the contrary, the high coupling of the protons in the base-doped sample does not lead to a noteworthy increase in the fuel cell performance.

5.4. Conclusions

Composite membranes based on electrospun poly(tetrafluoroethylene) (PVDF) nanofibers and the protic plastic crystal N,N-dimethylethylene diammonium triflate [DMEDAH][TFO] were synthesized through melting-casting technique. SEM characterization demonstrated the uniform distribution of the [DMEDAH][TFO] in the nanofibers.

The DSC characterization of the plastic crystal revealed a solid-solid phase transition at 55°C before its melting point at 70 °C. The ionic conductivity of [DMEDAH][TFO] increased with temperature, reaching $2.7 \times 10^{-5} \text{ S.cm}^{-1}$ at 50 °C.

In order to enhance the ionic conductivity of the plastic crystal, 5 mol% of triflic acid and 5 mol% of the base N,N-dimethylethylenediamine were added to the pure plastic crystal. The conductivity of the acid-doped plastic crystals increased more than twice due to the fast mobility of the triflic acid protons. However, the addition of the base did not enhance the ionic conductivity of [DMEDAH][TFO] probably due to a strong coupling of protons leading to a low mobility.

Membranes based on PVDF and pure, acid-doped and base-doped plastic crystal were developed and tested in a single proton exchange membrane fuel cell (PEMFC). The membrane based on pure [DMEDAH][Tfo]/PVDF showed open circuit voltage (OCV) about 0.53 V and current density of 0.45 mA.cm^{-2} at 0.15 V and 25 °C. It was demonstrated that the addition of triflic acid improved the fuel cell performance, reaching OCV of 0.74 V and current density of 61 mA.cm^{-2} at 0.15 V and 25 °C.

This work shows the potential of composite membranes based on electrospun polymers and protic plastic crystals as proton exchange membrane for fuel cell applications without external humidification. It is necessary to continue working developing new materials with fast proton mobility leading to higher ionic conductivity and fuel cell performance.

5.5. References

- [1] A. Mondal, A.P. Sunda and S. Balasubramanian. Thermal phase behavior and ion hopping in a 1,2,4-triazolium perfluorobutanesulfonate protic organic ionic plastic crystal. *Phys.Chem.Chem.Phys.*, 18 (2016) 2047.
- [2] K. Romanenko, L. Jin, P. Howlett and M. Forsyth. In Situ MRI of Operating Solid-State Lithium Metal Cells Based on Ionic Plastic Crystal Electrolytes. *Chem.Mater.*, 28 (2016) 2844.
- [3] X. Zhu, R. Zhao, W. Deng, X. Ai, H. Yang and Y. Cao. An All-solid-state and All-organic Sodium-ion Battery based on Redox-active Polymers and Plastic Crystal Electrolyte. *Electrochim.Acta*, 178 (2015) 55.
- [4] M. Díaz, A. Ortiz, M. Isik, D. Mecerreyes and I. Ortiz. Highly conductive electrolytes based on poly([HSO₃-BVIm][TfO])/[HSO₃-BMIm][TfO] mixtures for fuel cell applications. *Int J Hydrogen Energy*, 40 (2014) 11294.
- [5] M. Díaz, A. Ortiz and I. Ortiz. Progress in the use of ionic liquids as electrolyte membranes in fuel cells. *J.Membr.Sci.*, 469 (2014) 379.
- [6] J.M. Pringle, P.C. Howlett, D.R. MacFarlane and M. Forsyth. Organic ionic plastic crystals: Recent advances. *J.Mater.Chem.*, 20 (2010) 2056.
- [7] J.M. Pringle. Recent progress in the development and use of organic ionic plastic crystal electrolytes. *Phys.Chem.Chem.Phys.*, 15 (2013) 1339.
- [8] U.A. Rana, M. Forsyth, D.R. Macfarlane and J.M. Pringle. Toward protic ionic liquid and organic ionic plastic crystal electrolytes for fuel cells. *Electrochim.Acta*, 84 (2012) 213.
- [9] K. Liu, F. Ding, Q. Lu, J. Liu, Q. Zhang, X. Liu et al. A novel plastic crystal composite polymer electrolyte with excellent mechanical bendability and electrochemical performance for flexible lithium-ion batteries. *Solid State Ionics*, 289 (2016) 1.
- [10] X. Li, Z. Zhang, S. Li, L. Yang and S. Hirano. Polymeric ionic liquid-plastic crystal composite electrolytes for lithium ion batteries. *J.Power Sources*, 307 (2016) 678.
- [11] F. Chen, J.M. Pringle, and M. Forsyth. Insights into the transport of alkali metal ions doped into a plastic crystal electrolyte. *Chem.Mater.*, 27 (2015) 2666.

- [12] N.U. Taib, N.H. Idris. Plastic crystal-solid biopolymer electrolytes for rechargeable lithium batteries. *J.Membr.Sci.*, 468 (2014) 149.
- [13] M. Yoshizawa-Fujita, K. Fujita, M. Forsyth and D.R. MacFarlane. A new class of proton-conducting ionic plastic crystals based on organic cations and dihydrogen phosphate. *Electrochem.Comm.*, 9 (2007) 1202.
- [14] T.L. Greaves, C.J. Drummond. Protic ionic liquids: Properties and applications. *Chem.Rev.*, 108 (2008) 206.
- [15] H. Zhu, U.A. Rana, V. Ranganathan, L. Jin, L.A. O'Dell, D.R. MacFarlane et al. Proton transport behaviour and molecular dynamics in the guanidinium triflate solid and its mixtures with triflic acid. *J.Mater.Chem.A*, 2 (2014) 681.
- [16] X. Chen, H. Tang, T. Putzeys, J. Sniekers, M. Wübbenhorst, K. Binnemans et al. Guanidinium nonaflate as a solid-state proton conductor. *J.Mater.Chem.A*, 4 (2016) 12241.
- [17] J. Luo, A.H. Jensen, N.R. Brooks, J. Sniekers, M. Knipper, D. Aili et al. 1,2,4-Triazolium perfluorobutanesulfonate as an archetypal pure protic organic ionic plastic crystal electrolyte for all-solid-state fuel cells. *Energy Environ.Sci.*, 8 (2015) 1276.
- [18] N. Iranipour, D.J. Gunzelmann, A. Seeber, J. Vongsvivut, C. Doherty, F. Ponzio et al. Ionic transport through a composite structure of N-ethyl-N-methylpyrrolidinium tetrafluoroborate organic ionic plastic crystals reinforced with polymer nanofibres. *J.Mater.Chem.A*, 3 (2015) 6038.
- [19] G.W. Greene, F. Ponzio, N. Iranipour, H. Zhu, A. Seeber, M. Forsyth et al. Enhanced ionic mobility in Organic Ionic Plastic Crystal - Dendrimer solid electrolytes. *Electrochim.Acta*, 175 (2015) 214.
- [20] D. Hambali, Z. Zainuddin, I. Supa'At and Z. Osman, Studies of plastic crystal gel polymer electrolytes based on poly(vinylidene chloride-co-acrylonitrile), *AIP Conf. Proc.*, 1711 (2016).
- [21] M. Suleman, M. Deraman, M.A.R. Othman, R. Omar, M.A. Hashim, N.H. Basri et al. Electric double-layer capacitors with tea waste derived activated carbon electrodes and plastic crystal based flexible gel polymer electrolytes. *J.Phys.Conf.Ser.*, 739 (2016).

[22] U.A. Rana, I. Shakir, R. Vijayraghavan, D.R. MacEarlane, M. Watanabe and M. Forsyth. Proton transport in acid containing choline dihydrogen phosphate membranes for fuel cell. *Electrochim.Acta*, 111 (2013) 41.

[23] J. Hu, D. Kai, H. Ye, L. Tian, X. Ding, S. Ramakrishna et al. Electrospinning of poly(glycerol sebacate)-based nanofibers for nerve tissue engineering. *Mater.Sci.Eng.C*, 70 (2017) 1089.

[24] R. Kai, W. Jun and J. Huali. Electrospinning fibrous films doped with iridium complexes for high performance oxygen sensing: Synthesis and characterization. *Sens Actuators, B Chem*, 240 (2017) 697.

[25] T. Larsson, T.S. Li, M. Xu, I. Fransson, G. Yu, M. Andersson et al. Co-fabrication of nickel-YSZ cermet nanofibers via an electrospinning technique. *Mater.Res.Bull.*, 86 (2017) 38.

[26] N.H.A. Ngadiman, N.M. Yusof, A. Idris, E. Misran and D. Kurniawan. Development of highly porous biodegradable γ -Fe₂O₃/polyvinyl alcohol nanofiber mats using electrospinning process for biomedical application. *Mater.Sci.Eng.C*, 70 (2017) 520.

[27] D.B. Pal, P. Singh and P.K. Mishra. Composite ceria nanofiber with different copper loading using electrospinning method. *J Alloys Compd*, 694 (2017) S1.

[28] N. Qin, J. Xiong, R. Liang, Y. Liu, S. Zhang, Y. Li et al. Highly efficient photocatalytic H₂ evolution over MoS₂/CdS-TiO₂ nanofibers prepared by an electrospinning mediated photodeposition method. *Appl.Catal.B Environ.*, 202 (2017) 374.

[29] O. Rezaee, H. Mahmoudi Chenari, F.E. Ghodsi and H. Ziyadi. Preparation of PVA nanofibers containing tungsten oxide nanoparticle by electrospinning and consideration of their structural properties and photocatalytic activity. *J Alloys Compd*, 690 (2017) 864.

[30] J.B. Ballengee, P.N. Pintauro. Preparation of nanofiber composite proton-exchange membranes from dual fiber electrospun mats. *J.Membr.Sci.*, 442 (2013) 187.

[31] H. Li, Y. Lee, J. Lai and Y. Liu. Composite membranes of Nafion and poly(styrene sulfonic acid)-grafted poly(vinylidene fluoride) electrospun nanofiber mats for fuel cells. *J.Membr.Sci.*, 466 (2014) 238.

- [32] S. Martwiset, K. Jaroensuk. Electrospinning of poly(vinyl alcohol) and poly(4-styrenesulfonic acid) for fuel cell applications. *J Appl Polym Sci*, 124 (2012) 2594.
- [33] W. Pan, Z. Lü, K. Chen, X. Huang, B. Wei, W. Li et al. Novel polymer fibers prepared by electrospinning for use as the pore-former for the anode of solid oxide fuel cell. *Electrochim.Acta*, 55 (2010) 5538.
- [34] X. Zhang, D. He and S. Mu. Application of electrospinning technique in low temperature fuel cells. *Chem.Bull.*, 77 (2014) 490.
- [35] P.C. Howlett, F. Ponzio, J. Fang, T. Lin, L. Jin, N. Iranipour et al. Thin and flexible solid-state organic ionic plastic crystal-polymer nanofibre composite electrolytes for device applications. *Phys.Chem.Chem.Phys.*, 15 (2013) 13784.
- [36] X. Wang, H. Zhu, G.W. Greene, J. Li, N. Iranipour, C. Garnier et al. Enhancement of ion dynamics in organic ionic plastic crystal/PVDF composite electrolytes prepared by co-electrospinning. *J.Mater.Chem.A*, 4 (2016) 9873.
- [37] K. Gao, X. Hu, C. Dai and T. Yi. Crystal structures of electrospun PVDF membranes and its separator application for rechargeable lithium metal cells. *Materials Science and Engineering: B*, 131 (2006) 100.
- [38] J. Rao, R. Vijayaraghavan, F. Chen, J. Zhu, P. Howlett, D. R. MacFarlane et al. Protic organic ionic plastic crystals based on a difunctional cation and the triflate anion: a new solid-state proton conductor. *Chemical Communications*, (2016) DOI: 10.1039/c6cc07154f.

Chapter 6

CONCLUSIONS AND CHALLENGES FOR FUTURE RESEARCH

Abstract

This thesis aims to the development of new electrolyte membranes based on protic ionic liquids for improving the performance of PEMFC devices over the most widely used Nafion perfluorinated membranes at non-humidified conditions. After the detailed description of the objectives of this work, this chapter summarizes the main results that have been achieved, draws the conclusions derived from the analysis of the results and highlights future challenges and perspectives in proton exchange membranes based on ionic liquids for fuel cell applications.

6.1. Conclusions

A thorough study of the state of the art reveals the infeasibility of commercial perfluorinated polymers as proton exchange membranes for fuel cell applications under anhydrous conditions. Perfluorinated polymers are highly expensive membranes strongly dependent on humidity which require the use of external controlled humidity systems. In these electrolytes, the lack of water compromises the proton transport mechanisms leading to high ionic resistance electrolytes with deficient fuel cell performance. Consequently, the development of electrolytes with high ionic conductivity capable of working under non-humidified conditions constitutes a scientific and technical challenge. For this purpose, ionic liquids are attracting interest as electrolytes for this application due to their exceptional properties such as negligible volatility, non-flammability, high thermal and electrochemical stability and outstanding ionic conductivity even under anhydrous conditions. Due to the potential advantages of ionic liquids, this thesis focuses on the analysis of innovative polymeric membranes for proton exchange membrane fuel cells without external humidification using ionic liquids as favorable electrolytes.

With the aim of improving the low fuel cell performance under non-humidified conditions reported for commercial perfluorosulfonic membranes, impregnation of a Nafion membrane with two protic ionic liquids as proton carriers was carried out. As a result, Nafion membranes impregnated with $[\text{HSO}_3\text{-BBIm}][\text{TfO}]$ showed high fuel cell performance at 25°C without external humidification avoiding the water management systems and reducing the complexity of the fuel cell devices.

Having demonstrated the viability of protic ionic liquids as proton carriers under non-humidified conditions, the next step was the development of membranes based exclusively on polymerized protic ionic liquids. This strategy allows the design of high performance electrolytes under non-humidified conditions avoiding the use of expensive perfluorinated polymers. For this purpose, two different membrane structures were studied. The first membrane was based on the two polymerizable sulfoethylmethacrylate anion-based ionic liquids $[\text{HSO}_3\text{-BMIm}][\text{SEM}]$ and $[\text{HSO}_3\text{-}$

BVIm][SEM]. On the other hand, in the second studied structure, the triflate anion-based ionic liquid [HSO₃-BVIm][TfO] was polymerized at different compositional range of its analogous non-polymerizable ionic liquid [HSO₃-BMIm][TfO].

Thermogravimetric studies have demonstrated the ability of polymerized ionic liquids to retain atmospheric water inside its chemical structure. This property benefits the ionic conductivity, leading to higher ionic conductivity values for both membranes with high retained water content compared to that obtained with dried membranes. Thus, sulfoethylmethacrylate membranes with high water content showed ionic conductivity of $1.5 \times 10^{-3} \text{ S.cm}^{-1}$ at 70 °C whereas dried membranes registered $6.24 \times 10^{-6} \text{ S.cm}^{-1}$ at same temperature. Triflate anion-based membranes showed even higher ionic conductivity values, about $10^{-2} \text{ S.cm}^{-1}$ at 70°C for membranes with high water content. This behavior is explained due to the mobile protons produced in the dissociation of HSO₃ groups when they are exposed to water. These protons can be transferred through the H-bonded network formed by ions and water molecules. Therefore, the dependence of ionic conductivity with temperature of polymeric ionic liquids with high water content suggested two competing trends between the thermal activation and the water evaporation.

Broadband dielectric spectroscopy combined with temperature-modulated differential scanning calorimetry allows understanding the ionic transport mechanisms of the electrolytes. Ion dynamics studies under high pressure conditions have demonstrated an effective proton hopping mechanism in charge transport for sulfoethylmethacrylate anion-based membranes. On the other hand, this technique evidenced that the conductivity of triflate anion-base polymer is controlled by the Grotthuss mechanism, in contrast to the monomer controlled by vehicular mechanism. It was also observed that regardless of the amount of water present in the sample, the charge transport mechanism of the triflate polymer is permanently governed by fast proton hopping. Consequently, it was proven that using protic ionic liquids as polyelectrolytes it is possible to avoid the serious

problem of water management observed for perfluorinated membranes for low temperature fuel cell applications.

Due to the outstanding ionic conductivity values obtained for triflate anion-based membranes, these electrolytes were tested in a proton exchange membrane fuel cell device in order to evaluate their fuel cell performance. The membrane with 10 wt% [HSO₃-BMIm][TfO] showed the highest *in-situ* ionic conductivity, 2.92×10^{-1} S.cm⁻¹ and the best fuel cell performance at 40 °C, 189 mA.cm⁻² at 0.15 V and peak power density of 49 mW.cm⁻². These results exceeded that obtained with the neat poly([HSO₃-BVIIm][TfO]), 46 mA.cm⁻² at 0.15V and 15 mW.cm⁻² of peak power density.

Finally, protic plastic crystals, a new family of solid compounds similar to ionic liquids but with the benefits of a solid state electrolyte such as easier handling and the elimination of possible ionic liquid leaks and leachates, have been analyzed in their use as electrolytes for electrochemical applications. Taking advantage of the promising properties of protic plastic crystals, composite membranes based on electrospun poly(tetrafluoroethylene) (PVDF) nanofibers and the protic plastic crystal N,N-dimethylethylene diammonium triflate [DMEDAH][TFO] were synthesized through melting casting technique. SEM characterization demonstrated the uniform distribution of the [DMEDAH][TFO] in the nanofibers. The DSC characterization of the plastic crystal revealed a solid-solid phase transition at 55°C before its melting point at 70 °C. Ionic conductivity values of 2.7×10^{-5} S.cm⁻¹ at 50 °C were obtained for [DMEDAH][TFO]. In order to further increase the ionic conductivity of the plastic crystal, 5 mol% of triflic acid and 5 mol% of the base N,N-dimethylethylenediamine were added to [DMEDAH][TFO]. The conductivity of the acid-doped plastic crystals increased more than twice due to the fast mobility of the triflic acid protons. However, the addition of the base did not enhance the ionic conductivity of [DMEDAH][TFO] probably due to a strong coupling of protons leading to a low mobility. Membranes based on PVDF and pure, acid-doped and base-doped plastic crystal were developed and tested in a single proton exchange

membrane fuel cell (PEMFC). It was demonstrated that the addition of triflic acid improved the fuel cell performance, reaching an open circuit voltage (OCV) of 0.74 V and current density of 61 mA.cm⁻² at 0.15 V and 25 °C.

This thesis has demonstrated the suitability of protic ionic liquids as proton carriers for proton exchange membrane fuel cells under non-humidified conditions, avoiding the use of external humidity controllers necessary for perfluorinated polymers. As a summary, membranes with the highest fuel cell performance from each type of electrolyte studied in this thesis are shown in table 6.1.

Table 6.1. Electrolytes with higher fuel cell performance under non-humidified conditions at 25 °C

Electrolyte classification	Membrane	OCV	I (mA.cm ⁻²)	P (mW.cm ⁻²)
Ionic liquid-impregnated membranes	N212/[HSO ₃ -BBIIm][TfO]	0,82	217	43,6
Polymerized ionic liquids	[HSO ₃ -BVIIm][TfO] + 10wt% [HSO ₃ -BIMIIm][TfO]	0,83	174,4	43,3
Protic plastic crystal / polymeric nanofibers	acid [DMEDAH][TFO]/PVDF	0,74	61	9,5

In light of these results, ionic liquid-impregnated membranes and polymeric ionic liquids are the most promising electrolytes for proton exchange membrane fuel cell applications under non-humidified applications.

6.2. Challenges for future research

This thesis intends to open up the possibility of new proton exchange membranes based on protic ionic liquids for fuel cell devices under non-humidified conditions.

Thus far, ionic liquid-based electrolytes with outstanding ionic conductivity have been developed and characterized demonstrating their high fuel cell performance without external humidification at low temperature. Nevertheless, despite the achievements that have been described through the chapters of this thesis, there are still new challenges ahead and disadvantages that must be overcome before these membranes become a reality.

One of the most remarkable advantages of the use of proton exchange membrane fuel cells is their environmental friendly character. However, the low temperatures associated with this type of fuel cells hinder the use of hydrogen with low purity. The valorization of residual hydrogen as fuel in these electrochemical devices could promote the use of fuel cells increasing the sustainability of this technology. This valorization could be achieved by means of the use of high-performance catalyst and/or the use of higher temperatures.

On the other hand, one of the main disadvantages of polymeric ionic liquid membranes is their mechanical stability, especially if a non-polymerizable ionic liquid is incorporated between the polymer chains. Taking advantage of the design character of ionic liquids, it is recommendable the search of new chemical structures which led to a more mechanical stable and conductive polymers especially at high temperatures. Moreover, a complete and quantitative characterization of the resulting polymers in terms of mechanical stability and gas permeability is also advisable.

Another issue that must be improved is the contact between the membrane and the electrodes in order to obtain a better fuel cell performance. In this work, gas diffusion layers with platinum in their surface were used as electrodes. This is a fast and simple technique frequently reported in literature. However, other techniques, such as air brushing method, results in a membrane electrode assembly with optimized contact between all the elements involved in the electrochemical reactions. This resulting membrane must be analyzed in order to evaluate the influence of the contact between the electrodes and the membrane.

Finally, in order to bring these membranes to their real implementation, it is essential to scale-up the single fuel cell tests to a stack fuel cell system which allow obtaining the necessary power output for different real applications. One strategy to facilitate this scale-up is the fuel cell modeling because it provides valuable information about the fundamental phenomena that take place in the system. The speed of the simulation processes allows considering several alternatives enabling predict and optimize the behavior under different operating conditions.

Capítulo 6

CONCLUSIONES Y RETOS PARA FUTURAS INVESTIGACIONES

Resumen

Esta tesis se centra en el desarrollo de nuevos electrolitos basados en líquidos iónicos próticos con el objetivo de mejorar el rendimiento en PEMFCs reportado para las ampliamente utilizadas membranas perfluoradas bajo condiciones no humidificadas. Tras una detallada descripción de los objetivos de este trabajo, este capítulo resume los principales resultados alcanzados, establece las conclusiones derivadas del análisis de los resultados y destaca los retos futuros y perspectivas sobre las membranas de intercambio protónico basadas en líquidos iónicos para aplicaciones de pilas de combustible.

6.1. Conclusiones

El estudio minucioso del estado del arte ha revelado la inviabilidad del uso de las membranas comerciales perfluoradas como membranas de intercambio protónico para pilas de combustible bajo condiciones anhidras. Estas costosas membranas son fuertemente dependientes del contenido de agua, lo cual implica el uso de controladores de humedad externos. En estos electrolitos, la falta de agua perjudica los mecanismos de transporte protónico conduciendo a electrolitos de alta resistencia iónica con deficiente rendimiento en las celdas de combustible. Consecuentemente, el desarrollo de electrolitos con alta conductividad iónica capaces de funcionar bajo condiciones no humidificadas constituye un reto científico y técnico. Con este propósito, los líquidos iónicos están adquiriendo interés como electrolitos para esta aplicación debido a sus excepcionales propiedades como baja volatilidad, bajo riesgo de inflamabilidad, alta estabilidad térmica y electroquímica y alta conductividad iónica incluso en condiciones anhidras. Debido a las ventajas potenciales de los líquidos iónicos, esta tesis se centra en el desarrollo de membranas poliméricas innovadoras para PEMFCs sin humidificación externa empleado líquidos iónicos como electrolitos.

Con el objetivo de mejorar el bajo rendimiento en pilas de combustible bajo condiciones no humidificadas reportado para las membranas comerciales perfluoradas, se ha realizado una impregnación a una membrana de Nafion con dos líquidos iónicos próticos como transportadores de protones. Como resultado, la membrana de Nafion impregnada con $[\text{HSO}_3\text{-BBIm}][\text{TfO}]$ mostró alto rendimiento en la pila de combustible a 25 °C sin humidificación externa evitando de esta manera el uso de sistemas de gestión de humedad y reduciendo la complejidad de los dispositivos PEMFC.

Habiendo demostrado la viabilidad de los líquidos iónicos próticos como transportadores de protones en condiciones no humidificadas, el siguiente paso consistió en el desarrollo de membranas basadas exclusivamente en líquidos iónicos próticos polimerizados. Esta estrategia permite el diseño de electrolitos de alto

rendimiento bajo condiciones no humidificadas evitando el uso de los polímeros costosos perfluorados. Con este objetivo, dos membranas diferentes fueron estudiadas. La primera de ellas estuvo basada en dos líquidos iónicos próticos polimerizables de anión sulfoetilmacrilato $[\text{HSO}_3\text{-BMIm}][\text{SEM}]$ y $[\text{HSO}_3\text{-BVIIm}][\text{SEM}]$. Por otra parte, en la segunda membrana estudiada, el líquido iónico prótico $[\text{HSO}_3\text{-BVIIm}][\text{TfO}]$ fue polimerizado con diferentes proporciones de su líquido iónico análogo no polimerizable $[\text{HSO}_3\text{-BMIm}][\text{TfO}]$.

Los estudios termogravimétricos han demostrado la habilidad de los líquidos iónicos polimerizados de retener agua atmosférica dentro de su estructura polimérica. Esta propiedad beneficia la conductividad iónica, puesto que las membranas poliméricas presentaron mayores valores de conductividad iónica comparadas con las membranas sometidas a un proceso de secado. De esta manera, las membranas basadas en anión sulfoetilmacrilato con alto contenido de agua presentaron conductividades iónicas de $1.5 \times 10^{-3} \text{ S.cm}^{-1}$ a 70°C mientras que las membranas secas registraron $6.24 \times 10^{-6} \text{ S.cm}^{-1}$ a la misma temperatura. Las membranas basadas en anión triflato presentaron valores de conductividad aún mayores, $10^{-2} \text{ S.cm}^{-1}$ a 70°C para las membranas con alto contenido de agua. Este comportamiento es debido a los protones móviles producidos en la disociación de los grupos HSO_3 cuando se encuentran expuestos a humedad. Estos protones pueden ser transferidos a lo largo de la red de intercambio protónico formada por iones y moléculas de agua. De esta manera, la dependencia de la conductividad iónica con la temperatura sugirió dos tendencias competitivas entre la activación térmica y la evaporación del agua.

La espectroscopía dieléctrica de banda ancha combinada con calorimetría diferencial de barrido permite comprender los mecanismos de transporte protónicos de los electrolitos. Los estudios de dinámica molecular bajo presión elevada han demostrado un mecanismo de salto protónico efectivo para las membranas de anión sulfoetilmacrilato. Por otra parte, esta técnica evidenció que la conductividad en la membrana de anión triflato está controlada por el mecanismo

Grotthuss, mientras que en el monómero está controlado por un mecanismo vehicular. De la misma manera, ha sido demostrado que en el polímero de anión triflato, el transporte protónico está permanentemente controlado por el rápido salto protónico independientemente de la cantidad de agua de la membrana. Consecuentemente, se ha probado que el uso de líquidos iónicos próticos evita los problemas de la gestión de agua observados en las membranas perfluoradas en aplicaciones PEMFCs.

Debido al destacable valor de conductividad iónica obtenida en las membranas de anión triflato, estos electrolitos han sido probados en un dispositivo PEMFC con el objetivo de evaluar su rendimiento. La membrana con 10 wt% [HSO₃-BMIIm][TfO] mostró el mayor valor de conductividad *in-situ*, 2.92×10^{-1} S.cm⁻¹ y el mejor rendimiento a 40 °C, 189 mA.cm⁻² a 0.15 V y densidades de potencia de 49 mW.cm⁻². Estos resultados excedieron a los obtenidos con la membrana base poli([HSO₃-BVIm][TfO]), 46 mA.cm⁻² a 0.15V y 15 mW.cm⁻² de densidades de potencia máxima.

Finalmente, cristales plásticos próticos, una nueva familia de compuestos sólidos similares a los líquidos iónicos pero con los beneficios de un electrolito sólido tales como un fácil manejo y la eliminación de posibles fuga, han sido analizados para su uso como electrolitos en esta aplicación. Debido a las prometedoras ventajas de estos compuestos, membranas compuestas basadas en nanofibras de poli(tetrafluoroetileno) (PVDF) y el cristal plástico prótico N,N-dimetiletileno diamina triflato [DMEDAH][TFO] fueron sintetizadas. La caracterización mediante DSC del cristal plástico ha revelado una transición de fase sólido-sólido a 55°C antes de su fusión a 70 °C. Conductividades iónicas de 2.7×10^{-5} S.cm⁻¹ a 50 °C fueron alcanzadas. Con el objetivo de aumentar la conductividad iónica, 5 mol% de ácido trifílico y 5 mol% de base N,N-dimetiletilenodiamina fueron añadidos al cristal plástico [DMEDAH][TFO]. La conductividad del cristal dopado con ácido se incrementó más del doble debido a la rápida movilidad de los protones del ácido trifílico. Sin embargo, la adición de la base no mejoró significativamente la conductividad del cristal plástico probablemente debido a un fuerte acoplamiento

entre los protones. Las membranas basadas en PVDF y en cristal plástico puro y dopado fueron desarrolladas y testeadas en un dispositivo PEMFC. Se demostró que la adición del ácido mejoró el rendimiento de la pila, alcanzando OCV de 0.74 V y densidades de corriente de 61 mA.cm⁻² a 0.15 V y 25 °C.

Esta tesis ha demostrado la viabilidad del uso de líquidos iónicos próticos como transportadores protónicos para PEMFCs en condiciones no humidificadas evitando el uso de controladores de humedad. Como resumen, las membranas que han obtenido un mejor rendimiento a lo largo de esta tesis se muestran en la tabla 6.1.

Tabla 6.1. Electrolitos con mejor rendimiento en pila de combustible bajo condiciones no humidificadas a 25 °C

Tipo de electrolito	Membrana	OCV	I (mA.cm ⁻²)	P (mW.cm ⁻²)
Membrana impregnada de líquido iónico	N212/[HSO ₃ -BBIm][TfO]	0,82	217	43,6
Líquidos iónicos polimerizados	[HSO ₃ -BVIm][TfO] + 10wt% [HSO ₃ -BMIm][TfO]	0,83	174,4	43,3
Cristal plástico / nanofibras poliméricas	ácido [DMEDAH][TFO]/PVDF	0,74	61	9,5

En vista de los resultados obtenidos, las membranas basadas en líquidos iónicos impregnados y en líquidos iónicos poliméricos son los electrolitos más prometedores para PEMFCs sin humidificación externa.

6.2. Retos para investigaciones futuras

Esta tesis pretende abrir la posibilidad hacia nuevas membranas de intercambio protónico basadas en líquidos iónicos próticos para PEMFCs bajo condiciones no humidificadas.

Hasta ahora, se han desarrollado y caracterizado electrolitos con destacable conductividad iónica demostrando su alto rendimiento en pilas de combustible sin humidificación externa. Sin embargo, a pesar de los logros que han sido descritos a lo largo de los capítulos de esta tesis, aún quedan por superar nuevos retos y desventajas antes de que estas membranas se conviertan en una realidad.

Una de las ventajas más destacables de las pilas de combustible de intercambio protónico es su carácter no contaminante. Sin embargo, las bajas temperaturas asociadas a esta tecnología impide el uso de hidrógeno de baja pureza. La valorización de hidrógeno residual como combustible en estos dispositivos podría promover el uso de las pilas de combustible incrementando la sostenibilidad de esta tecnología. Esta valorización puede realizarse mediante el uso de catalizadores de alto rendimiento y/o el uso de altas temperaturas.

Por otra parte, una de las mayores desventajas de los líquidos iónicos polimerizados es su estabilidad mecánica, especialmente si un líquido iónico no polimerizable es incorporado entre las cadenas poliméricas. Gracias al posible diseño de los líquidos iónicos, es recomendable la búsqueda de nuevas estructuras químicas que permitan polímeros conductores mecánicamente más estables especialmente a altas temperaturas. Además, es recomendable una caracterización completa y cuantitativa de estos polímeros en relación a su estabilidad mecánica y permeabilidad de gases.

Otro aspecto que debe ser mejorado es el contacto entre la membrana y los electrodos con el objetivo de obtener un mejor rendimiento en la pila de combustible. En este trabajo, se han utilizado como electrodos capas de difusión de gases con platino en su superficie. Ésta es una técnica rápida y simple frecuentemente reportada en bibliografía. Sin embargo, existen otras técnicas, como la deposición de catalizador mediante aerógrafo, que permiten obtener MEAs con un contacto optimizado entre los elementos involucrados en las reacciones electroquímicas. Estas membranas resultantes deben ser analizadas con el objetivo de evaluar la influencia del contacto entre la membrana y los electrodos.

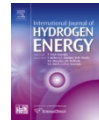
Finalmente, con el objetivo de implementar estas membranas, es esencial realizar su escalado a stacks de pilas de combustible para poder obtener la potencia real que requieren las diferentes aplicaciones. Una estrategia para facilitar este proceso es el modelado ya que proporciona información valiosa sobre los fenómenos fundamentales que tienen lugar en el sistema. Además, la rapidez de la simulación del proceso permite considerar diferentes alternativas permitiendo predecir y

optimizar el comportamiento de la pila de combustible bajo diferentes condiciones de operación.

LIST OF SCIENTIFIC CONTRIBUTIONS

Publications in international journals

1. Performance of PEMFC with new polyvinyl-ionic liquids based membranes as electrolytes. **M. Díaz**, A. Ortiz, M. Vilas, E. Tojo, I. Ortiz. International Journal of Hydrogen Energy 39 (2014) 3970-3977.



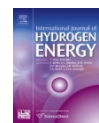
2) Progress in the use of ionic liquids as electrolyte membranes in fuel cells. **M. Díaz**, A. Ortiz, I. Ortiz. Journal of Membrane Science 469 (2014) 379–396.



3) Conductivity Mechanism in Polymerized Imidazolium-Based Protic Ionic Liquid [HSO₃-BVIIm][OTf]: Dielectric Relaxation Studies. Z. Wojnarowska, J. Knapik, **M. Díaz**, A. Ortiz, I. Ortiz, M. Paluch. Macromolecules 47 (2014) 4056-4065.



4) Highly conductive electrolytes based on poly([HSO₃-BVIIm][TfO])/[HSO₃-BMIm][TfO] mixtures for fuel cell applications. **M. Díaz**, A. Ortiz, M. Isik, D. Mecerreyes, I. Ortiz. International Journal of Hydrogen Energy 40 (2015) 11294-11302



Contributions to international conferences

1) Membranes based on ionic liquids for their use as electrolyte in fuel cells. **M. Díaz**, A. Ortiz, I. Ortiz. 5TH International summer school on advanced studies of polymer electrolyte fuel cells. Graz (Austria). September 2012. Poster.



2) Protic Ionic Liquids as Electrolyte Membranes for Fuel Cells under non-humidified conditions. **M. Díaz**, A. Ortiz, M. Vilas, E. Tojo, I. Ortiz. REFGALIs summer school. Pontevedra (Spain). June 2013. Poster.



3) Nuevos polielectrolitos basados en líquidos iónicos para su aplicación en PEMFC. **M. Díaz**, A. Ortiz, M. Vilas, E. Tojo, I. Ortiz. V congreso nacional de pilas de combustible. Madrid (Spain). November 2012. Conference.



4) Towards protic ionic liquid electrolyte membranes for fuel cells. **M. Díaz**, A. Ortiz, M. Vilas, E. Tojo, I. Ortiz. 5TH International congress on ionic liquids. Algarve (Portugal). April 2013. Conference.



5) Ionic Liquid-based polymers as potential electrolytes for fuel cell applications. **M. Díaz**, A. Ortiz, I. Ortiz. Europolymer Conference (EUPOC 2013). Gargnano (Italy). September 2013. Poster.



6) Development of new electrolytes based on ionic liquids for their use in fuel cells. **M. Díaz**, A. Ortiz, I. Ortiz. XXXIV Reunión Bienal de la Real Sociedad Española de Química. Santander (Spain). September 2013. Conference.



7) High conductivity electrolytes based on polymerized ionic liquid and ionic liquid mixtures. **M. Díaz**, A. Ortiz, I. Ortiz. IX Ibero-American congress on membrane science and technology. Santander (Spain). May 2014. Conference.



8) Electrolitos de alta conductividad basados en mezclas de liquido iónico/líquido iónico polimerizado. **M. Díaz**, A. Ortiz, M. Isik, D. Mecerreyes, I. Ortiz. Iberconappice 2014. Barcelona (Spain). October 2014. Conference.



9) Highly proton conductive membranes based on polymerized ionic liquids for non humidified fuel cell application. A. Ortiz, **M. Díaz**, I. Ortiz. Eupoc 2015. Gargnano (Italy). May 2015. Conference.



10) Polymerized ionic liquid for non-humidified proton exchange fuel cell applications. **M. Díaz**, A. Ortiz, I. Ortiz. ECCE 10. Nice (France). September 2015. Conference.



11) Ionic liquids membranes as highly proton conductive electrolytes for non-humidified fuel cell. A. Ortiz, **M. Díaz**, I. Ortiz. Euromembrane 2015. Aachen (Germany). September 2015. Conference.



12) Membranas basadas en [DMEDAH][TFO] soportado sobre nanofibras de PVDF y SPEEK como electrolitos para PEMFCs sin humidificación externa. **M. Díaz**, A. Ortiz, J. Pringle, M. Forsyth, I. Ortiz. Iberconappice 2016. Málaga (Spain). April 2016. Conference.



13) Design of proton exchange membranes based on polymeric ionic liquids for fuel cell applications. A. Ortiz, **M. Díaz**, I. Ortiz. Citem 2016 México (México). May 2016. Conference.



14) [DMEDAH][TFO] soportado sobre nanofibras de PVDF, SPEEK y PBI como membranas para PEMFC sin humidificación externa. **M. Díaz**, A. Ortiz, I. Ortiz. GE-RSEQ. Alicante (Spain). July 2016. Conference.



15) Proton exchange membranes based on polymeric ionic liquids for fuel cell applications. A. Ortiz, **M. Díaz**, I. Ortiz. PRiME 2016. Honolulu (USA). October 2016. Conference.

